(12) INTERNATIONAL APPLICATION PUBLISHED UNDER THE PATENT COOPERATION TREATY (PCT)

(19) World Intellectual Property Organization
International Bureau

(43) International Publication Date
13 September 2012 (13.09.2012)

WIPO | PCT

(10) International Publication Number
WO 2012/120048 A1

(51) **International Patent Classification**:
A61P 1/00 (2006.01) ***A61P 25/00*** (2006.01)
A61P 3/00 (2006.01) ***A61K 31/00*** (2006.01)
A61P 21/00 (2006.01)

(21) **International Application Number**:
PCT/EP2012/053928

(22) **International Filing Date**:
7 March 2012 (07.03.2012)

(25) **Filing Language**: English

(26) **Publication Language**: English

(30) **Priority Data**:
61/449,751 7 March 2011 (07.03.2011) US
61/579,793 23 December 2011 (23.12.2011) US
61/596,485 8 February 2012 (08.02.2012) US

(71) **Applicant** *(for all designated States except US)*: **Fondazione Telethon** [IT/IT]; Via Carlo Spinola 16, I-00154 Roma (IT).

(72) **Inventors; and**
(75) **Inventors/Applicants** *(for US only)*: **SETTEMBRE, Carmine** [IT/IT]; c/o TIGEM, Via Pietro Castellino 111, I-80131 Napoli (IT). **BALLABIO, Andrea** [IT/IT]; c/o TIGEM, Via Pietro Castellino 111, I-80131 Napoli (IT). **MEDINA SANABRIA, Diego Luis** [IT/IT]; c/o TIGEM, Via Pietro Castellino 111, I-80131 Napoli (IT).

(74) **Agents**: **CAPASSO, Olga** et al.; de Simone & Partners SpA, Via Vincenzo Bellini, 20, I-00198 Rome (IT).

(81) **Designated States** *(unless otherwise indicated, for every kind of national protection available)*: AE, AG, AL, AM, AO, AT, AU, AZ, BA, BB, BG, BH, BR, BW, BY, BZ, CA, CH, CL, CN, CO, CR, CU, CZ, DE, DK, DM, DO, DZ, EC, EE, EG, ES, FI, GB, GD, GE, GH, GM, GT, HN, HR, HU, ID, IL, IN, IS, JP, KE, KG, KM, KN, KP, KR, KZ, LA, LC, LK, LR, LS, LT, LU, LY, MA, MD, ME, MG, MK, MN, MW, MX, MY, MZ, NA, NG, NI, NO, NZ, OM, PE, PG, PH, PL, PT, QA, RO, RS, RU, RW, SC, SD, SE, SG, SK, SL, SM, ST, SV, SY, TH, TJ, TM, TN, TR, TT, TZ, UA, UG, US, UZ, VC, VN, ZA, ZM, ZW.

(84) **Designated States** *(unless otherwise indicated, for every kind of regional protection available)*: ARIPO (BW, GH, GM, KE, LR, LS, MW, MZ, NA, RW, SD, SL, SZ, TZ, UG, ZM, ZW), Eurasian (AM, AZ, BY, KG, KZ, MD, RU, TJ, TM), European (AL, AT, BE, BG, CH, CY, CZ, DE, DK, EE, ES, FI, FR, GB, GR, HR, HU, IE, IS, IT, LT, LU, LV, MC, MK, MT, NL, NO, PL, PT, RO, RS, SE, SI, SK, SM, TR), OAPI (BF, BJ, CF, CG, CI, CM, GA, GN, GQ, GW, ML, MR, NE, SN, TD, TG).

Published:

— *with international search report (Art. 21(3))*

— *before the expiration of the time limit for amending the claims and to be republished in the event of receipt of amendments (Rule 48.2(h))*

— *with sequence listing part of description (Rule 5.2(a))*

WO 2012/120048 A1

(54) **Title**: TFEB PHOSPHORYLATION INHIBITORS AND USES THEREOF

(57) **Abstract**: The invention refers to TFEB phosphorylation inhibitors. Such molecules have a therapeutic applicability in all disorders that need induction of the cell authophagic/lysosomal system, such as lysosomal storage disorders, neurodegenerative diseases, hepatic diseases, muscle diseases and metabolic diseases.

TFEB PHOSPHORYLATION INHIBITORS AND USES THEREOF

Field of the invention

The invention refers to TFEB phosphorylation inhibitors. Such molecules have a therapeutic applicability in all disorders that need induction of the cell authophagic/lysosomal system, such as lysosomal storage disorders, neurodegenerative diseases, hepatic diseases, muscle diseases and metabolic diseases.

Background and prior art

Autophagy is a catabolic process that relies on the cooperation of two distinct types of cellular organelles, autophagosomes and lysosomes (1). During starvation the cell expands both compartments to enhance degradation and recycling processes.

The lysosome maintains cellular homeostasis and mediates a variety of physiological processes, including cellular clearance, lipid homeostasis, energy metabolism, plasma membrane repair, bone remodeling, and pathogen defense. All these processes require an adaptive and dynamic response of the lysosome to environmental cues. Indeed, physiologic cues, such as aging and diet, and pathologic conditions, which include lysosomal storage diseases (LSDs), neurodegenerative diseases, injuries and infections may generate an adaptive response of the lysosome (34, 35, 36).

The understanding of the mechanisms that regulate lysosomal function and underlying lysosomal adaptation is still in an initial phase. A major player in the regulation of lysosomal biogenesis is the basic Helix-Loop-Helix (bHLH) leucine zipper transcription factor, TFEB (2). Among the identified TFEB transcriptional targets are lysosomal hydrolases, which are involved in substrate degradation, lysosomal membrane proteins that mediate the interaction of the lysosome with other cellular structures, and components of the vacuolar H+-ATPase (vATPase) complex, which participate to lysosomal acidification (37, 2).

WO2010/092112 refers to molecules able to enhance the cellular degradative pathway acting on the so called CLEAR element; among them TFEB is listed.

WO2010/044885 refers to mTOR modulators.

Description of the invention

The applicants showed that during starvation the cell activated a transcriptional program that controls major steps of the autophagic pathway, including autophagosome

formation, autophagosome-lysosome fusion and substrate degradation. The transcription factor EB (TFEB), a previously identified master gene for lysosomal biogenesis (2), coordinates this program by driving expression of both autophagy and lysosomal genes. TFEB is a main player in the transcriptional response to starvation and controls autophagy by positively regulating autophagosome formation and autophagosome-lysosome fusion both in vitro and in vivo.

The applicants found that nuclear localization and activity of TFEB are regulated by specific serine phosphorylations. Similar to starvation, pharmacological or gene mutation based inhibition of specific phosphorylation induces autophagy by activating TFEB. These data unveil a novel, kinase-dependent, mechanism involved in the regulation of the lysosomal-autophagic pathway by controlling the biogenesis and partnership of two cooperating cellular organelles.

The applicants found that pharmacological inhibition of TFEB phosphorylation can be used *in vivo* to activate the lysosomal and autophagic system of the cells and thus it represents a tool to treat different pathologic conditions.

TFEB activity and its nuclear translocation correlate with its phosphorylation status. In particular phosphorylation of TFEB by mTORC1 inhibits TFEB activity when nutrients are present. Conversely, pharmacological inhibition of mTORC1, as well as starvation and lysosomal dysruption, activates TFEB by promoting its nuclear translocation. In addition, the transcriptional response of lysosomal and autophagic genes to either lysosomal dysfunction or pharmacological inhibition of mTORC1 is suppressed in TFEB-/- cells.

This is even more surprising in view of Peña-Lopis et al. that found that mTOR was able to phosphorylate TFEB but reached an opposite conclusion (38), indicating that mTOR-mediated phosphorylation of TFEB promoted nuclear translocation and consequently inhibiting mTOR resulted in the inhibition of TFEB activity.

Finally applicants showed that pharmacological activation of the TFEB regulatory network can be exploited to promote cellular clearance in disorders due to the accumulation of toxic molecules, such as Lysosomal Storage Disorder and common neurodegenerative diseases.

Therefore it is an object of the invention an inhibitor of TFEB phosphorylation for medical use. Preferably the inhibitor of TFEB phosphorylation according to the invention acts on a kinase of the pathway of the TFEB phosphorylation, more preferably the kinase

is mTOR and/or PI3K. Examples of such inhibitors are those belonging to the group of compounds listed in Table 4 par.1 PI3K-mTOR pathway.

In an alternative embodiment the inhibitor acts inhibiting a kinase that directly phosphorylates TFEB molecule, preferably a serine specific Extracellular Regulated Kinase (ERK), more preferably the ERK2 kinase. Examples of such inhibitors are those belonging to the group of compounds listed in Table 4 par. 2 Ras-ERK pathway.

In an alternative embodiment the inhibitor acts inhibiting a Mitogen activated protein kinase. Examples of such inhibitors are those belonging to the group of compounds listed in Table 4 par. 3 Mitogen activated protein kinases.

In an alternative embodiment the inhibitor acts inhibiting an Aurora kinase. Examples of such inhibitors are those belonging to the group of compounds listed in Table 4 par. 4 Aurora kinases.

In an alternative embodiment the inhibitor acts inhibiting a Receptor Tyrosine kinase. Examples of such inhibitors are those belonging to the group of compounds listed in Table 4 par. 5 Receptor Tyrosine kinases.

In an alternative embodiment the inhibitor acts inhibiting a Polo-like kinase. Examples of such inhibitors are those belonging to the group of compounds listed in Table 4 par. 6 Polo-like kinases.

In an alternative embodiment the inhibitor acts inhibiting a kinase belonging to the JAK-STAT pathway. Examples of such inhibitors are those belonging to the group of compounds listed in Table 4 par. 7 JAK-STAT pathway.

In an alternative embodiment the inhibitor acts inhibiting a cyclin dependent kinase. Examples of such inhibitors are those belonging to the group of compounds listed in Table 4 par. 8 cyclin dependent kinases.

In an alternative embodiment the inhibitor acts inhibiting a kinase belonging to the Wnt signaling pathway. Examples of such inhibitors are those belonging to the group of compounds listed in Table 4 par. 9 Wnt signaling pathway.

In an alternative embodiment the inhibitor acts inhibiting a Src family kinase. Examples of such inhibitors are those belonging to the group of compounds listed in Table 4 par. 10 Src family kinases.

In an alternative embodiment the inhibitor acts inhibiting a kinase belonging to the family of Protein kinases C. Examples of such inhibitors are those belonging to the group of compounds listed in Table 4 par. 11 Protein kinase C family.

The inhibitor of TFEB phosphorylation as above disclosed is advantageously used in the treatment of a disorder that needs the induction of the cell authophagic/lysosomal system, preferably for use in the treatment of any of the following pathologies: lysosomal storage disorders, neurodegenerative diseases, hepatic diseases, muscle diseases and metabolic diseases.

Examples of lysosomal storage disorder are: activator deficiency/GM2 gangliosidosis, alpha-mannosidosis, aspartylglucosaminuria, cholesteryl ester storage disease, chronic hexosaminidase A deficiency, cystinosis, Danon disease, Fabry disease, Farber disease, fucosidosis, galactosialidosis, Gaucher disease (including Type I, Type II, and Type III), GM1 gangliosidosis (including infantile, late infantile/juvenile, adult/chronic), I-cell disease/mucolipidosis II, infantile free sialic acid storage disease/ISSD, juvenile hexosaminidase A deficiency, Krabbe disease (including infantile onset, late onset), metachromatic leukodystrophy, pseudo-Hurler polydystrohpy/mucolipidosis IIIA, MPS I Hurler syndrome, MPS I Scheie syndrome, MPS I Hurler-Scheie syndrome, MPS II Hunter syndrome, Sanfilippo syndrome type A/MPS IIIA, Sanfilippo syndrome type B/MPS IIIB, Morquio type A/MPS IVA, Morquio Type B/MPS IVB, MPS IX hyaluronidase deficiency, Niemann-Pick disease (including Type A, Type B, and Type C), neuronal ceroidlipofuscinoses (including CLN6 disease, atypical late infantile, late onset variant, early juvenile Baten-Spielmeyer-Vogt/juvenile NCL/CLN3 disease, Finnish variant late infantile CLN5, Jansky-Bielschowsky disease/late infantile CLN2/TPP1 disease, Kufs/adult-onset NCL/CLN4 disease, northern epilepsy/variant late infantile CLN8, and Santavuori-Haltia/infantile CLN1/PPT disease), beta-mannosidosis, Pompe disease/glycogen storage disease type II, pycnodysostosis, Sandhoff disease/adult onset/GM2 gangliosidosis, Sandhoff disease/GM2 gangliosidosis infantile, Sandhoff disease/GM2 gangliosidosis juvenile, Schindler disease, Salla disease/sialic acid storage disease, Tay-Sachs/GM2 gangliosidosis, Wolman disease, Multiple Sulfatase Deficiency.

Examples of hepatic diseases are: Alpha1 antitrypsin deficiency and Fatty liver disease.

Examples of muscle diseases are: Autophagic Vacuolar Myopathies and X-linked myopathy with excessive autophagy.

Examples of metabolic diseases are: hypercholesterolemy and fatty liver disease.

Examples of neurodegenerative diseases are: Alzheimer's disease, Parkinson's disease, Huntington's disease, Creutzfeldt-Jakob disease, and spinocerebellar ataxia.

It is a further object of the invention the use of the above disclosed inhibitors of TFEB phosphorylation for increasing the productivity of cells producing endogeneous or recombinant lysosomal enzymes.

It is a further object of the invention a method of producing lysosomal endogeneous or recombinant enzymes comprising: (1) contacting the inhibitor of TFEB phosphorylation as above disclosed with the autophagic/lysosomal system in a cell; (2) inducing said autophagic/lysosomal system; and (3) increasing production of said lysosomal enzymes.

It is a further object of the invention a method of treating a disorder by administering to a subject a therapeutically effective amount of the inhibitor of TFEB phosphorylation as above disclosed. Preferably the disorder is alleviated by the induction of the cell authophagic/lysosomal system. More preferably the disorder is selected from the group comprising lysosomal storage disorders, neurodegenerative diseases, hepatic diseases, muscle diseases and metabolic diseases. Examples of such diosrers were above provided.

In a preferred embodiment the method of treating a disorder according to the invention comprises the steps of: (1) administering an inhibitor as above disclosed; (2) inducing the autophagic/lysosomal system in a cell; and (3) increasing cellular clearance.

The invention will be described in experimental and non-limiting examples.

Figure Legends

Fig. 1 TFEB induces autophagy. (**A**) HeLa cells stably overexpressing TFEB were transfected with a GFP-LC3 plasmid and treated as indicated. Approximately 100 cells were analyzed in triplicate for each experiment. The graph shows quantification of GFP-positive vesicles. (**B-F**) Western blot analysis of LC3 in (**B**) TFEB-3xflag stable overexpressing (+) and control cells (-).Graph represents the quantification using imageJ software analysis of LC3II expression (relative to actin) from three independent blots; (**C**) TFEB stable overexpressing cells, which were serum and aminoacid-starved (Starv) for the indicated time (h= hours), (**D-F**) cellular lysates isolated from TFEB-RNAi and control cells treated with scrambled RNAi (ctr) cultured in (**D**) normal media, (**E**) starved media, or (**F**) starved media supplemented with bafilomycin (4h; 400nM). The graph represents the quantification of LC3II expression (relative to actin) from three independent blots and band intensities were quantified using imageJ software analysis. (**G**) TFEB mRNA levels were analyzed by qPCR using cDNAs prepared from cells transfected with 3 different

siRNAoligos targeting TFEB (oligo #1, #2, #3), or with a scrambled siRNAoligo (ctr). (**H**) Representative confocal images of fixed HeLa cells stably expressing GFP-mRFP-LC3 transfected with empty (control) or TFEB vector. A minimum of 2000 cells was counted and the values represent the average number of vesicles (relative to the control, %) obtained from three independent experiments. AL (autolysosomes) = mRFP positive/GFP negative vesicles; total: mRFP positive vesicles. (All error bars represent standard deviations. T-test (unpaired) *p* value (*)<0.05, (**)<0.01)

Fig. 2 Starvation regulates TFEB nuclear translocation and activity. (**A**) Scatter Plot graphs displaying the logarithmic value of the fold change differences in the relative expression levels of 51 autophagy-related genes in HeLa cells cultured in different conditions. X-axis=control group. Y-axis=treated group. Circles represent genes with increased (red) or decreased (green) fold change. Comparisons were as indicated. (**B**) Chromatin immunoprecipitation (ChIP) analysis. The histogram shows the amount of immunoprecipitated DNA as detected by qPCR assay. Values were normalized to the input and plotted as relative enrichment over a mock control. Experiments were performed in triplicate. (**C**) qPCR analysis of TFEB-target gene expression in normal, starved, and in TFEB-siRNA starved cells. GAPDH and HPRT represents housekeeping genes, while ATG10, ATG9A and ATG4D represent control genes (non-TFEB target genes). (**D-F**) HeLa cells stably overexpressing TFEB were left untreated or nutrient starved for 4h. (**D**) Five fields containing 50-100 cells/each were analyzed for TFEB nuclear localization. *P value* (*) = <0.01. (**E**) Cells were subjected to nuclear/cytosolic fractionation and blotted with Flag antibody. H3 and tubulin were used as nuclear and cytosolic markers, respectively. (**F**) Nuclear fractions were blotted with Flag and H3 (loading control) antibodies. (**G**) Western blot analysis of Flag, tubulin and H3 in nuclear extracts prepared from normal, starved and starved/stimulated with normal media cells for 1h (normal) or pretreated with AP-2 (AKT inhibitor), Rapamycin (mTOR inhibitor) and U0126 (MEK inhibitor) 1h prior to media stimulation. Total extracts were used to verify the efficiency of the inhibitors. (**H**) qPCR analysis of lysosomal and autophagic genes in TFEB siRNA or TFEB-scrambled control cells transfected with either a constitutive active MEK (caMEK) plasmid or with an empty vector. Starvation was performed where indicated. (All error bars represent standard deviations. T-test (unpaired) *p* value (*)<0.05, (**)<0.01)

Fig. 3 Serine phosphorylation regulates TFEB activation. (**A**) TFEB subcellular localization in HeLa cells expressing mutated versions of TFEB-3xFlag, immunostained with Flag antibody. Five fields from three independent experiments, containing 50-100

cells each were analyzed. (**B**) qPCR analysis of TFEB target gene expression 24h post-transfection with empty, normal and mutant TFEB plasmids. (**C, D**) Western blot analysis of LC3II (**C**) and Lamp1 (**D**) in protein extracts from HeLa cells transfected with equal amounts of empty (pCDNA), TFEB-3xFlag or TFEBS142A-3xFlag vectors. Bafilomycin was added where indicated. Experiments were done in triplicate and the quantification of proteins levels were normalized to actin levels. (**E**) Analysis of autolysosomes (AL= RFP positive/GFP negative) in HeLa cells stably expressing GFP-mRFP-LC3 and transfected with either pcDNA, Tfeb or Ser-Tfeb for 24h. Quantification as reported in Fig 1H. (**F**) Western blot analysis using anti-Erk antibody on HeLa cells transfected with HA-Erk2 kept and/or TFEB-3xFlag, kept in full serum or nutrient starved for 4h and immunoprecipitated with anti-Flag antibody. Lysates were immunoprecipitated with anti-FLAG and blotted with an anti-Erk antibody. (**G**) In vitro kinase assay. Recombinant kinases were incubated in the presence of ATP-γ ^{32}P and of a peptide spanning from amino acid 120 to 170 of TFEB protein (TFEB-S-142) or with a similar peptide in which serine 142 was substituted with alanine (TFEB-A-142). Phosphorylation efficiency ("phosphorylation sensitivity") was measured as the amount of radioactivity incorporated by the peptides. (**H**) HeLa stable clones overexpressing TFEB were transfected with siRNA oligos specific for ERK1/2 or with control siRNA. 48h later cells were left untreated, serum starved or serum and amino acid (a.a.) starved for 4h, harvested and subjected to nuclear isolation and Flag immunoblotting. Total lysates were probed with ERK antibody. All error bars represent standard deviations. *P value* (*) = <0.05.

Fig. 4 *In vivo* analysis of TFEB-mediated induction of autophagy. (A) Immunofluorescence analysis of GFP-positive vesicles in fed, 16h-fasted, and 24h-fasted mice. Quantification of vesicles is shown in the graph. **(B)** qPCR analysis of TFEB target gene expression in liver samples from fed and fasted animals (n=3; Error bars represent standard deviations. p value (*)<0.05). Gapdh and Hprt were used as reference genes. (**C,D**) Analysis of TFEB subcellular localization in two month-old wild type mice infected with AAV2/9*Tcfeb*-HA and fasted 16h prior to sacrifice. (**C**) HA-immunofluorescence analysis. The graph shows quantification of nuclear HA signal. 100 transduced cells were counted for each liver. n=3 mice/group. *= <0.001. (**D**) Western blot analysis of HA, Tubulin and H3 in liver specimens subjected to nuclear fractionation. Total liver lysates were probed with an HA antibody to verify comparable transgene expression between fed and fasted animals. (**E**) Western blot analysis of LC3, actin, p-ERK1/2 and ERK1/2 in liver extracts from mice injected AAV2/9*Tcfeb*-HA. (**F**) Western blot analysis of GFP and

DAPI staining in cryopreserved liver slices from 2-month old GFP-LC3 transgenic mice injected with either AAV-Tcfeb-HA or with saline solution (control group) and fed ad libitum or fasted for 24h prior sacrifice. Quantification of GFP-positive vesicles is shown in the graph. (**G**) qPCR analysis of both autophagic and lysosomal TFEB-target gene expression in liver samples isolated from conditional *Tcfeb*-3xFLAG transgenic mice (Tcfeb-3xflag;AlbCRE), in which transgene expression is driven by a liver-specific CRE recombinase (i.e. Albumin-CRE). (**H**) Western blot analysis of LC3 and actin in liver protein extracts from Alb-CRE, Tcfeb-3xFlag and Tcfeb-3xFlag;Alb-CRE mice.

Fig. 5 TFEB transient overexpression induces autophagy. (A) HeLa cells were transiently transfected with a plasmid encoding for flagged TFEB protein. 48h after transfection cells were collected, lysed and 10 mg of protein samples were analyzed for LC3, Flag and actin immunoreactivity. Experiments were performed in triplicate and band intensities were quantified using image j software analysis (Error bars represent standard deviations. p value (*)<0.05) (B) COS-7 cells were transiently transfected with an empty vector or with a TFEB-3xFlag vector. 24 hours later cells were treated for 4h with lysosomal inhibitors (pepstatin/E64, 10μg/ml, SIGMA). 10 μg of cell lysates were subjected to LC3 and actin immunoblotting.

Fig. 6 Induction of autophagy in TcFEB overexpressing MEFs. (A, B) Electron micrograph of MEFs infected with lentivirus expressing TcFEB and control cells. (a) Autophagic structures were observed upon TcFEB expression, including autophagosomes (AV) and autolysosomes (AL). (B) Formation of early autophagosome. Isolation membrane (arrows) surrounding electron-dense cytoplasmatic material. (C) Quantitation of number of autophagic structure (AV and AL) and (D) of early autophagosomes. At least 30 cells/group were analyzed. Error bar represent SEM; p value (*) < 0.05; (***) < 0.0001.

Fig. 7 TFEB promotes autophagosome formation. (A) Control and stable TFEB-overexpressing cells were treated with bafilomycin (baf; 12h 400nM) harvested and subjected to LC3II, Flag and actin immunoblotting. (B) Control and TFEB-overexpressing cells were left untreated or treated with 10μg/ml lysosomal inhibitor pepstatin/E64 for 4h, lysed and subjected to LC3, Flag and actin immunoblotting. Experiments were performed in triplicate and band intensities were quantified using imageJsoftware analysis (Error bars represent standard deviations. p value (*) <0.05).

Fig. 8 TFEB increases autophagic proteolysis. Rate of long-lived protein degradation in TFEB-overexpressing, TFEB-depleted and control cells in either normal or

starved condition. 3-methyl adenine (3MA) was added where indicated (Error bars represent standard deviations. p value (*) <0.05).

Fig. 9 Distribution of the TFEB putative binding elements in the promoter regions of a subset of autophagy genes. Numbers indicate the distance of the binding element from the transcription start site (TSS).

Fig. 10 Starvation enhances TFEB activity. Luciferase report assay using a construct carrying four tandem copies of TFEB binding sites. Both normal and TFEB-overexpressing HeLa cells were transfected with an artificial promoter with TFEB binding sites. Both cells types displayed increased transactivation potential when cultured in starved conditions. (Error bars represent standard deviations p (*)< 0.05)

Fig. 11 Starvation induces TFEB nuclear translocation through MAPK. (A) Starvation induces cytosolic TFEB mobility shift and nuclear translocation. Normal medium; starved medium (4h); starved + normal, indicates that cell were cultured in starved medium (4h) and supplemented with normal medium 1h prior to harvesting. Cytosolic and nuclear fractions were subjected to Flag immunoblotting. (B) Analysis of TFEB cellular localization by immunofluorescence in HeLa cells treated as indicated in fig. 2G. The graph shows percentage of cells that display TFEB nuclear localization. Error bars represent standard deviations. P value (*) < 0.05

Fig. 12 TFEB nuclear traslocation is dependent on S142 phosphorylation. (A) HeLa cells expressing TFEB-3xFlag, S142A-3xFlag, S332-3xFlag or S423-3xFlag proteins were subjected to nuclear protein isolation. Equal amounts of nuclear proteins were verified by ponceau staining. (B) HeLa cells expressing TFEB-3xFlag, S142A-3xFlag and S142D-3xFlag proteins were subjected to nuclear protein isolation in normal and in starved conditions. (C) Flag immunoblotting of cytosolic protein isolated from HeLa cells expressing TFEB-3xFlag and TFEB-S142A-3xFlag showing that in normal media S142A migrates as lower MW band compared to WT TFEB while this shift is not evident anymore in starved conditions. (D) Flag immunoblotting of cytosolic protein isolated from starved HeLa cells expressing TFEB-3xFlag, S142A-3xFlag and S142D-3xFlag showing a reduced shift of TFEB-S142D

Fig. 13 S142A TFEB mutant displays enhanced activity. Hela cells stably overexpressing GFP-LC3 were transfected with equal amounts of empty, TFEB-3xFlag or S142A-TFEB-3xFlag plasmids and the number of autophagosomes was quantified. At least ten fields (containing 4-10 cells) were analyzed for each point. Experiments were performed in triplicate. Error bars represent standard deviations. p value (*) < 0.05.

Fig. 14 Multiple sequence alignment of TFEB-human S142 phosphorylation site with TFEB paralogues, MITF and relevant TFEB-related family members. TFEB_human homologs were identified by BLAST (2.2.17) search against UniProtKB database at ExPASy Proteomics Server. The applicantsAuthors removed the hits with "putative", "uncharacterized" and "cDNA" keywords and hits without gene names. Next, the applicantsauthors aligned the remaining homologs with ClustalW (1.82). The multiple sequence alignment was generated by Seaview. The figure shows only a 20 amino acid-long segment of TFEB_HUMAN sequence aligned with other proteins from TFEB, MITF, TCFEB, TFE3 and TCFE3 families. "sp" stands for SwissProt entry, while "tr" denotes Tremble entry. P19484 is a UniProrKB accession code. TFEB_HUMAN indicates gene name and species name respectively.

Fig. 15 Strategy for TcFEB overexpression in vivo. (A) Representative images of cryopreserved liver slices immunostained with anti-HA antibody (to verify viral transduction efficiency). (B) Liver protein extracted from Tcfeb-HA injected and control mice were immunoblotted HA and actin antibodies. (C) Generation of a transgenic mouse line for TcFEB conditional overexpression. The map of the transgene vector, before and after CRE recombinase is illustrated at the top. Representative genotypes of littermates are shown on the left, while the correspondent liver-specific TFEB overexpression in mouse n4 is shown on the right.

Fig. 16 TFEB overexpression increases the release of lysosomal enzymes in the culture medium of MEFs, NSCs, HeLa, and COS-7 cells. Activities of lysosomal enzymes acid phosphatase, beta-galactosidase, and beta-hexosaminidase were determined in the culture medium and in cells transfected with either an empty vector or with a TFEB-expression vector. HeLa, Cos7 cells and mouse embryonic fibroblasts from mouse models of MLIV (S7), MPSIIIA (S7), and MSD were transfected using PolyFect Transfection Reagent (Qiagen) or lipofectamine 2000 Reagent (Invitrogen), according to the manufacturer's protocols. TFEB-3xFLAG HeLa stable cell lines (CF7) was previously described (2). The figure shows percentages of enzyme activities released compared to total activities.

Fig. 17 TFEB exerts a positive control on lysosomal exocytosis. MPSIIIA MEF Cells were maintained in DMEM supplemented with 10% FBS and penicillin/streptomycin (normal culture medium). Sub-confluent cells were transfected using LipofectamineTM 2000 (Invitrogen) according to manufacturer's protocols. MPS-IIIA MEFs were co-transfected with a plasmid encoding a tagged sulfamidase (SGSH3XFlag) and either an

empty plasmid or a plasmid encoding TFEB. One day after transfection the medium was replaced with DMEM 0,5% FBS. Two days after transfection the conditioned medium and the pellet were collected for sulfamidase activity measurement and the percentage of the enzyme released in the medium calculated.

Fig. 18 Lysosomal stress induces TFEB nuclear translocation. Immunoblotting of proteins extracted from HeLa cells that express TFEB–3 x Flag treated with chloroquine (CQ) or Salicylihalamide A (SalA), subjected to nuclear/cytosolic fractionation and blotted with antibody against FLAG to detect TFEB. Histone 3 (H3) and tubulin were used as nuclear and cytosolic markers, respectively. Blots are representative of triplicate experiments.

Fig. 19 mTORC1 regulates TFEB. (A) Lysosomal stress inhibits mTOR signaling. Immunoblotting of protein extracts isolated from HeLa cells treated overnight, as indicated. Membranes were probed with antibodies for p-T202/Y204-ERK1/2, ERK1/2, p-T389-S6K, and S6K to measure ERK and mTORC1 activities. (B) Torin 1 induces TFEB dephosphorylation and nuclear translocation. FLAG immunoblotting of cytosolic and nuclear fractions isolated from TFEB–3 x FLAG HeLa cells cultured in amino acid-free media and subsequently stimulated as indicated for at least 3 h. Correct subcellular fractionation was verified with H3 and tubulin antibodies. (C, D) Effects and dose–response curves of ERK and mTOR inhibitors on TFEB nuclear translocation. TFEB–GFP HeLa cells were seeded in 384-well plates, incubated for 12 h, and treated with 10 different concentrations of the ERK inhibitor U0126 or the mTOR inhibitors Rapamycin, Torin 1 and Torin 2 ranging from 2.54 nM to 50 μM. After 3 h at 37 °C in RPMI medium containing one of each of the compounds, the cells were washed, fixed, and stained with DAPI and photographed by using confocal automated microscopy (Opera high content system, Perkin Elmer). (C) Representative images of test concentrations for each compound. Scale bars represent 30 μm. (D) The graph shows the percentage of nuclear translocation at the 10 different concentrations of each compound (in log of the concentration). The EC50 for each compound was calculated using Prism software (see Materials and methods for details). (E) Amino acids induce TFEB molecular weight shift. Immunoblotting of protein extracts isolated from HEK-293T cells transfected either TFEB-3XFLAG or with an empty vector were nutrient starved and stimulated for 50 minutes with amino acids (a.a.). Antibody used were p-T389-S6K, S6K and FLAG. (F) Rag knockdown induces TFEB nuclear translocation. HeLa cells stably expressing Flag–3 x TFEB were infected with lentiviruses encoding a Short hairpin (Sh-) RNA targeting

luciferase (control) or RagC and RagD mRNAs. In all, 96 h post infection, cells were left untreated (N=normal media), starved (S=starved media) or treated with Torin 1 (T=Torin 1) for 4 h and then subjected to nuclear/cytosolic fractionation. TFEB localization was detected with a FLAG antibody, whereas tubulin and H3 were used as controls for the cytosolic and nuclear fraction, respectively; levels of S6K phosphorylation were used to test RagC and RagD knockdown efficiency. (G) mTORC2 does not affect TFEB phosphorylation. Mouse embryonic fibroblasts (MEFs) isolated from Sin1-/- or control embryos (E14.5) were infected with a retrovirus encoding TFEB–3 x FLAG; 48 h post infection, cells were treated with Torin 1 (T) for 4 h, where indicated, subjected to nuclear/cytosolic fractionation and immunoblotted for FLAG, tubulin, and H3.

Fig. 20 mTORC1 phosphorylates TFEB at serine 142 (S142). (A) Torin 1 induces S142 dephosphorylation. HeLa cells were treated as indicated and total and nuclear extracts were probed with a TFEB p-S142 phospho-antibody and with anti-FLAG antibody. (B) Schematic representation of TFEB protein structure with the predicted mTORC1 phosphorylation sites and their conservation among vertebrates. Numbering is according to human isoform 1. (C) Sequence conservation scores of the phosphorylation sites and quantitative agreement between mTOR consensus motif and the sequence around the phosphorylation sites of TFEB. (D) S142 and S211 regulate TFEB localization. Flag immunostaining of TFEB subcellular localization in HeLa cells expressing serine-to-alanine mutated versions of TFEB–3 x Flag. Nuclei were stained with DAPI. Values are means of five fields containing at least 50 transfected cells. Student's t-test (unpaired) ***P <0.001. Scale bars represent 30 μm.

Fig. 21 The lysosome regulates gene expression by TFEB. (A) Chloroquine treatment inhibits mTORC1 activity in primary hepatocytes. Primary hepatocytes isolated from 2-month-old Tcfebflox/flox (control) and Tcfebflox/flox;Alb-Cre(Tcfeb-/-) mice were left untreated or treated overnight with Torin 1, U0126, or Chloroquine. Subsequently, cells were lysed and protein extracts were immunoblotted with the indicated antibodies. (B, C) TFEB mediates the transcriptional response to chloroquine and Torin 1. Quantitative PCR (qPCR) of TFEB target genes in primary hepatocytes from control (flox/flox) and Tcfeb-/- (flox/flox; alb-Cre) mice. Cells were treated with Chloroquine (left) and Torin 1 (right). The expression levels are shown as % increased expression of the treated versus the corresponding untreated samples. Values represent means±s.d. of three independent hepatocyte preparations (three mice/genotype). Student's t-test (two tailed) *P-value ≤0.05.

Fig. 22 Treatment with Torin 1 and its analog Torin 2 reduces glycosaminoglycan (GAG) accumulation in neural stem cells (NSCs) from Multiple Sulfatase Deficiency mouse model (MSD). Differentiated neuronal stem cells (NSCs) isolated from MSD mice were treated with DMSO, 10nM of Torin 1 or 10nM of torin 2. After 24 hours, the GAG content was determined by alcian blue (AB) staining. Both torins were able to reduce GAG staining in MSD treated cells as compared to DMSO treated cells. A representative image of GAG staining in WT NSCs is showed in the lowest panel.

Fig. 23 Treatment with Torin 2 reduces vacuolization in MSD cells. Differentiated NSC were fixed on glutaraldehyde and processed for standard electron microscopy.

Fig. 24 Torin 2 reduces GAG accumulation in the liver of MSD mice. MSD mice were treated with placebo (MSD_750) or torin2 (MSD_727) during 10 days (oral administration; 0.3 mg torin 2/day/mouse in 50% PEG400). After the treatment liver tissues were collected and GAG accumulation was determined by alcian blue staining (black spots). Torin 2-treated mice showed a reduction of GAG accumulation in liver tissue (n=3). A representative image of WT liver stained with alcian blue is showed (WT_739).

Materials and methods

Cell culture and media and drugs and cellular treatment

HeLa and COS and HEK-293T cells were purchased from ATCC. Cells were cultured in the following media: (normal) DMEM high glucose supplemented with 10% FBS; (starvation) HBSS media with Ca and Mg supplemented with 10mM HEPES; (Serum) EBSS supplemented with 20%FBS; (amino acid media) Glucose and serum free DMEM; Drugs treatment: Rapamycin (2.5mg/ml, SIGMA) 2-4h otherwise indicated; Bafilomycin, (400nM, SIGMA) 2-4h; Insulin (100ng/ml SIGMA) for 2h; EGF, FGF (BD biosciences); LIF (100ng/ml; ESGRO, Millipore) 2h; PMA (1μg/ml) 2h. U0126 (MEKi) were used at 25 mM (Cell Signaling), API2 (AKT inhibitor) were used at 1 mM. Lysosomal inhibitors were pepstatin and E64 (10 mg/ml 4h SIGMA). The following drugs were used in experiments of Figs.18-21: Rapamycin (2.5μM, otherwise indicated) from SIGMA; Torin1 (250 nM, otherwise indicated) from TOCRIS; U0126 (50 μM) from Cell Signaling technology; Chloroquine (100 μM) from SIGMA; Salicylihalamide A (2 μM) was a kind gift from Jeff De Brabander (UT Southwestern).

Primary hepatocytes were generated as follow: 2-month-old mice were deeply anaesthetized with Avertin (240 mg/kg) and perfused first with 25 ml of HBSS (Sigma

H6648) supplemented with 10mM HEPES and 0.5mM EGTA and after with a similar solution containing 100 U/ml of Collagenase (Wako) and 0.05 mg/ml of Trypsin inhibitor (Sigma). Liver was dissociated in a petri dish, cell pellet was washed in HBSS and plated at density of $5x10^5$ cells/35mm dish and cultured in William's medium E supplemented with 10%FBS, 2mM glutamine, 0.1mM Insulin, 0.1mM Dexamethasone and pen/strep. The next day, cells were treated as described in the text. Sin1-/- and control MEFs were generated as previously described (53) and maintained in DMEM supplemented with 10% FBS, glutamine and pen/strep.

Generation of a Tcfeb^{flox} mouse line

The applicants used publicly available embryonic stem (ES) cell clones (http://www.eucomm.org/) in which Tcfeb was targeted by homologous recombination at exons 4 and 5. The recombinant ES cell clones were injected into blastocysts, which were used to generate a mouse line carrying the engineered allele. Liver-specific KO was generated crossing the Flox/Flox mice with a transgenic line expressing the CRE under the Albumin promoter (ALB-CRE) obtained from the Jackson laboratory. All procedures involving mice were approved by the Institutional Animal Care and Use Committee of the Baylor College of Medicine.

Transfection, plasmids and siRNA

Both plasmids and siRNA were transfected with lipofectamine LTX (Invitrogen) using a reverse transfection protocols. siRNA-transfected cells were collected after 48 or 72h. siRNA TFEB were used at 50nM (Dharmacon), siRNA ERK1/2 were used at 100nM (Cell Signaling).

Cells were transiently transfected with DNA plasmids pRK5-mycPAT1, pCEP4-TFEB-his, pC1G2-TFEB, and p3 x FLAG-CMVTFEB using lipofectamine2000 or LTX (Invitrogen) according to the protocol from manufacturer. Site-direct mutagenesis was performed according to the manufacturer instructions (Stratagene) verifying the correct mutagenesis by sequencing.

Western blotting

Cells or tissues were solubilized in RIPA buffer supplemented with protease (ROCHE) and Phosphatase (SIGMA) inhibitors. From 10 to 30 micrograms were loaded on 4-12% Bis-Tris gel (NUPAGE, Invitrogen), transferred to PVDF membranes and analyzed by western blot using the ECL method (Pierce). The following antibodies were used: LC3 (Novus Biological), FLAG, b-ACTIN, TUBULIN (SIGMA), HA (Covance),

H3, ERK1/2, p-ERK1/2, p-AKT, p-70S6K (Cell Signaling), ERK2 (Santa Cruz). Protein levels were quantified by using ImageJ software analysis.

Nuclear/cytosolic fractionation

Cells were seeded at 50% of confluence in 6 well dishes and serum starved overnight (ON). Normal medium was added the following day either in presence of DMSO or kinase inhibitors. Subcellular fractionation was carried out as previously reported. Briefly, cells were lysed in 0.5 Triton X-100 lysis buffer (50mM Tris-HCl, 0.5% triton, 137.5 mM NaCl, 10% glycerol, 5 mM EDTA supplemented with fresh protease and phosphatase inhibitors. Supernatant represented cytosolic fraction while nuclear pellet was washed twice and lysed in 0.5 Triton X-100 buffer 0.5% SDS and sonicated.

Degradation of long-lived proteins

Sub-confluent cells were incubated with L-U^{14}C-serine for 20h and chased for 1h with cold media to degrade short-lived proteins. Subsequently cells were incubated with either normal media or starvation media (eventually in the presence of 3-MA) for 4h. The rate of long-lived protein degradation was calculated from the ratio of soluble radioactivity in the media to that insoluble in the acid-precipitable cell pellet.

RNA extraction, reverse transcription, ChIP and quantitative PCR

Total RNA was extracted from tissues using TRIzol (Invitrogen) or from cells using RNAesy column (Qiagen). Reverse transcription was performed using TaqMan reverse transcription reagents (Applied Biosystems). Lysosomal and autophagic gene specific primers were previously reported[2]. Autophagy gene primers and mouse primers were purchased from SABiosciences. Fold change calculations were calculated using SABiosciences' online data analysis website (http://www.sabiosciences.com/pcr/arrayanalysis.php) which uses the DDC_t method. In brief, the average of the most stable housekeeping genes (GAPDH, ACTB, B2M, RPL13A, HPRT and Cyclophillin) were used as "normalizer" genes to calculate the DC_t value. Next, the DDC_t value is calculated between the "control" group and the "experimental" group. Lastly, the fold change is calculated using $2^{(-DDCt)}$. Biological replicates were grouped to allow calculating the fold change values. Unpaired T-Test was used to calculate statistical significance. Asterisks in the graph indicate that the P-value was <0.05.

Protein kinase prediction

The applicants used five methods including CrPhos0.8, GPS-2.1, PhosphoMotifFinder, Networkin and PHOSIDA (15-19) using the default parameters.

They further filtered CrPhos0.8 and GPS-2.1 predictions according to their confidence scores. For the former, we took into account the predictions with a false positive rate (FPR) equals or less than 30%. For the latter, they considered the predictions with score equals or higher than 5. GPS-2.1 scores were calculated as the difference between actual score and threshold values. We took all the predictions from other three methods. In the case of Networkin, we combined predictions from both Networkin and Networkin 2. Each method describes the kinases associated by S142 site in a different kinase classification, which simply involves four hierarchical levels: kinase group, kinase family, kinase subfamily and kinase itself. To obtain a general consensus in each hierarchical level, we classified each prediction in these four hierarchical levels, if the predictions were not already classified in that manner. They searched for the missing classifications at the http://kinase.org/kinbase database under vertebrate clade and human species. Consensus in each classification is found according to the majority vote in each classification.

***In vitro* kinase assay**

TFEB-S-142: aa. o 117-166 of Seq Id No. 2:
PPPAASPGVRAGHVLSSSAGNSAPNSPMAMLHIGSNPERELDDVIDNIMR and
TFEB-A-142: Seq Id No. 4, corresponding to aa. of 117-166 of Seq Id No. 2 where Ser 142 was substituted with Ala (bold):
PPPAASPGVRAGHVLSSSAGNSAPN**A**PMAMLHIGSNPERELDDVIDNIMR
were synthesized by GENESCRIPT corp. The test peptides TFEB-A-142 and TFEB-S-142 were made up to 1 mM in 50 mM HEPES pH7. There appeared to be no issue with dissolution. The kinase assay was performed at room temperature for 40 minutes at 200 μM ATP and 100 μM of each peptide, using Millipore's standard radiometric assay. All protein kinases were used at their standard KinaseProfiler™ assay concentration. Following incubation, all assays were stopped by the addition of acid and an aliquot spotted onto P30 and Filtermat A to separate products. All tests were carried out in triplicate, and the usual substrate for each protein kinase included as a control.

***In vivo* gene delivery**

The mice were housed in the transgenic mouse facility of Baylor College of Medicine (Houston, TX, USA). GFP-LC3 transgenic mice were a kind gift of N. Mizushima. C57B6 female mice (4 weeks old) were used, if not otherwise specified. The AAV vector was produced by the TIGEM AAV Vector Core Facility. Briefly, the mouse TFEB (TcFEB) coding sequence was cloned into the pAAV2.1-CMV-GFP plasmid by replacing the GFP sequence and fused in frame with a HA tag. The resulting pAAV2.1-

CMV-TcFEB-HA was then triple transfected in sub-confluent 293 cells along with the pAd-Helper and the pack2/9 packaging plasmids. The recombinant AAV2/9 vectors were purified by two rounds of CsCl. Vector titers, expressed as genome copies (GC/mL), were assessed by both PCR quantification using TaqMan (Perkin-Elmer, Life and Analytical Sciences, Waltham, MA) and by dot blot analysis. Each mouse was retro-orbital injected with 1.25 $x10^{11}$ viral particle and sacrificed after 3 weeks. Starved mice were food-deprived for 16h when analyzed for gene expression, or for 24h when analyzed for GFP-LC3 dots number.

Histology and immunofluorescence

Liver samples were collected and fixed overnight in 4% paraformaldehyde in PBS. After cryoprotection in 10 and 30% sucrose in PBS, the specimens were frozen in OCT (Sakura Finetech, Torrance, CA) and sectioned 30μm thick. Images were taken on an Axioplan2 (Zeiss, Thorwood, NY). For immunofluorescence, slices were blocked for 2h at RT in 2.5% BSA in PBS+0.1% Triton X-100. After blocking, specimens were incubated for 20h with the primary antibody and, after 3X washes in PBS+0.05% TX-100, for 3h with secondary antibodies conjugated either with Alexafluor 488 or Alexafluor 555 (Invitrogen). For immunohistochemistry analyses of HA the avidin-biotin complex (ABC) method was used (Vectastain Elite ABC kit). Anti-GFP was from Abcam; (diluition 1:500)

Electron microscopy

Control and TFEB-overexpressing cells were washed with PBS, and fixed in 1% glutaraldehyde dissolved in 0.2 M Hepes buffer (pH 7.4) for 30 min at room temperature. The cells were then postfixed for 2 h in OsO4. After dehydration in graded series of ethanol, the cells were embedded in Epon 812 (Fluka) and polymerized at 60°C for 72 h. Thin sections were cut at the Leica EM UC6, counterstained with uranyl acetate and lead citrate. EM images were acquired from thin sections using a Philips Tecnai-12 electron microscope equipped with an ULTRA VIEW CCD digital camera (Philips, Eindhoven, The Netherlands). Quantification of vacuolization was performed using the AnalySIS software (Soft Imaging Systems GmbH, Munster, Germany). Selection of cells for quantification was based on their suitability for stereologic analysis, i.e. only cells sectioned through their central region (detected on the basis of the presence of Golgi membranes) were analyzed.

Animal Models

All procedures involving mice were approved by the Institutional Animal Care and Use Committee of the Baylor College of Medicine. GFP-LC3 transgenic line was

described previously. Tissue specific overexpression of Tcfeb was generated as follows: *Tcfeb*-3xFlag cDNA was inserted after a CAGCAT cassette [chicken actin promoter (CAG) followed by chloramphenicol acetyltransferase (CAT) cDNA flanked by 2 loxP sites] and used to generate transgenic mice (Baylor College of Medicine transgenic core). Mice were then crossed with Albumin-CRE (obtaine from the Jackson laboratory) line. For 48 Starvation protocol the mice were food deprived for 22h, subsequently were fed for 2h and fasted again for 24h prior sacrifice.

Enzymatic activities

Lysosomal enzymes acid phosphatase, beta-galactosidase, and beta-hexosaminidase activities were measured using the appropriate fluorimetric or colorimetric substrates. SGSH activity was measured following protocols described in Fraldi*et* al., *Hum Mol Gen* 2007 (33).

Immunoblotting and antibodies

The mouse anti-TFEB monoclonal antibody was purchased from My Biosource catalogue No. MBS120432. To generate anti-pS142 specific antibodies, rabbits were immunized with the following peptide coupled to KLH: AGNSAPN{pSer}PMAMLHIC. Following the fourth immunization, rabbits were sacrificed and the serum was collected. Non-phosphospecific antibodies were depleted from the serum by circulation through a column containing the nonphosphorylated antigene. The phosphospecific antibodies weresubsequently purified using a column containing the phosphorylated peptide.

Cells were lysed with M-PER buffer (Thermo) containing protease and phosphatase inhibitors (Sigma); nuclear/cytosolic fractions were isolated as above described. Proteins were separated by SDS–PAGE (Invitrogen; reduced NuPAGE 4–12% Bis-tris Gel, MES SDS buffer). If needed, the gel was stained using 20 ml Imperial Protein Stain (Thermo Fisher) at room temperature for 1 h and de-stained with water. Immunoblotting analysis was performed by transferring the protein onto a nitrocellulose membrane with an I-Blot (Invitrogen). The membrane was blocked with 5% non-fat milk in TBS-T buffer (TBS containing 0.05% Tween-20) and incubated with primary antibodies anti-FLAG and anti-TUBULIN (Sigma; 1:2000), anti-H3 (Cell Signaling; 1:10 000) at room temperature for 2 h whereas the following antibodies were incubated ON in 5% BSA: anti-TFEB (My Biosource; 1:1000), anti-P TFEB (1:1000) ERK1/2, p-ERK1/2, p-P70S6K, P70S6K (Cell Signaling; 1:1000). The membrane was washed three times with TBS-T buffer and incubated with alkaline phosphatase-conjugated IgG (Promega; 0.2 mg/ml) at room temperature for 1 h. The membrane was washed three times with TBS buffer and the

expressed proteins were visualized by adding 10 ml Western Blue Stabilized Substrate (Promega).

High content nuclear translocation assay

TFEB-GFP cells were seeded in 384-well plates, incubated for 12 hours, and treated with ten different concentrations (50000 nM, 16666,66 nM, 5555,55 nM, 1851,85 nM, 617,28 nM, 205,76 nM, 68,58 nM, 22,86 nM, 22,86 nM, 7,62 nM, and 2,54 nM) of ERK inhibitor U0126 (Sigma-Aldrich) or mTOR inhibitors Rapamycin (Sigma-Aldrich), Torin 1, and Torin 2. After 3 hours at 37°C in RPMI medium cells were washed, fixed, and stained with DAPI. For the acquisition of the images, ten pictures per each well of the 384-well plate were taken by using confocal automated microscopy (Opera high content system, Perkin Elmer). A dedicated script was developed to perform the analysis of TFEB localization on the different images (Acapella software, Perkin Elmer). The script calculates the ratio value resulting from the average intensity of nuclear TFEB-GFP fluorescence divided by the average of the cytosolic intensity of TFEB-GFP fluorescence. The results were normalized using negative (RPMI medium) and positive (HBSS starvation) control samples in the same plate. The data are represented by the percentage of nuclear translocation at the different concentrations of each compound using Prism software (GraphPad software). The EC50 for each compound was calculated using non-linear regression fitting (Prism software). Same method was used to screen a library of 145 kinase inhibitors.

Methods for cellular and a mouse model of lysosomal storage disorders experiments

Cell culture

Neuronal progenitor cells were isolated from cortices of WT and MSD pups (P0) by tissue homogenization using the neural tissue dissociation kit and separation using magnetic sorting of cells expressing the stem cell marker prominin-1 (Miltenyi Biotec Srl). Neuronal progenitor cells were maintained in ESGRO complete medium (Hyclone) in the presence of EGF and FGF2 growth factors (Prepotech). Where indicated, neural stem cells (NSCs) were differentiated by removing growth factors and incubate in ESGRO medium containing 2% of serum for at least 48h.

Mice treatment

Multiple Sulfatase Deficiency (MSD) mice were treated with placebo (n=3) or torin 2 (n=3) during 10 days (gavage-oral administration; 0.3mg torin 2/day/mouse in 50% PEG400). During the treatment period the treated mice were monitored and weighted (no weight differences were observed after treatment), and all the mice treated survived. After

the treatment liver tissues were collected and GAG accumulation was determined by alcian blue staining.

Alcian blue staining of NSCs

Neuronal progenitor cells were isolated from cortices of WT and MSD pups (P0) by using standard protocols. Neuronal stem cells (NSCs) were fixed in Methacarn (60% Methanol; 10% Acetic Acid; 30% Chloroform) for 15min at RT. After washing the cells were stained for 3 hours in 1% alcian blue pH 2.5, rinsed in 0.3% acetic acid and water and mounted in 100% for visualization.

Alcian blue staining of tissue samples

Sections of paraffin-embedded liver tissue were stained with 1% Alcian blue (Sigma-Aldrich) and counterstained with Nuclear-Fast red (Sigma-Aldrich).

Electron microscopy

Cells were washed with PBS, fixed in 0.05% glutaraldehyde, and dissolved in 0.2 M Hepes buffer (pH 7.4) for 30 min at room temperature. The cells were then post-fixed for 2 h in OsO4. After dehydration in graded series of ethanol, the cells were embedded in Epon 812 (Fluka) and polymerized at 60°C for 72 h. Thin sections were cut at the Leica EM UC6, counterstained with uranyl acetate and lead citrate.

Results

TFEB induces autophagy

(Macro)autophagy is an evolutionary conserved mechanism that targets intracytoplasmic material to lysosomes, thus providing energy supply during nutrient starvation (3). Autophagy activation during starvation is regulated by mTOR, whose activity is dependent on cellular energy needs.

As autophagy is the result of a tight partnership between autophagosomes and lysosomes (1), the applicants tested whether TFEB, a transcription factor that controls lysosomal biogenesis, regulated autophagy. As TFEB exerts a positive control on lysosomal biogenesis and function (2) and on lysosomal exocytosis (Figs 16 and 17), one would expect that TFEB overexpression should decrease the number of autophagosomes due to their increased degradation by the lysosomes. Surprisingly, stable TFEB overexpression in HeLa cells increased significantly the number of autophagosomes, as determined by using the LC3 marker, which specifically associates with autophagosomes (4-7) (Fig. 1a,b). Similar data were obtained by transient overexpression of TFEB in HeLa and Cos cells (Fig. 5). An increase in the number of autophagosomes was also detected by

electron microscopy on mouse embryonic fibroblast (MEFs) infected with a lentivirus overexpressing TFEB (Fig. 6). This increase persisted in cells treated with lysosomal inhibitors of autophagosome/LC3II degradation bafilomycin and pepstatin/E64 (8), indicating that TFEB activates the formation of autophagosomes (Fig. 1a and 7). Nutrient starvation did not further increase the number of autophagosomes in TFEB-overexpressing cells (Fig. 1a,c), suggesting a saturating effect of TFEB overexpression on autophagy and raising the possibility that TFEB may be an important mediator of starvation-induced autophagy.

Consistent with these findings, RNA interference (RNAi) of *TFEB* in HeLa cells resulted in decreased levels of LC3II both in normal and starved conditions, either in the presence or absence of bafilomycin (Fig. 1d-f). Notably, the decrease of LC3II correlated with the levels of *TFEB* downregulation achieved by the different RNAi oligos, demonstrating the specificity of the assay (Fig. 1g). These gain and loss of function data suggest that the biogeneses of autophagosomes and lysosomes are co-regulated by TFEB. The applicants next measured the rate of delivery of autophagosome to lysosome using an RFP-GFP tandem tagged LC3 protein (9), which discriminates early autophagic organelles (GFP-positive/mRFP-positive) from acidified autolysosomes (GFP-negative/mRFP-positive), as the GFP signal (but not the mRFP) is quenched inside acidic compartments (9). They found that the number of autophagolysosomes is higher in TFEB overexpressing cells compared to control cells, indicating that TFEB promotes autophagosome-lysosome fusion, thus enhancing the autophagic flux (Fig. 1h). Functional evidence of TFEB role in the regulation of autophagy came from the observation that degradation of long-lived proteins was enhanced by TFEB overexpression, and reduced by TFEB knock-down. This enhancement was abolished by the autophagy inhibitor 3-methyl adenine (3-MA) (10) (Fig. 8).

To test whether TFEB regulated the expression of autophagy genes, the applicants analyzed the mRNA levels of a group of 51 genes reported to be involved in several steps of the autophagic pathway (1, 12, 13). They observed that the enhancement of the expression levels of autophagy genes in cells overexpressing TFEB was very similar to the one obtained during starvation (HeLa cells 4h in EBSS media) (Pearson correlation: r value = 0.42; *p*value =0.001), while they were downregulated after TFEB silencing (Fig. 2a and Tables 1,2). Among them the expression of *UVRAG*, *WIPI*, *MAPLC3B*, *SQSTM1*, *VPS11*, *VPS18* and *ATG9B* was most significantly affected by TFEB overexpression (Tables 1,2). These genes are known to play a role in different steps of autophagy and

appeared to be direct targets of TFEB, as they carry at least one CLEAR site (2) in their promoters (Fig. 9). In addition, in four of these genes we validated the binding of TFEB to the target sequence by quantitative chromatin immunoprecipitation assay (QChip) (Fig. 2b). Interestingly, *VPS11*,*VPS18* and *UVRAG* play roles in autophagosome delivery to lysosomes (14), consistent with the observation of a significant enhancement of lysosome-autophagosome fusion in cells overexpressing TFEB.

These data indicate that TFEB is involved in the transcriptional regulation of starvation-induced autophagy. This conclusion is strongly bolstered by the following observations. First, nutrient starvation induced an increased binding of TFEB to the promoters of both lysosomal and autophagy genes as measured by QChIP (Fig. 2b). Second, the luciferase reporter assay (2) showed that starvation enhanced the effects of TFEB on target gene transcription (Fig. 10). Third, the expression of TFEB direct targets was upregulated in starved cells and this upregulation was inhibited by TFEB silencing (Fig. 2a,c).

Starvation regulates TFEB nuclear translocation and activity

To identify the mechanism of starvation-induced activation of TFEB, the applicants analyzed its subcellular localization and post-translational modifications in starved cells. In normal conditions TFEB is localized to the cytoplasm (2). They observed that nutrient starvation (EBSS media) rapidly induced TFEB nuclear translocation (Fig. 2d,e), and that cytosolic TFEB from starved cells appeared to have a lower molecular weight compared to that of normally fed cells, as revealed by western blot analysis (Fig. 11a). This molecular weight shift occurred rapidly but transiently and was abolished within 1h after re-adding normal media to starved cells, concomitant with a decrease of nuclear TFEB (Fig. 11a). By supplementing EBSS media either with serum, amino acids or growth factors (i.e. insulin or EGF) the applicants observed a significant inhibition of TFEB nuclear translocation compared to starved media alone (Fig. 2f). Almost no effect was observed when EBSS was supplemented with cytokines (i.e. INF or LIF) (Fig. 2f), suggesting that activation of TFEB is a process regulated by a signaling mechanism, which is sensitive to nutrient and growth factors. The applicants stimulated starved cells with normal medium supplemented with drugs inhibiting the mTOR (Rapamycin), PI3K-AKT (Triciribin) and MEK (U0126) kinases. MEKi-inhibition resulted in TFEB nuclear localization, at level similar to starvation, while AKT and mTOR inhibition had no effect (Fig. 2g and Fig. 11b). These data suggest that TFEB activity is regulated by MAP kinase, uncovering an unexpected role of this signaling pathway in the regulation of starvation-induced autophagy.

Furthermore, the expression of a constitutively active MEK (caMEK) in HeLa cells resulted in downregulation of TFEB target gene expression during starvation, thus mimicking the effect of TFEB knockdown (Fig. 2h), while caMEK overexpression in TFEB-depleted cells had no effect on the expression of TFEB target genes (Fig. 2h).

Serine phosporylation regulates TFEB activation

To analyze more in detail the relationship between MAPK signaling and TFEB, the applicants performed a mass-spectrometry analysis and identified at least three serines (i.e. S142, S332, and S402) that were phosphorylated in nutrient rich medium but not in starved medium. They mutated each of these three serines to alanines to abolish phosphorylation. Mutant TFEB proteins were individually expressed into HeLa cells and TFEB nuclear translocation analyzed. The TFEB(S142A) mutant showed a significantly increased nuclear localization compared to TFEB(WT), TFEB(S332A) and TFEB(S402A) (Fig. 3a and Fig. 12a). Conversely the phospho-mimetic mutant (TFEB S142D) was unable to translocate into the nucleus upon nutrient starvation (Fig. 12b). The S142A TFEB mutant migrates at lower molecular weight in normal but not in starved media, while the S142D mutant displayed a reduced shift during starvation compared to WT TFEB (Fig. 12c,d), further demonstrating that S142 is phosphorylated in normal but not in starved media. The expression of TFEB(S142A) resulted in increased expression levels of TFEB target genes compared to TFEB(WT), TFEB(S332A) and TFEB(S402A) (Fig. 3b). Consistently, TFEB(S142A) caused a stronger induction of the autophagic/lysosomal system, compared to wt TFEB, as demonstrated by the increased number of autophagosomes (Fig 3c and Fig. 13), lysosomes (Fig. 3d) and autophagolysosomes (Fig. 3e). Thus, TFEB nuclear translocation and activation are regulated by the phosphorylation of serine 142.

To identify the specific kinase responsible for the phosphorylation of serine 142, the applicants performed bioinformatic analyses using methods that are based on computational models built upon a set of experimentally validated phosphorylation sites (15-19) (see methods for details). Consistently with previous results, they identified the serine-specific Extracellular Regulated Kinases (ERKs) as the top-ranking candidates for the phosphorylation of serine 142 (Table 3). Interestingly, serine 142 is highly conserved in other members of the HLH-leucine zipper gene family, such as the Microphthalmia Transcription Factor (MITF) (Fig. 14), where it was found to be phosphorylated by ERK2 (20). Further evidence of ERK2-mediated TFEB phosphorylation came from ERK2-TFEB co-immunoprecipitation (Fig. 3f) in normal but not in starved media Furthermore siRNA-

mediated knock-down of ERK1/2 proteins induced TFEB nuclear translocation to a similar extent as nutrient starvation (Fig. 3h).

***In vivo* analysis of TFEB-mediated induction of autophagy**

The applicants analyzed the physiological relevance of TFEB-mediated control of the lysosomal/autophagic pathway *in vivo* in GFP-LC3 transgenic mice (11). They focused studies on the liver, due to the reported autophagic response observed in liver upon nutrient depletion. In liver, the number of GFP-positive vesicles started to increase after 24hrs of fasting, and peaked at 48hrs (see mat and methods for 48h starvation protocol) (Fig. 4a), while the transcriptional induction of both autophagic and lysosomal TFEB target genes was evident after 16 hrs of fasting (Fig. 4b). Therefore, transcriptional activation precedes autophagosome formation *in vivo*. Importantly, at 16 hrs of fasting the sub-cellular localization of TFEB was completely nuclear (Fig. 4c,d) and the level of ERK phosphorylation was reduced compared to fed animals (Fig. 4e), indicating that starvation regulates TFEB activity *in vivo*, similarly to what was observed in cultured cells.

The applicants evaluated if TFEB was sufficient to induce autophagy *in vivo* using both viral- and transgene-mediated TFEB overexpression. GFP-LC3 transgenic mice (11) were injected systemically with an adeno-associated viral (AAV) vector containing the murine *Tcfeb*cDNA tagged with an HA epitope (AAV 2/9–*Tcfeb*-HA) (Fig. 15a,b). Liver specimens from *Tcfeb*-injected animals showed a significant increase in the number of GFP positive vesicles, and this increase was further enhanced by starvation (Fig. 4e,f). In addition, liver samples from conditional *Tcfeb*-3xFLAG transgenic mice, in which transgene expression is driven by a liver-specific CRE recombinase (i.e. Albumin-CRE) (Fig. 15c), displayed a significant increase in the expression of lysosomal and autophagic genes and in the number of autophagosomes compared to control littermates (Fig. 4g,h). Together, these data point to an important role of TFEB in the transcriptional regulation of starvation-induced autophagy.

TORC1 regulates TFEB subcellular localization

TFEB subcellular localization was then analysed in HeLa and HEK-293T cells transiently transfected with a TFEB–3 x FLAG plasmid and treated overnight with inhibitors of lysosomal function. These treatments included the use of chloroquine, an inhibitor of the lysosomal pH gradient, and Salicylihalamide A (SalA) a selective inhibitor of the v-ATPase (39). Immunoblotting performed after nuclear/cytoplasmic fractionation revealed that also lysosomal stress induced nuclear translocation of exogenously expressed TFEB and that again TFEB nuclear accumulation was associated with a shift of TFEB–3 x

FLAG to a lower molecular weight, suggesting that lysosomal stress may affect TFEB phosphorylation status (Fig. 18).

Based on the observation that mTORC1 resides on the lysosomal membrane and its activity is dependent on both nutrient and lysosomal function (40, 41), the applicants postulated that the effects of lysosomal stress on TFEB nuclear translocation may be mediated by mTORC1. Consistent with this idea, chloroquine or SalA inhibited mTORC1 activity as measured by level of p-P70S6K, a known mTORC1 substrate (Fig. 19A, 41). The involvement of mTOR appears in contrast with our previous observation that Rapamycin, a known mTOR inhibitor, did not affect TFEB activity. However, recent data indicate that Rapamycin is a partial inhibitor of mTOR, as some substrates are still efficiently phosphorylated in the presence of this drug (42). Therefore, applicants used kinase inhibitors Torin 1 and Torin 2, which belong to a novel class of molecules that target the mTOR catalytic site, thereby completely inhibiting mTOR activity (42, 46, 47).

Applicants stimulated starved cells, in which TFEB is dephosphorylated and localized to the nucleus, with an amino-acid rich medium supplemented with Torin 1 (250 nM), Rapamycin (2.5 μM), or ERK inhibitor U0126 (50 μM). Stimulation of starved cells with nutrients alone induced a significant TFEB molecular weight shift and re-localization to the cytoplasm (Fig. 19B). Nutrient stimulation in the presence of the ERK inhibitor U0126 at a concentration of 50 μM induced only a partial TFEB molecular weight shift, suggesting that phosphorylation by ERK partially contributes to TFEB cytoplasmic localization. Treatment with 2.5 μM Rapamycin also resulted in a partial molecular weight shift but did not affect TFEB subcellular localization (Fig. 19B). However, Torin 1 (250 nM) treatment entirely prevented the molecular weight shift induced by nutrients and, in turn, resulted in massive TFEB nuclear accumulation.

As Torin 1 inhibits both mTORC1 and mTORC2 complexes, applicants next evaluated the contribution of each complex to TFEB regulation. Three main observations suggest that TFEB is predominantly regulated by mTORC1: (1) stimulation of starved cells with amino acids, which activate mTORC1 but not mTORC2, induced an extensive TFEB molecular weight shift, which is highly suggestive of a phosphorylation event (Fig. 19E); (2) knockdown of RagC and RagD, which mediate amino-acid signals to mTORC1, caused TFEB nuclear accumulation even in cells kept in full nutrient medium (Fig. 19F); (3) in cells with disrupted mTORC2 signalling (Sin1-/- mouse embryonic fibroblasts (MEFs)) (52-54) TFEB underwent a molecular weight shift and nuclear translocation upon Torin 1 treatment that were similar to control cells (Fig. 19G).

mTORC1 controls TFEB subcellular localization via the phosphorylation of S142

To test whether mTORC1 phosphorylates TFEB at S142, the applicants generated a phosphospecific antibody that recognizes TFEB only when phosphorylated at S142. Using this antibody, the applicantsauthors observed that TFEB was no longer phosphorylated at S142 in HeLa cells stably overexpressing TFEB–3 x FLAG and cultured in nutrient-depleted media, consistent with the applicants' results above reported (Fig. 20A).

Subsequently, they analysed the levels of S142 phosphoryation in starved cells supplemented with normal media with or without either Torin 1 or Rapamycin. While Torin 1 clearly blunted nutrient-induced S142 phosphorylation, rapamycin did not, suggesting that S142 represents a rapamycin-resistant mTORC1 site (Fig. 20A). These results clearly demonstrate that TFEB is an mTOR substrate and that S142 is a key residue for the phosphorylation of TFEB by mTOR.

Recent findings suggest that mTORC1 phosphorylates its target proteins at multiple sites (43, 44, 45). To identify additional serine residues that may be phosphorylated by mTOR, the applicants searched for consensus phosphoacceptor motif for mTORC1 (43) in the coding sequence of TFEB (Fig. 20B and C). They mutagenized all TFEB amino-acid residues that were putative mTORC1 targets into alanines. Then they tested the effects of each of these mutations on TFEB subcellular localization and found that, similarly to S142A, a serine-to-alanine mutation at position 211 (S211A) resulted in a constitutive nuclear localization of TFEB (Fig. 20D). Mutations of the other serine residues behaved similarly to the wild-type TFEB (Fig. 20D).

Together, these data indicate that, other than S142, S211 also plays a role in TFEB subcellular localization and suggest that S211 represents an additional target site of mTORC1.

The lysosome regulates gene expression in TFEB

As the interaction of TFEB with mTORC1 controls TFEB nuclear translocation, the applicants tested whether the ability of TFEB to regulate gene expression was also influenced by this interaction. The expression of several lysosomal/autophagic genes that were shown to be targets of TFEB (37) was tested in primary hepatocytes from a conditional knockout mouse line in which TFEB was deleted in the liver (Tcfebflox/flox; alb-CRE), and in a control mouse line (Tcfebflox/flox). Cells were treated with either chloroquine or Torin 1, or left untreated. These treatments inhibited mTOR as measured by the level of p-S6K, whereas the levels of p-ERK were unaffected (Fig. 21A). Primary hepatocytes isolated from TFEB conditional knockout mice cultured in regular medium did

not show significant differences in the expression levels of several TFEB target genes compared with control hepatocytes. However, while the expression of TFEB target genes was upregulated in hepatocytes from control mice after treatment with chloroquine, this upregulation was significantly blunted in hepatocytes from TFEB conditional knockout mice (Fig. 21B). Similarly, the transcriptional response upon Torin 1 treatment was significantly reduced in hepatocytes from TFEB conditional knockout mice (Fig. 21C). Together, these results indicate that TFEB plays a key role in the transcriptional response induced by the lysosome via mTOR.

Identification of additional kinase inhibitors that induce the mobilization of cytosolic TFEB to the nucleus

In order to find additional small molecules able to induce the translocation of TFEB from the cytosol to the nucleus, the applicants developed a cell-based high content assay using stable HeLa cells overexpressing TFEB fused to the green fluorescent protein (TFEB-GFP). In the assay imaging of treated cells is acquired by an automated confocal microscope (OPERA system) and the analysis of those images with Acapella image software calculates the ratio of the average of fluorescence intensity of TFEB-GFP between the cytosol and nucleus of the cell (see Materials and methods for details). To validate the assay authors tested the ERK inhibitor U0126 and the mTOR inhibitors rapamycin, torin 1 and torin 2. (Figs 19C). They tested ten concentrations for each inhibitor. The most potent compound activating TFEB nuclear translocation was Torin 1 (EC50; 147.9 nM) as well as its analogs Torin 2 (EC50; 1666 nM). The partial mTOR inhibitor rapamycin and the ERK inhibitor U016 showed EC50s of 104.3 μM and 80.4 μM, respectively (Figs 19 D). They used Torin 1 as the reference compound to perform the screening of a kinase inhibitor library of 145 compounds (SelleckChem). TFEB-GFP cells were seeded in 384-well plates, incubated for 12 h, and treated with ten different concentrations of each compound ranging from 50 μM to 2.54 nM. After 3 h at 37 °C in RPMI medium containing one of each of the compounds, the cells were washed, fixed, stained with DAPI and photographed by using confocal automated microscopy. The EC50 for each compound was calculated from the dose-response curves using Prism software as a result of 4 different runs. Active compounds are grouped in Table 4. The results clearly showed that the most enriched category of active compounds were inhibitors of the PI3K-mTOR pathway (Table 1, in bold), suggesting that this pathway represents a major player in the regulation of TFEB mobilization from cytosol to the nucleus. In addition to this category the applicantsauthors found hits belonging to inhibitors of protein tyrosine kinase

receptors (EGFR, VEGFR, PDGFR, Met, IGFR, ALK), and inhibitors of kinases involved in cell division (CDKs, Aurora, and polo-like kinases). Other represented categories were p38 kinase JAK2, JNK, GSK3, PKC, and MAPK inhibitors (Tab. 4). In the following Table 4, "A" means the compound had an EC50 equal to or less than 7000 nM; "B" means the compound had an EC50 of greater than 7000 but less than or equal to 15000; "C" means the compound had an EC50 of greater than 15000.

Table 4 Kinase inhibitors that induce the mobilization of cytosolic TFEB to the nucleus.

1. PI3K-mTOR pathway

MC Mendoza et al. The Ras-ERK and PI3K-mTOR pathways: cross-talk and compensation. (2011) Trends in Biochemical Sciences 36(6):320

Compound name	CAS No.	Structure	Target	Average EC50
MK-2206	1032350-13-2	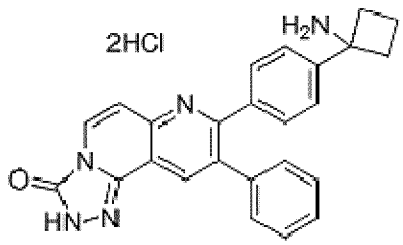	Akt	B
AT7867	857531-00-1	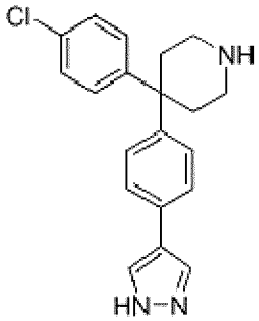	Akt	A

XL147	**956958-53-5**	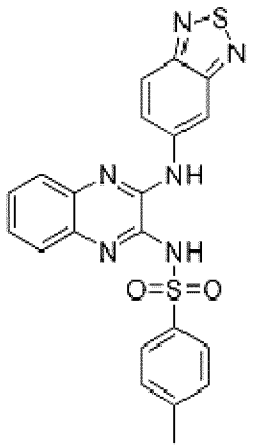	**Class I PI3K**	**A**
GDC0941	**957054-30-7**	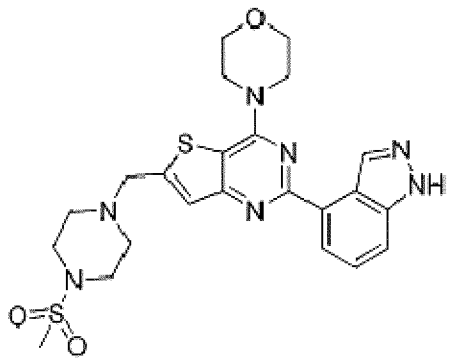	**Class I PI3K,p110a**	**B**
KU0063794	**938440-64-3**	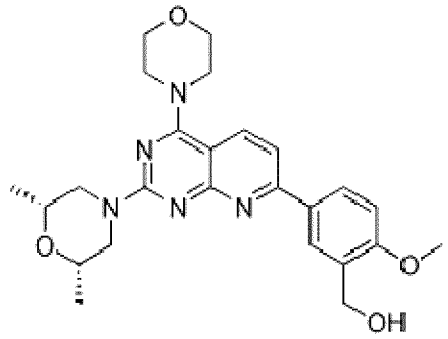	**mTOR**	**A**
WYE354	**1062169-56-5**	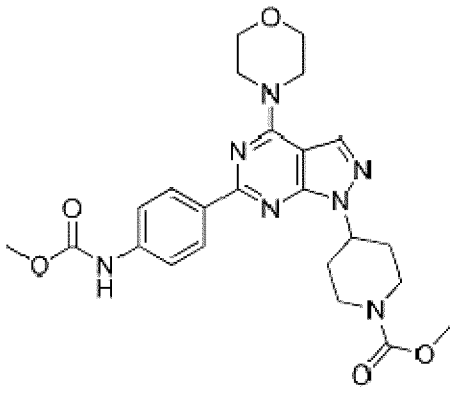	**mTOR**	**B**

Deforolimus	**572924-54-0**	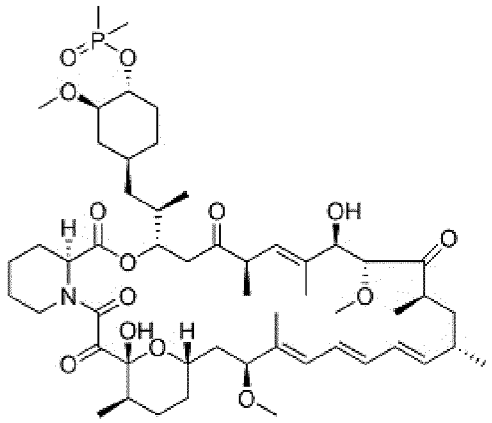	**mTOR**	**B**
TORIN 1	**1222998-36-8**	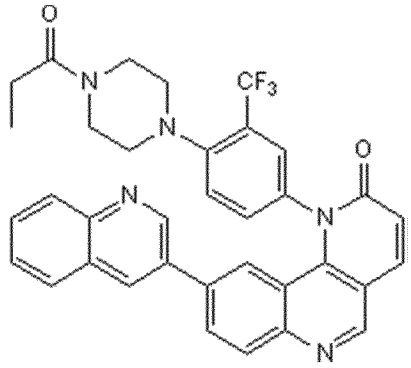	**mTOR**	**A**
TORIN 2	**1223001-51-1**	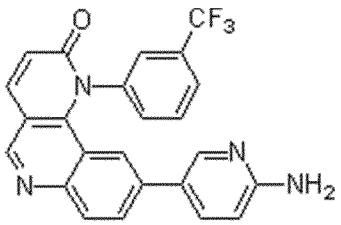	**mTOR**	**A**
RAPAMYCIN	**53123-88-9**	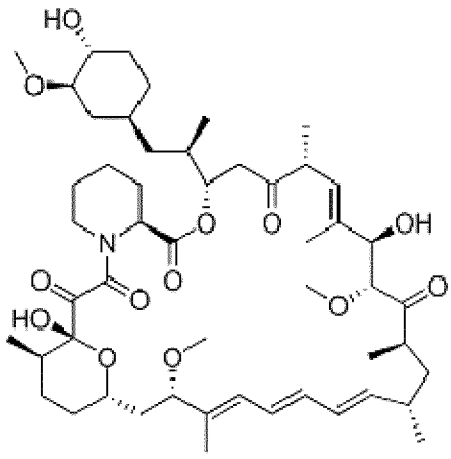	**mTOR**	**C**

Temsirolimus	**162635-04-3**	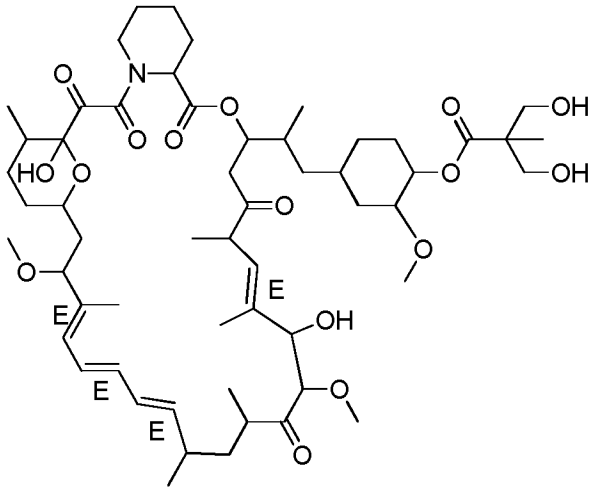	**mTOR**	**B**
Everolimus (RAD001)	**159351-69-6**	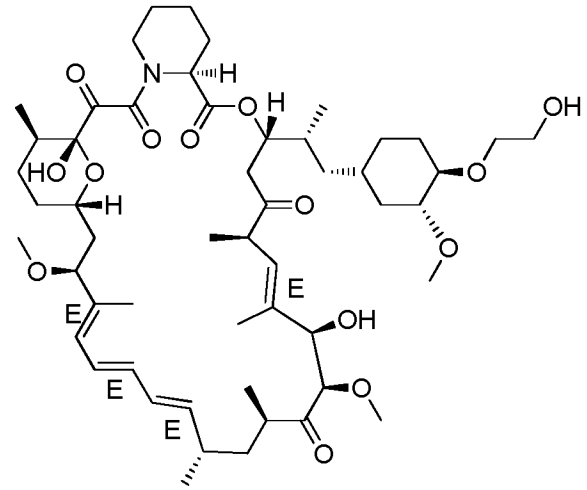	**mTOR**	**C**
Sirolimus	**53123-88-9**	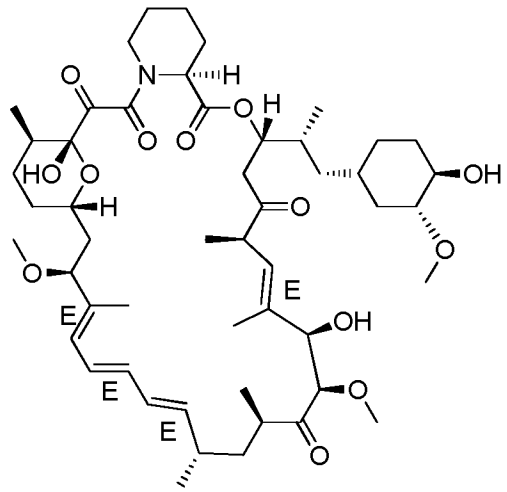	**mTOR**	**C**
GSK1059615	**958852-01-2**	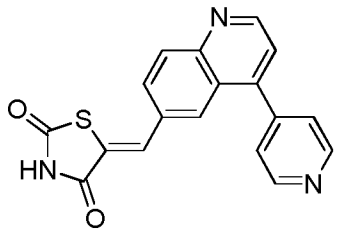	**PI3K**	**A**

NVP-BEZ235	**915019-65-7**	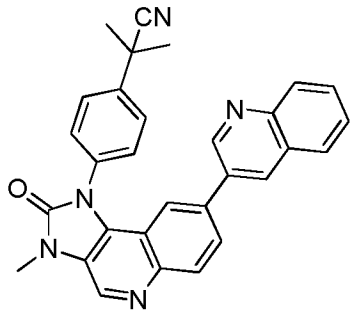	**PI3K / mTOR**	**A**
ZSTK474	**475110-96-4**	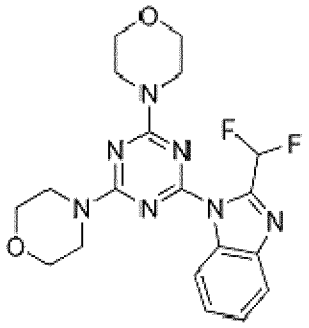	**PI3K γ**	**A**
TGX 221	**663619-89-4**	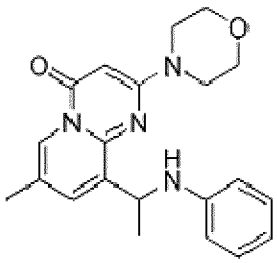	**PI3Kβ**	**A**
PIK75	**372196-77-5**	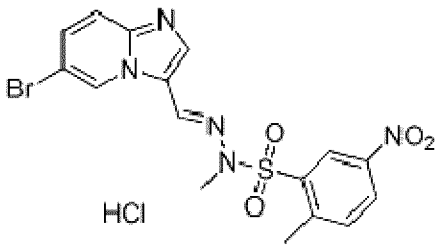	**Pan-PI3K**	**A**
PI103	**371935-74-9**	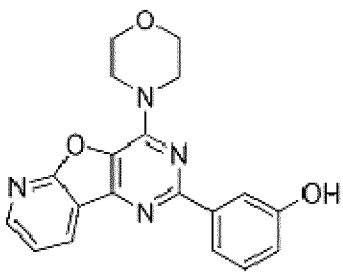	**Pan-PI3K and mTORC 1,C2**	**A**

ridaforolimus	**572924-54-0**	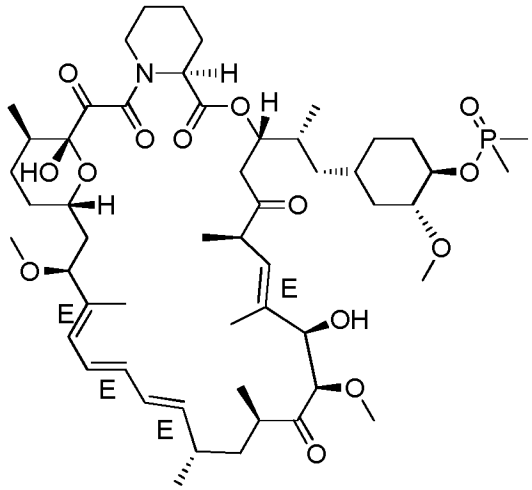	**mTOR**	**not tested**
WYE125132	**1144068-46-1**	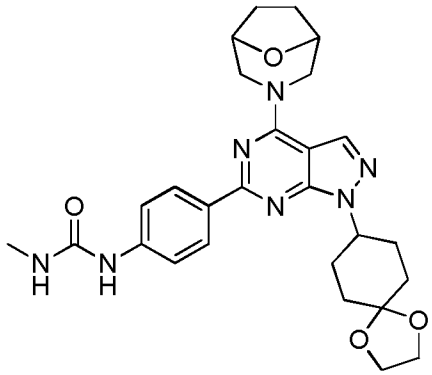	**mTOR**	**not tested**
GDC-0980	**1032754-93-0**	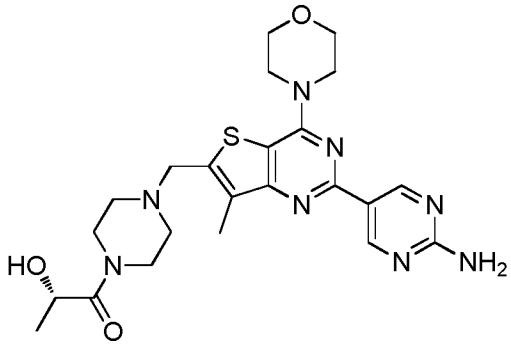	**PI3K**	**not tested**
BKM120	**944396-07-0**	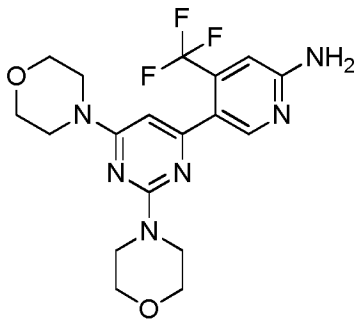	**PI3K**	**not tested**

PX866	**502632-66-8**	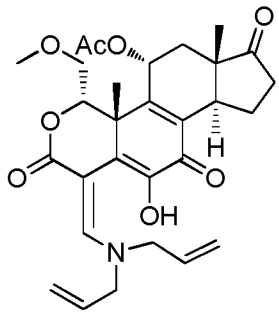	**PI3K**	**not tested**
PKI402	**1173204-81-3**	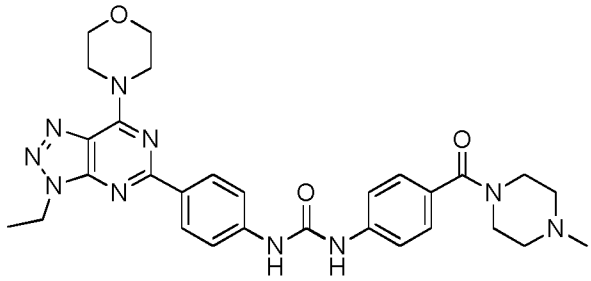	**PI3K**	**not tested**
AZD6482	**1173900-33-8**	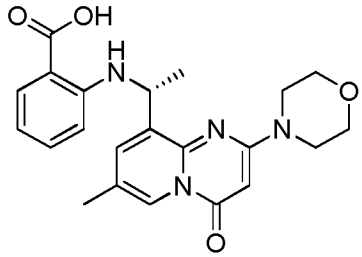	**PI3K**	**not tested**
SF1126	**936487-67-1**	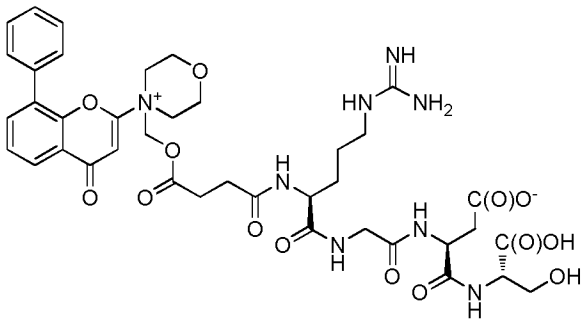	**PI3K**	**not tested**
TG100115	**677297-51-7**	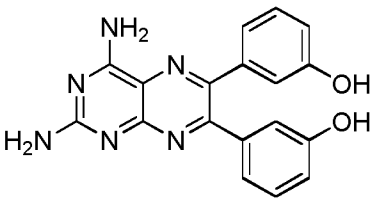	**PI3K**	**not tested**
LY294002	**154447-36-6**	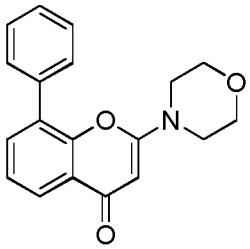	**PI3K**	**not tested**

PF04691502	**1013101-36-4**	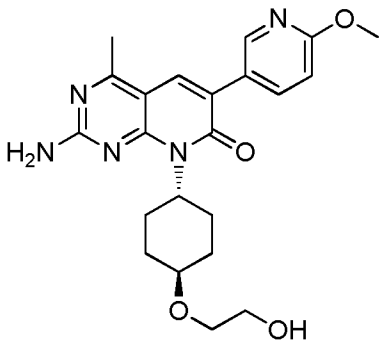	**PI3K / mTOR**	**not tested**
GSK2126458	**1086062-66-9**	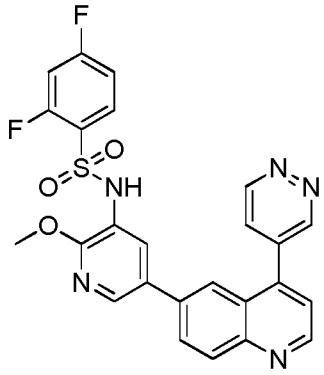	**PI3K / mTOR**	**not tested**
PF-05212384 (PKI-587)	**1197160-78-3**	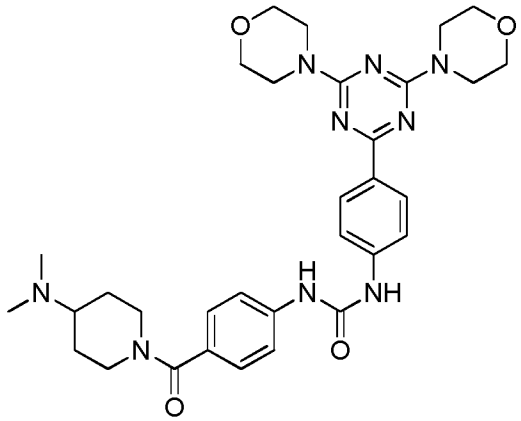	**PI3K / mTOR**	**not tested**
PP121	**1092788-83-4**	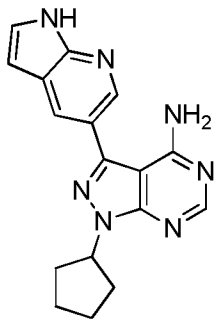	**PI3K, mTOR**	**not tested**

2. Ras-ERK pathway

MC Mendoza et al. (2011) The Ras-ERK and PI3K-mTOR pathways: cross-talk and compensation. Trends in Biochemical Sciences 36(6):320

Compound name	CAS No.	Structure	Target	Average EC50
not applicable	1173097-76-1	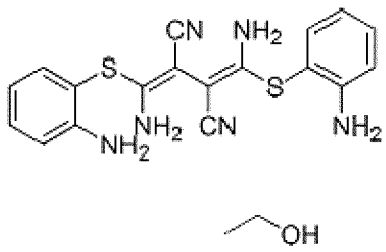	ERK	C
PD0325901	391210-10-9	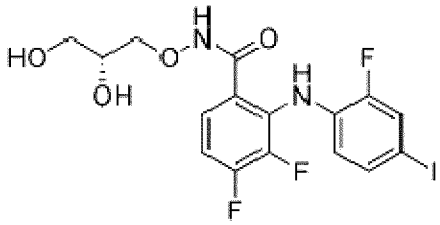	ERK	C
BIX 02188	1094614-84-2	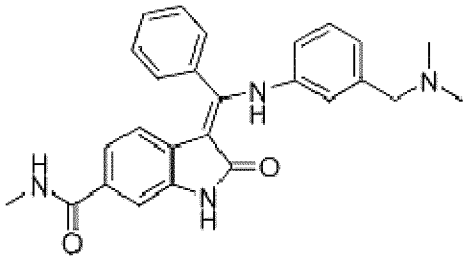	MEK	C
PD98059	167869-21-8	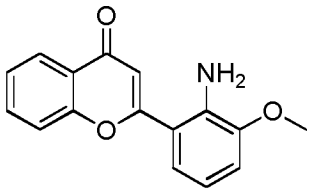	MEK	not tested
AS 703026	1236699-92-5	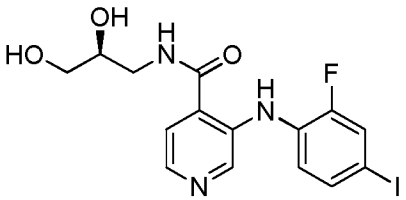	MEK	not tested
Trametinib	871700-17-3	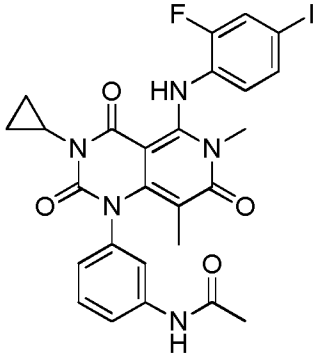	MEK	not tested

RDEA 119	**23032-37-5**	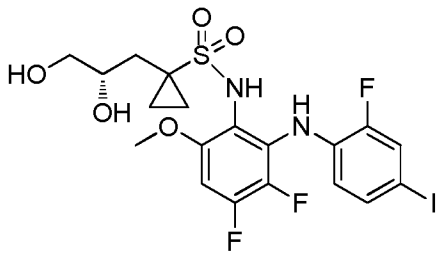	**MEK**	**not tested**
TAK 733	**1035555-63-5**	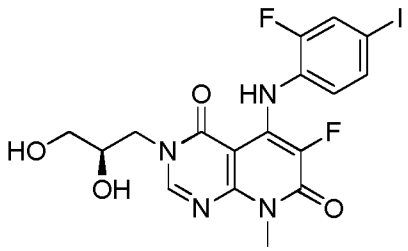	**MEK**	**not tested**
PD 184352	**212631-79-3**	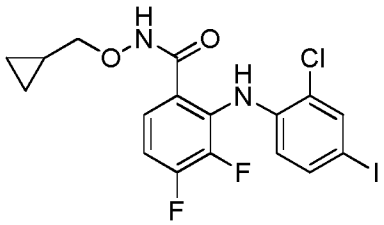	**MEK**	**not tested**
Selumetinib	**606143-52-6**	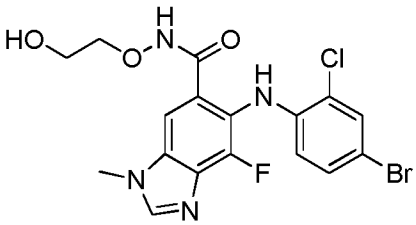	**MEK**	**not tested**
not applicable	**869357-68-6**	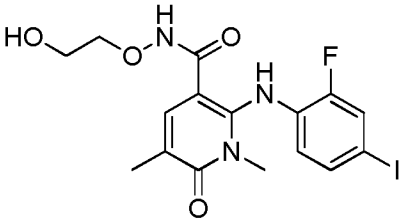	**MEK**	**not tested**
CH4987655	**874101-00-5**	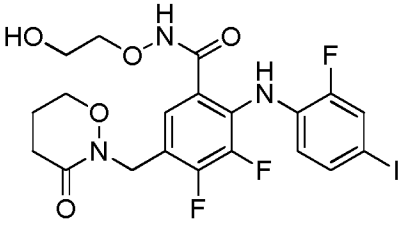	**MEK**	**not tested**

GDC 0973 (XL 518)	934660-93-2	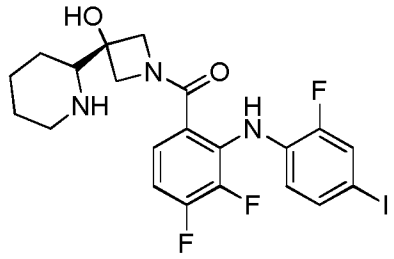	MEK	not tested
not applicable	847372-67-2	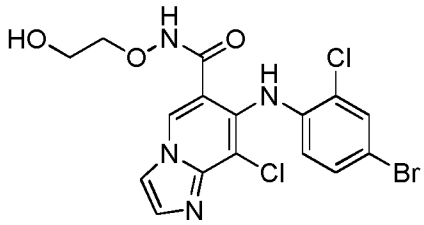	MEK	not tested
not applicable	946128-88-7	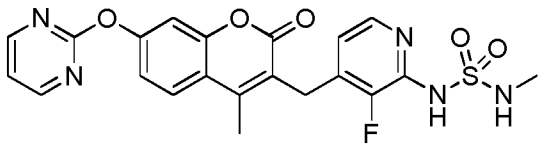	MEK	not tested
U0126	109511-58-2	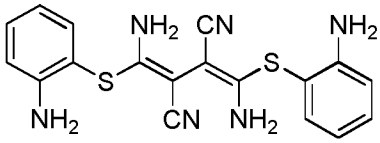	MEK	not tested
E 6201	603987-35-5	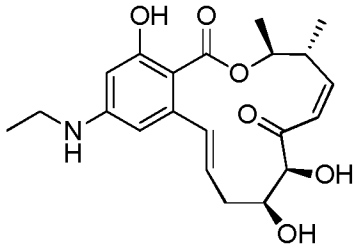	MEK	not tested

3. Other Mitogen-activated protein kinases

GL Johnson (2011) Defining MAPK Interactomes. ACS Chemical Biology 6(1):18

Compound name	CAS No.	Structure	Target	Average EC50
BIX02189	1094614-85-3	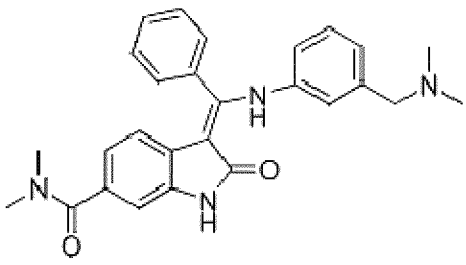	MEK5 / ERK5	B

Vinorelbine	**71486-22-1**	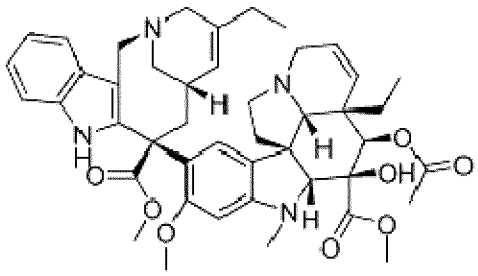	**P38 kinase**	**A**
SB203580	**152121-47-6**	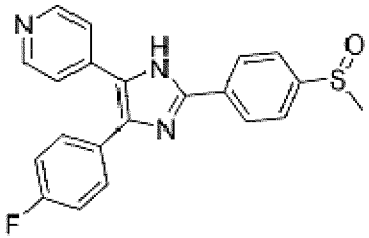	**P38 kinase**	**B**
LY2228820	**862507-23-1**	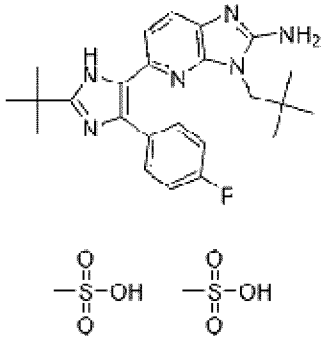	**p38 MAPK**	**A**
SP600125	**129-56-6**	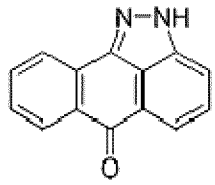	**JNK**	**C**

4) Aurora Kinase family:

G Vader and SMA Lens (2008) The Aurora kinase family in cell division and cancer. Biochimica et Biophysica Acta 1786:60

Compound name	CAS No.	Structure	Target	Average EC50
ENMD-2076	**934353-76-1**	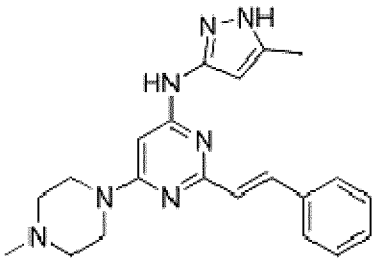	**Aurora**	**A**

Hesperadin	**422513-13-1**	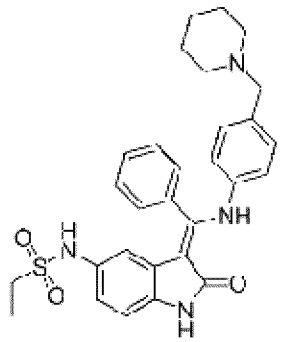	**Aurora**	**B**
JNJ-7706621	**443797-96-4**	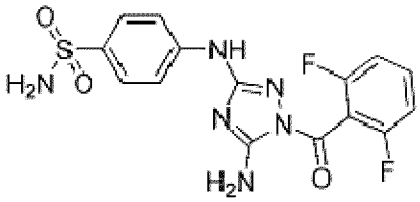	**Aurora / CDK**	**B**
CYC116	**693228-63-6**	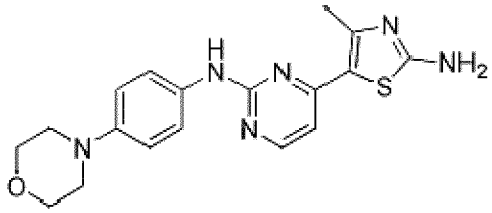	**Aurora | VEGFR-PDGFR**	**A**
Aurora A inhibitor 1	**1158838-45-9**	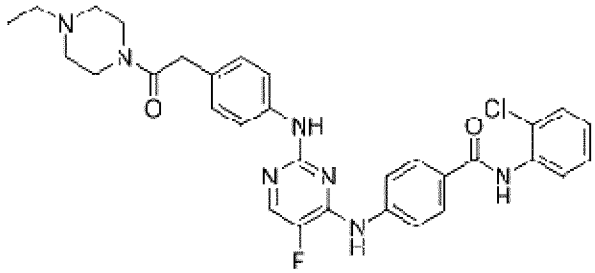	**Aurora A**	**A**
CCT129202	**942947-93-5**	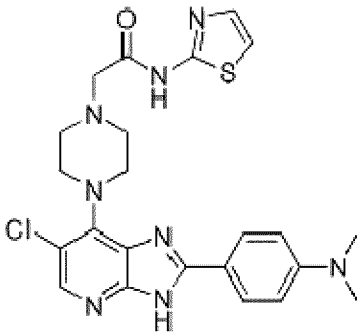	**AuroraA /B/C**	**A**

5) Receptor Tyrosine Kinases

MA Lemmon and J Schlessinger (2010) Cell Signaling by Receptor Tyrosine Kinases. Cell 141:1117

Compound name	CAS No.	Structure	Target	Average EC50
Ki8751	228559-41-9	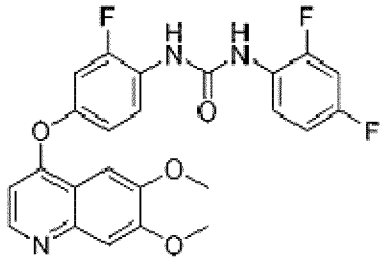	c-Kit | VEGFR-PDGFR	A
Masitinib (AB1010)	790299-79-5	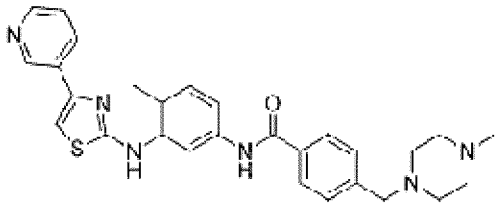	c-Kit | VEGFR-PDGFR	A
XL880 (GSK1363089)	849217-64-7	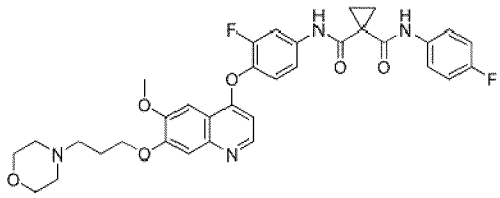	c-Met | VEGFR-PDGFR	A
CI-1033	267243-28-7	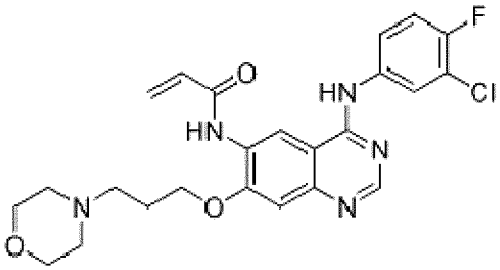	EGFR	A
Gefitinib (Iressa)	184475-35-2	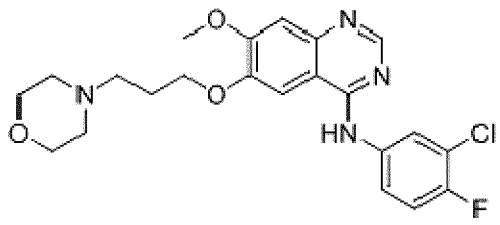	EGFR (HER)	B
Neratinib	698387-09-6	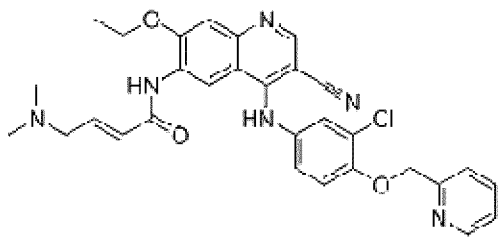	EGFR (HER)	C

AEE788	**497839-62-0**	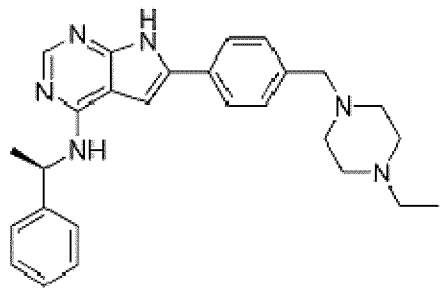	**EGFR (HER)**	**A**
BIBW2992 (Tovok)	**439081-18-2**	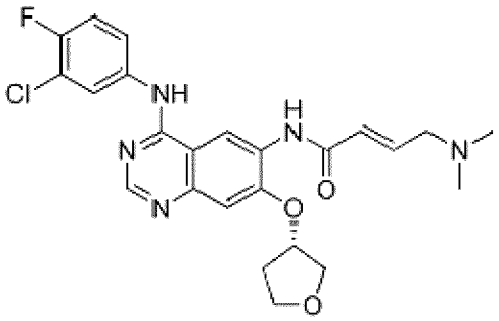	**EGFR (HER)**	**A**
Lapatinib Ditosylate	**388082-77-7**	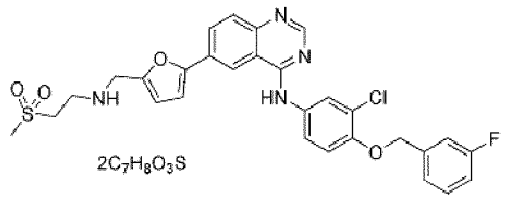	**EGFR (HER)**	**A**
WZ4002	**213269-23-8**	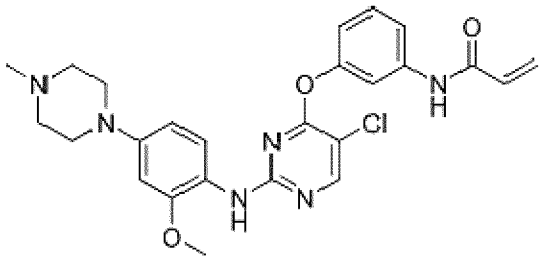	**EGFR T790M**	**B**
AP24534	**943319-70-8**	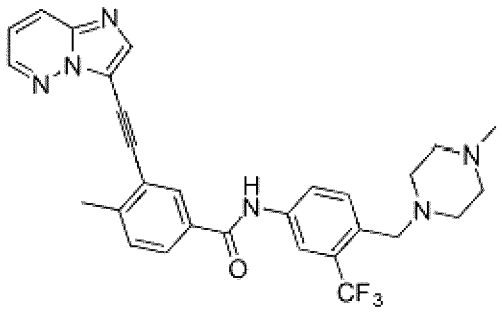	**FGFR | FLT-3 | Src-bcr-Abl | VEGFR-**	**A**

Vandetanib	**443913-73-3**	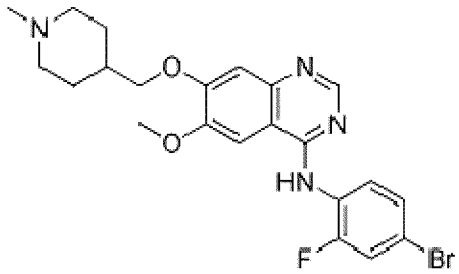	**VEGFR - EGFR**	**A**
Imatinib Mesylate STI571	**220127-57-1**	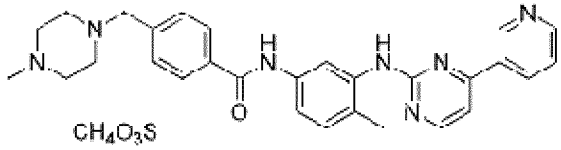	**VEGFR-PDGFR**	**A** **A**
BMS 794833	**1174046-72-0**	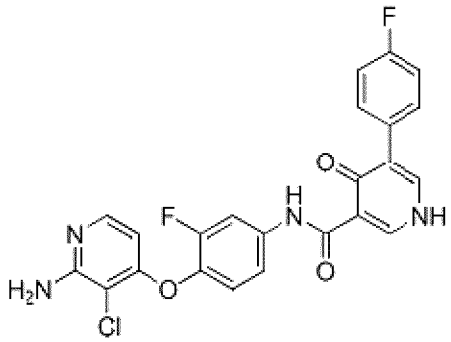	**VEGFR-PDGFR**	**B**
Cediranib (AZD2171)	**288383-20-0**	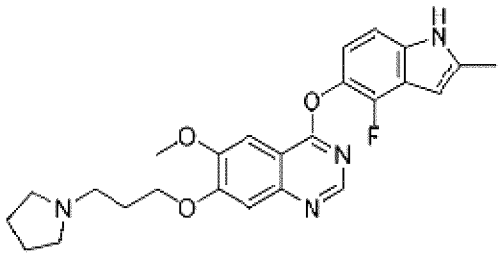	**VEGFR-PDGFR**	**A**
Sunitinib Malate	**341031-54-7**	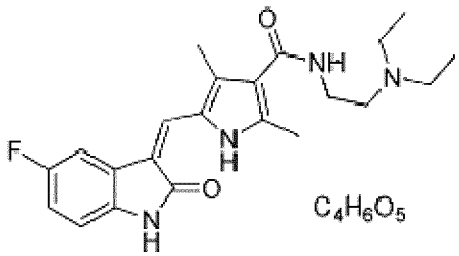	**VEGFR-PDGFR**	**A**

NVP-TAE684	**761439-42-3**	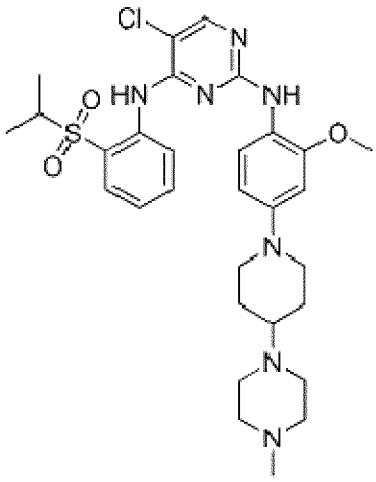	**ALK**	**A**
PF-02341066	**877399-52-5**	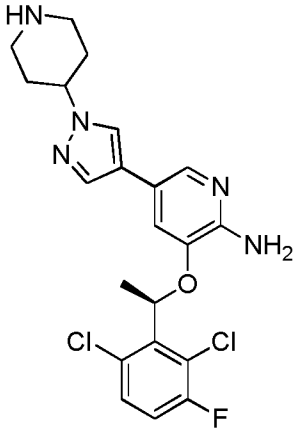	**Met kinase / ALK**	**A**
NVP-ADW742	**475488-23-4**	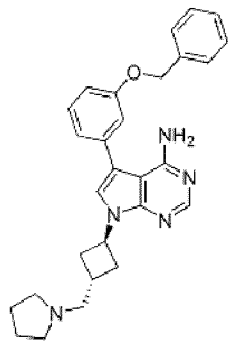	**IGFR**	**A**

6) Polo-like kinases

F Eckerdt (2005) Polo-like kinases and oncogenesis. Oncogene 24:267

Compound name	**CAS No.**	**Structure**	**Target**	**Average EC50**

BI2536	**755038-02-9**	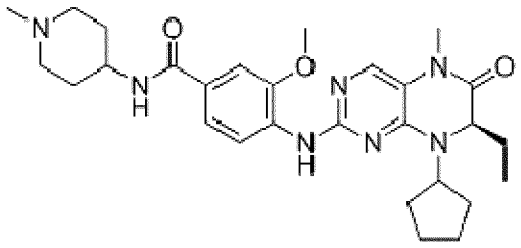	**PLK1/2/3**	**A**
GSK461364	**929095-18-1**	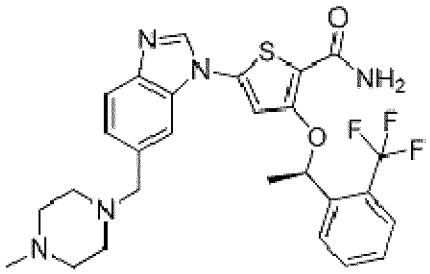	**PLK1/2/3**	**A**
KU-55933	**587871-26-9**	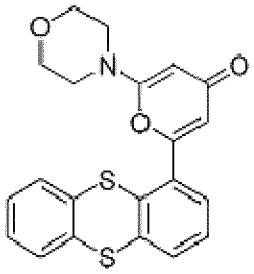	**ATM**	**A**
KU-60019	**925701-49-1**	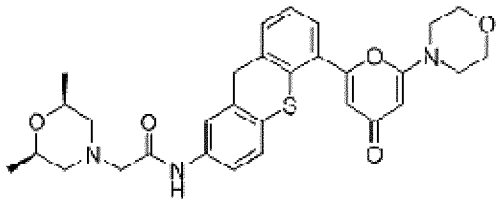	**ATM**	**C**

7) JAK-STAT pathway

SN Constantinescu (2007) Mining for JAK–STAT mutations in cancer. Trends in Biochemical Sciences 33(3):122

Compound name	**CAS No.**	**Structure**	**Target**	**Average EC50**

LY2784544	**1229236-86-5**	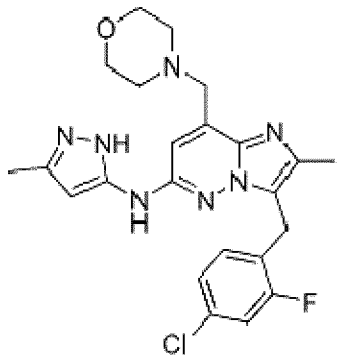	**JAK2**	**A**

8) Cyclin-dependent kinases

Ali S et al. Cancer Res. 2009 Aug 1;69(15):6208-15.

Compound name	CAS No.	Structure	Target	Average EC50
BS181	***1092443-52-1***	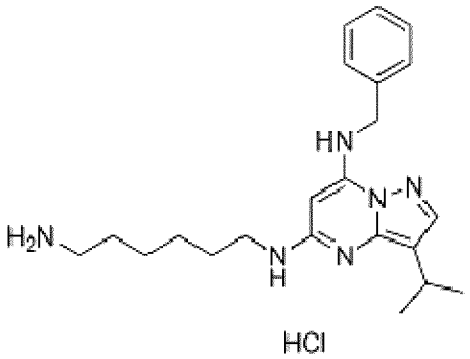	CDK2/CDK7	**A**

9) Wnt signaling pathway

J Huelsken and J Behrens (2002) The Wnt signalling pathway. J Cell Sci 115:3977

Compound name	CAS No.	Structure	Target	Average EC50
CHIR99021	**252917-06-9**	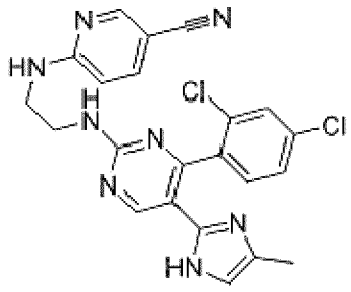	GSK-3	**A**

10) Src family kinases

SM Thomas_and JS Brugge (1997) Cellular functions regulated by Src family kinases Annu. Rev. Cell Dev. Biol 13:513

Compound name	CAS No.	Structure	Target	Average EC50
AZD0530 (Saracatinib)	***379231-04-6***	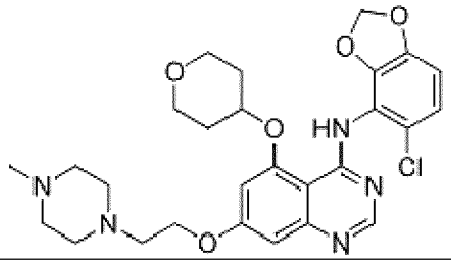	Src-bcr-Abl	**B**

11) Protein kinase C family

H MELLOR1 and PJ PARKER (1998) The extended protein kinase C superfamily. Biochem. J. 332:281

Compound name	CAS No.	Structure	Target	Average EC50
Enzastaurin	***170364-57-5***	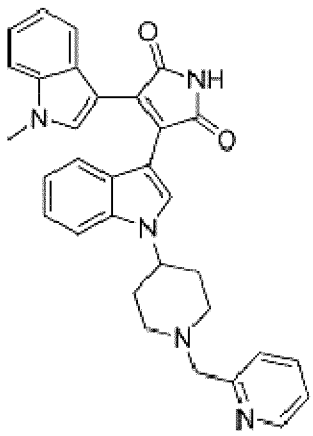	PKC BETA	**A**

Compound name	CAS No.	Structure	Target	Average EC50
Tamoxifen citrate	***54965-24-1***	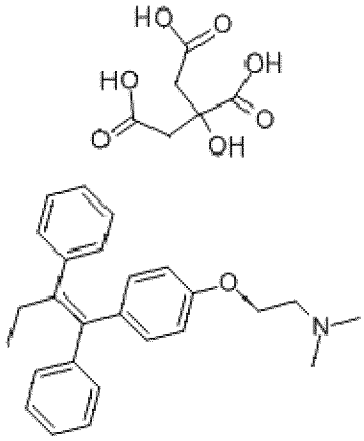	PKC	A

TFEB phosphorylation inhibitors promote cellular clearance in a cellular and a mouse model of lysosomal storage disorders.

The applicants tested whether TFEB phosphorylation inhibitors could be exploited to induce cellular clearance in Multiple Sulfatase Deficiency (MSD), a Lysosomal Storage Disorder with a severe neurodegenerative outcome due to the progressive accumulation of glycosaminoglycans (GAGs) in post-mitotic neurons and glial cells (49-51).

They evaluated the effects of Torin 1 and its analog Torin 2 on the clearance of GAGs in glia-differentiated NSCs and observed a striking reduction of alcian blue-stained GAGs (Fig. 22). Remarkably, electron microscopy analyses revealed that TFEB phosphorylation inhibitors-mediated clearance of GAGs in MSD NSCs was associated to a complete rescue of the cellular vacuolization, resulting in a normal cellular morphology (Fig. 23). Moreover, Torin 2 treatment of MSD mice resulted in a significant reduction of GAG staining also in liver as detected by alcian blue staining (Fig. 24).

Data indicate that pharmacological activation of the TFEB regulatory network can be exploited to promote cellular clearance in disorders due to the accumulation of toxic molecules, such as Lysosomal Storage Disorder and common neurodegenerative diseases.

Both transcriptional-dependent (24, 25) and independent mechanisms regulating autophagy have been described (26, 27). The study identifies novel, kinase-dependent, regulatory circuits that control multiple crucial steps of the autophagic pathway such as autophagosome formation, autophagosome-lysosome fusion and lysosome-mediated degradation of the autophagosomal content. Interestingly, the applicants observed that the

transcriptional induction of the autophagic/lysosomal genes precedes autophagosome formation. It could be envisaged that such transcriptional-dependent mechanism ensures a more prolonged and sustained activation of autophagy.

Autophagy dysfunction has been linked to several genetic disorders (28-30) and previous studies showed that enhancement of autophagy has a therapeutic effect in animal models of neurodegenerative diseases and hepatic fibrosis (29, 31, 32).

The discovery of a novel mechanism that controls, at the transcriptional level, the lysosomal-autophagic pathway suggests novel approaches to modulate cellular clearance in these diseases. Furthermore, it provides a spin-off for therapeutic approaches based on lysosomal enzymes, suggesting new strategies for increasing the productivity of cell lines producing endogeneous or recombinant lysosomal enzymes (Figs. 16 and 17). Moreover, TFEB overexpression was able to promote substrate clearance and to rescue cellular vacuolization in LSDs (Figs. 22, 23, 24), (48); thus, the identification of a phosphorylation-mediated mechanism that regulates TFEB activity offers a new tool to promote cellular clearance in health and disease.

Table 1: Gene expression changes in response to TFEB overexpression or cell starvation (Pearson Correlation 0.42)

TFEB stable OVEREXPRESSION	
GENE SYMBOL	**FOLD INCREASE**
AKT1	1.2
AMBRA1	1.2
APP	1.4
ARSA	1.3
ATG10	1.1
ATG12	1.2
ATG16L1	-1.2
ATG16L2	1.1
ATG3	1.2
ATG4A	1.2
ATG4B	1.3
ATG4C	1.1
ATG4D	1.6
ATG5	1.2
ATG7	1.2
ATG9A	1.1
ATG9B	**5.6**
BAD	1.0

CELL STARVATION	
GENE SYMBOL	**FOLD INCREASE**
AKT1	1.1
AMBRA1	1.3
APP	1.2
ARSA	1.4
ATG10	1.0
ATG12	1.2
ATG16L1	-1.5
ATG16L2	1.0
ATG3	1.0
ATG4A	-1.2
ATG4B	1.1
ATG4C	1.1
ATG4D	1.8
ATG5	1.1
ATG7	1.0
ATG9A	1.3
ATG9B	**1.8**
BAD	1.0

BAK1	1.4
BAX	1.2
BCL2	1.5
BECN1	1.2
BID	1.2
BNIP3	1.1
CLN3	1.5
CXCR4	1.3
DRAM	1.8
EIF2AK3	1.4
EIF4G1	1.3
FAM176A	1.6
GAA	1.3
GABARAP	1.1
GABARAPL1	1.0
GABARAPL2	1.1
HGS	-1.1
HTT	1.0
MAP1LC3A	1.1
MAP1LC3B	1.2
PIK3C3	-1.2
PIK3R4	1.1
PTEN	1.1
RAB24	1.2
RGS19	1.2
SNCA	1.6
SQSTM1	2.4
TP53	1.1
ULK1	1.1
UVRAG	1.8
VPS11	1.4
VPS18	1.4
WIPI	2.5

BAK1	1.0
BAX	1.1
BCL2	1.4
BECN1	1.0
BID	1.1
BNIP3	1.1
CLN3	1.2
CXCR4	1.2
DRAM	-1.3
EIF2AK3	1.2
EIF4G1	-1.2
FAM176A	-1.3
GAA	1.2
GABARAP	1.3
GABARAPL1	1.2
GABARAPL2	1.0
HGS	-1.2
HTT	1.0
MAP1LC3A	1.4
MAP1LC3B	1.2
PIK3C3	-1.2
PIK3R4	-1.2
PTEN	1.1
RAB24	1.2
RGS19	-1.2
SNCA	-1.2
SQSTM1	1.6
TP53	1.0
ULK1	2.0
UVRAG	2.4
VPS11	1.6
VPS18	1.4
WIPI	1.5

Pearson product-moment correlation coefficient (PMCC) was obtained by comparing the gene expression profiles shown, i.e. TFEB stable overexpression vs. gene expression profiles of starved HeLa cells.

Table 2: Gene expression changes in response to TFEB inhibition using siRNA

GENE SYMBOL	FOLD INCREASE
AKT1	-2.1962
AMBRA1	1.1134
APP	-1.1769

ARSA	-2.858
ATG10	1.0389
ATG12	1.0461
ATG16L1	-1.6529
ATG16L2	-1.3333
ATG3	1.2702
ATG4A	-1.3333
ATG4B	-1.244
ATG4C	-1.6077
ATG4D	-1.1527
ATG5	-1.0607
ATG7	-1.6994
ATG9A	-1.9793
ATG9B	-4.4229

BAK1	1.4489
BAX	-1.3803
BCL2	-2.3054
BECN1	-1.1769
BID	1.3241
BNIP3	-1.1212
CLN3	-1.4692
CXCR4	-1.5529
DRAM	-1.1769
EIF2AK3	-1.3996
EIF4G1	-2.3702
ESR1	-1.676
GAA	-1.3613
GABARAP	1.4093
GABARAPL1	-1.2016
GABARAPL2	1.3899
HGS	-1.5594
HTT	-1.3899
MAP1LC3A	-1.0389
MAP1LC3B	-1.4175

PIK3R4	-1.6189
PTEN	-1.2702
RAB24	1.3333

SNCA	1.2269
SQSTM1	-1.4093
TP53	-1.279
ULK1	-3.668
UVRAG	-1.3059
VPS11	-1.84
VPS18	-2.1
WIPI	-1.94

Down-regulated genes upon siRNA-mediated TFEB knock-down. Fold change represents the average of 4 independent experiments. Genes significantly down-regulated are indicated in red ($p < 0.05$).

Table 3: Prediction of S142 phosphorylation using different methods

METHODS	Cutoff	Actual prediction for S142	Group	Family	Subfamily	Kinase
CrPhos0.8	FPR ≤ 30%	MAPK8	CMGC	MAPK	JNK	MAPK8
CrPhos0.8	FPR ≤ 30%	MAPK3	CMGC	MAPK	ERK	MAPK3
CrPhos0.8	FPR ≤ 30%	MAPK1	CMGC	MAPK	ERK	MAPK1
CrPhos0.8	FPR ≤ 30%	CDK2	CMGC	CDK	CDK2	CDK2
GPS-2.1	Score ≥ 5	CMGC/CDK/CDK5	CMGC	CDK	CDK5	
GPS-2.1	Score ≥ 5	CMGC/CDK/CDK4/CDK4	CMGC	CDK	CDK4	CDK4
GPS-2.1	Score ≥ 5	CMGC/MAPK/ERK/MAPK1	CMGC	MAPK	ERK	MAPK1
GPS-2.1	Score ≥ 5	CMGC/MAPK/ERK/MAPK3	CMGC	MAPK	ERK	MAPK3
GPS-2.1	Score ≥ 5	CMGC/MAPK/JNK/MAPK8	CMGC	MAPK	JNK	MAPK8
GPS-2.1	Score ≥ 5	CMGC/MAPK/JNK/MAPK10	CMGC	MAPK	JNK	MAPK10
GPS-2.1	Score ≥ 5	STE/STE7/MAP2K7	STE	STE7	MAP2K7	
GPS-2.1	Score ≥ 5	CMGC/MAPK/p38/MAPK12	CMGC	MAPK	p38	MAPK12
PhosphoMotifFinder		GSK3	CMGC	GSK	GSK3	
PhosphoMotifFinder		ERK1	CMGC	MAPK	ERK	MAPK3
PhosphoMotifFinder		ERK2	CMGC	MAPK	ERK	MAPK1
PhosphoMotifFinder		ERK3	CMGC	MAPK	ERK	MAPK6
PhosphoMotifFinder		CDK5	CMGC	CDK	CDK5	CDK5
Networkin		p38MAPK/MAPK9	CMGC	MAPK	JNK	MAPK9

Networkin		GSK3/GSK3B	CMGC	GSK	GSK3	GSK3B
Networkin		CDK5/CDK2	CMGC	CDK	CDK2	CDK2
networkin 2		CDK2_CDK3/CDK2	CMGC	CDK	CDK2	CDK2
PHOSIDA		CK1_group	CK1	CK1		
PHOSIDA		ERK	CMGC	MAPK	ERK	

Results of the prediction of phosphorylation of S142 using five different methods. Methods are given in the first column. The second column indicates confidence score cutoff as described in methods, when available. The third column shows the actual format of prediction obtained by the corresponding method. The next four columns show the prediction in the kinase group, kinase family, kinase subfamily and kinase protein classifications, respectively.

References

1 He, C. & Klionsky, D. J. Regulation mechanisms and signaling pathways of autophagy. *Annu Rev Genet* **43**, 67-93 (2009).

2 Sardiello, M. *et al.* A gene network regulating lysosomal biogenesis and function. *Science* **325**, 473-477 (2009).

3 Lum, J. J. *et al.* Growth factor regulation of autophagy and cell survival in the absence of apoptosis. *Cell* **120**, 237-248 (2005).

4 Klionsky, D. J., Elazar, Z., Seglen, P. O. & Rubinsztein, D. C. Does bafilomycin A1 block the fusion of autophagosomes with lysosomes? *Autophagy* **4**, 849-950 (2008).

5 Xie, Z. & Klionsky, D. J. Autophagosome formation: core machinery and adaptations. *Nat Cell Biol* **9**, 1102-1109 (2007).

6 Rubinsztein, D. C. *et al.* In search of an "autophagomometer". *Autophagy* **5**, 585-589 (2009).

7 Mizushima, N., Yoshimori, T. & Levine, B. Methods in mammalian autophagy research. *Cell* **140**, 313-326 (2010).

8 Klionsky, D. J., Cuervo, A. M. & Seglen, P. O. Methods for monitoring autophagy from yeast to human. *Autophagy* **3**, 181-206 (2007).

9 Kimura, S., Noda, T. & Yoshimori, T. Dissection of the autophagosome maturation process by a novel reporter protein, tandem fluorescent-tagged LC3. *Autophagy* **3**, 452-460 (2007).

10 Bauvy, C., Meijer, A. J. & Codogno, P. Assaying of autophagic protein degradation. *Methods Enzymol* **452**, 47-61 (2009).

11 Mizushima, N., Yamamoto, A., Matsui, M., Yoshimori, T. & Ohsumi, Y. In vivo analysis of autophagy in response to nutrient starvation using transgenic mice expressing a fluorescent autophagosome marker. *Mol Biol Cell* **15**, 1101-1111 (2004).

12 Mizushima, N. Autophagy: process and function. *Genes Dev* **21**, 2861-2873 (2007).

13 Behrends, C., Sowa, M. E., Gygi, S. P. & Harper, J. W. Network organization of the human autophagy system. *Nature* **466**, 68-76 (2010).

14 Liang, C. *et al.* Beclin1-binding UVRAG targets the class C Vps complex to coordinate autophagosome maturation and endocytic trafficking. *Nat Cell Biol* **10**, 776-787 (2008).

15 Dang, T. H., Van Leemput, K., Verschoren, A. & Laukens, K. Prediction of kinase-specific phosphorylation sites using conditional random fields. *Bioinformatics* **24**, 2857-2864 (2008).

16 Xue, Y. *et al.* GPS 2.0, a tool to predict kinase-specific phosphorylation sites in hierarchy. *Mol Cell Proteomics* 7, 1598-1608 (2008).

17 Amanchy, R. *et al.* A curated compendium of phosphorylation motifs. *Nat Biotechnol* **25**, 285-286 (2007).

18 Linding, R. *et al.* Systematic discovery of in vivo phosphorylation networks. *Cell* **129**, 1415-1426 (2007).

19 Gnad, F. *et al.* PHOSIDA (phosphorylation site database): management, structural and evolutionary investigation, and prediction of phosphosites. *Genome Biol* **8**, R250 (2007).

20 Hemesath, T. J., Price, E. R., Takemoto, C., Badalian, T. & Fisher, D. E. MAP kinase links the transcription factor Microphthalmia to c-Kit signalling in melanocytes. *Nature* **391**, 298-301 (1998).

21 Kolch, W. Coordinating ERK/MAPK signalling through scaffolds and inhibitors. *Nat Rev Mol Cell Biol* **6**, 827-837 (2005).

22 Corcelle, E. *et al.* Disruption of autophagy at the maturation step by the carcinogen lindane is associated with the sustained mitogen-activated protein kinase/extracellular signal-regulated kinase activity. *Cancer Res* **66**, 6861-6870 (2006).

23 Lipinski, M. M. *et al.* A genome-wide siRNA screen reveals multiple mTORC1 independent signaling pathways regulating autophagy under normal nutritional conditions. *Dev Cell* **18**, 1041-1052 (2010).

24 Zhao, J. *et al.* FoxO3 coordinately activates protein degradation by the autophagic/lysosomal and proteasomal pathways in atrophying muscle cells. *Cell Metab* **6**, 472-483 (2007).

25 Mammucari, C. *et al.* FoxO3 controls autophagy in skeletal muscle in vivo. *Cell Metab* **6**, 458-471 (2007).

26 He, C. & Levine, B. The Beclin 1 interactome. *Curr Opin Cell Biol* **22**, 140-149 (2010).

27 Neufeld, T. P. TOR-dependent control of autophagy: biting the hand that feeds. *Curr Opin Cell Biol* **22**, 157-168 (2010).

28 Wong, E. & Cuervo, A. M. Autophagy gone awry in neurodegenerative diseases. *Nat Neurosci* **13**, 805-811 (2010).

29 Levine, B. & Kroemer, G. Autophagy in the pathogenesis of disease. *Cell* **132**, 27-42 (2008).

30 Settembre, C. *et al.* A block of autophagy in lysosomal storage disorders. *Hum Mol Genet* **17**, 119-129 (2008).

31 Hidvegi, T. *et al.* An autophagy-enhancing drug promotes degradation of mutant alpha1-antitrypsin Z and reduces hepatic fibrosis. *Science* **329**, 229-232 (2010).

32 Rubinsztein, D. C., Gestwicki, J. E., Murphy, L. O. & Klionsky, D. J. Potential therapeutic applications of autophagy. *Nat Rev Drug Discov* **6**, 304-312 (2007).

33 Fraldi, A., Hemsley, K., Crawley, A., Lombardi, A., Lau, A., Sutherland, L., Auricchio, A., Ballabio, A. and Hopwood, J.J. Functional correction of CNS lesions in an MPS-IIIA mouse model by intracerebral AAV-mediated delivery of sulfamidase and SUMF1 genes. *Hum Mol Genet,* **16,** 2693-702 (2007).

34 Ballabio A, Gieselmann V (2009) Lysosomal disorders: from storage to cellular damage. *Biochim Biophys Acta***1793:** 684-696

35 Luzio JP, Pryor PR, Bright NA (2007) Lysosomes: fusion and function. *Nat Rev Mol Cell Biol***8:** 622-632

36 Saftig P, Klumperman J (2009) Lysosome biogenesis and lysosomal membrane proteins: trafficking meets function. *Nat Rev Mol Cell Biol***10:** 623-635

37 Palmieri M, Impey S, Kang H, di Ronza A, Pelz C, Sardiello M, Ballabio A (2011) Characterization of the CLEAR network reveals an integrated control of cellular clearance pathways. *Hum Mol Genet***20:** 3852-3866

38 Pena-Llopis S, Vega-Rubin-de-Celis S, Schwartz JC, Wolff NC, Tran TA, Zou L, Xie XJ, Corey DR, Brugarolas J (2011) Regulation of TFEB and V-ATPases by mTORC1. *Embo J***30:** 3242-3258

39 Xie XS, Padron D, Liao X,Wang J, Roth MG, De Brabander JK (2004) Salicylihalamide A inhibits the V0 sector of the V-ATPase through a mechanism distinct from bafilomycin A1. J Biol Chem**279**: 19755–19763

40 Sancak Y, Bar-Peled L, Zoncu R, Markhard AL, Nada S, Sabatini DM (2010) Ragulator-Rag complex targets mTORC1 to the lysosomal surface and is necessary for its activation by amino acids. Cell**141**: 290–303

41 Zoncu R, Bar-Peled L, Efeyan A, Wang S, Sancak Y, Sabatini DM (2011a) mTORC1 senses lysosomal amino acids through an inside-out mechanism that requires the vacuolar H-ATPase. *Science***334:** 678-683

42 Thoreen CC, Kang SA, Chang JW, Liu Q, Zhang J, Gao Y, Reichling LJ, Sim T, Sabatini DM, Gray NS (2009) An ATP-competitive mammalian target of rapamycin inhibitor reveals rapamycin-resistant functions of mTORC1. *J Biol Chem***284:** 8023-8032

43 Hsu PP, Kang SA, Rameseder J, Zhang Y, Ottina KA, Lim D, Peterson TR, Choi Y, Gray NS, Yaffe MB, Marto JA, Sabatini DM (2011) The mTOR-regulated phosphoproteome reveals a mechanism of mTORC1-mediated inhibition of growth factor signaling. Science**332**: 1317–1322

44 Peterson TR, Sengupta SS, Harris TE, Carmack AE, Kang SA, Balderas E, Guertin DA, Madden KL, Carpenter AE, Finck BN, Sabatini DM (2011) mTOR complex 1 regulates lipin 1 localization to control the SREBP pathway. Cell**146**: 408–420

45 Yu Y, Yoon SO, Poulogiannis G, Yang Q, Ma XM, Villen J, Kubica N, Hoffman GR, Cantley LC, Gygi SP, Blenis J (2011) Phosphoproteomic analysis identifies Grb10 as an mTORC1 substrate that negatively regulates insulin signaling. Science 332: 1322–1326

46 Feldman ME, Apsel B, Uotila A, Loewith R, Knight ZA, Ruggero D, Shokat KM (2009) Active-site inhibitors of mTOR target rapamycin-resistant outputs of mTORC1 and mTORC2. *PLoS Biol***7:** e38

47 Garcia-Martinez JM, Moran J, Clarke RG, Gray A, Cosulich SC, Chresta CM, Alessi DR (2009) Ku-0063794 is a specific inhibitor of the mammalian target of rapamycin (mTOR). *Biochem J***421:** 29-42

48 Medina DL, Fraldi A, Bouche V, Annunziata F, Mansueto G, Spampanato C, Puri C, Pignata A, Martina JA, Sardiello M, Palmieri M, Polishchuk R, Puertollano R, Ballabio A (2011) Transcriptional activation of lysosomal exocytosis promotes cellular clearance. *Dev Cell***21:** 421-430

49 Di Graham, P.L., ed. (2002). Suzuki K: Lysosomal diseases (Hodder Arnold Publication)

50 Futerman, A.H., and van Meer, G. (2004). The cell biology of lysosomal storage disorders. Nat Rev Mol Cell Biol *5*, 554-565

51 Platt, F.M., walkley S. U. (2004). lysosomal disorders of the brain (New York, Oxford University Press

52 Frias MA, Thoreen CC, Jaffe JD, Schroder W, Sculley T, Carr SA, Sabatini DM (2006) mSin1 is necessary for Akt/PKB phosphorylation, and its isoforms define three distinct mTORC2s. *Curr Biol***16:** 1865-1870

53 Jacinto E, Facchinetti V, Liu D, Soto N, Wei S, Jung SY, Huang Q, Qin J, Su B (2006) SIN1/MIP1 maintains rictor-mTOR complex integrity and regulates Akt phosphorylation and substrate specificity. *Cell***127:** 125-137

54 Yang Q, Inoki K, Ikenoue T, Guan KL (2006) Identification of Sin1 as an essential TORC2 component required for complex formation and kinase activity. *Genes & development***20:** 2820-2832

CLAIMS

1. An inhibitor of TFEB phosphorylation for medical use.

2. The inhibitor of TFEB phosphorylation according to claim 1 acting on a kinase of the pathway of the TFEB phosphorylation.

3. The inhibitor according to claim 2 wherein the kinase is mTOR and/or PI3K.

4. The inhibitor according to claim 3 belonging to the group of compounds listed in Table 4 par.1 PI3K-mTOR pathway.

5. The inhibitor according to claim 1 or 2 acting on a kinase that directly phosphorylates TFEB molecule.

6. The inhibitor according to claim 5 inhibiting a serine specific Extracellular Regulated Kinase (ERK).

7. The inhibitor according to claim 6 wherein the ERK kinase is the ERK2 kinase.

8. The inhibitor according to claim 2 belonging to the group of compounds listed in Table 4 par. 2 Ras-ERK pathway.

9. The inhibitor according to claim 2 wherein the kinase is a Mitogen activated protein kinase.

10. The inhibitor according to claim 9 belonging to the group of compounds listed in Table 4 par. 3 of Mitogen activated protein kinases.

11. The inhibitor according to claim 2 wherein the kinase is a Aurora kinase.

12. The inhibitor according to claim 11 belonging to the group of compounds listed in Table 4 par. 4 Aurora kinases.

13. The inhibitor according to claim 2 wherein the kinase is a Receptor Tyrosine kinases.

14. The inhibitor according to claim 13 belonging to the group of compounds listed in Table 4 par. 5 Receptor Tyrosine kinases.

15. The inhibitor according to claim 2 wherein the kinase is a Polo-like kinase.

16. The inhibitor according to claim 15 belonging to the group of compounds listed in Table 4 par. 6 Polo-like kinases.

17. The inhibitor according to claim 2 wherein the kinase belongs to the JAK-STAT pathway.

18. The inhibitor according to claim 17 belonging to the group of compounds listed in Table 4 par. 7 JAK-STAT pathway.

19. The inhibitor according to claim 2 wherein the kinase is a cyclin dependent kinase.

20. The inhibitor according to claim 19 belonging to the group of compounds listed in Table 4 par. 8 cyclin dependent kinases.

21. The inhibitor according to claim 2 wherein the kinase belongs to the Wnt signaling pathway.

22. The inhibitor according to claim 21 belonging to the group of compounds listed in Table 4 par. 9 Wnt signaling pathway.

23. The inhibitor according to claim 2 wherein the kinase is a Src family kinase.

24. The inhibitor according to claim 23 belonging to the group of compounds listed in Table 4 par. 10 Src family kinases.

25. The inhibitor according to claim 2 wherein the kinase belongs to the family of Protein kinases C.

26. The inhibitor according to claim 25 belonging to the group of compounds listed in Table 4 par. 11 Proteine kinase C family.

27. The inhibitor according to any of previous claims for use in the treatment of a disorder that needs the induction of the cell authophagic/lysosomal system.

28. The inhibitor according to claim 27 for use in the treatment of any of the following pathologies: lysosomal storage disorders, neurodegenerative diseases, hepatic diseases, muscle diseases and metabolic diseases.

29. The inhibitor according to claim 28 wherein the lysosomal storage disorder belongs to the group of: activator deficiency/GM2 gangliosidosis, alpha-mannosidosis, aspartylglucosaminuria, cholesteryl ester storage disease, chronic hexosaminidase A deficiency, cystinosis, Danon disease, Fabry disease, Farber disease, fucosidosis, galactosialidosis, Gaucher disease (including Type I, Type II, and Type III), GM1 gangliosidosis (including infantile, late infantile/juvenile, adult/chronic), I-cell disease/mucolipidosis II, infantile free sialic acid storage disease/ISSD, juvenile hexosaminidase A deficiency, Krabbe disease (including infantile onset, late onset), metachromatic leukodystrophy, pseudo-Hurler polydystrohpy/mucolipidosis IIIA, MPS I Hurler syndrome, MPS I Scheie syndrome, MPS I Hurler-Scheie syndrome, MPS II Hunter syndrome, Sanfilippo syndrome type A/MPS IIIA, Sanfilippo syndrome type B/MPS IIIB, Morquio type A/MPS IVA, Morquio Type B/MPS IVB, MPS IX hyaluronidase deficiency, Niemann-Pick disease (including Type A, Type B, and Type C), neuronal ceroid lipofuscinoses (including CLN6 disease, atypical late infantile, late onset variant, early juvenile Baten-Spielmeyer-Vogt/juvenile NCL/CLN3 disease, Finnish variant late infantile CLN5, Jansky-Bielschowsky disease/late infantile CLN2/TPP1 disease, Kufs/adult-onset

NCL/CLN4 disease, northern epilepsy/variant late infantile CLN8, and Santavuori-Haltia/infantile CLN1/PPT disease), beta-mannosidosis, Pompe disease/glycogen storage disease type II, pycnodysostosis, Sandhoff disease/adult onset/GM2 gangliosidosis, Sandhoff disease/GM2 gangliosidosis infantile, Sandhoff disease/GM2 gangliosidosis juvenile, Schindler disease, Salla disease/sialic acid storage disease, Tay-Sachs/GM2 gangliosidosis, Wolman disease, Multiple Sulfatase Deficiency.

30. The inhibitor according to claim 28 wherein the hepatic disease belongs to the group of Alpha1 antitrypsin deficiency and Fatty liver disease.

31. The inhibitor according to claim 28 wherein the muscle disease belongs to the group of Autophagic Vacuolar Myopathies and X-linked myopathy with excessive autophagy.

32. The inhibitor according to claim 28 wherein the metabolic disease belongs to the group of hypercholesterolemy and fatty liver disease.

33. The inhibitor according to claim 28 wherein the neurodegenerative disease belongs to the group of Alzheimer's disease, Parkinson's disease, Huntington's disease, Creutzfeldt-Jakob disease, and spinocerebellar ataxia.

34. Use of the inhibitor according to any of claims 1 to 26 for increasing the productivity of cells producing endogeneous or recombinant lysosomal enzymes.

35. A method of producing lysosomal endogeneous or recombinant enzymes comprising: (1) contacting the inhibitor according to any of claims 1 to 26 with the autophagic/lysosomal system in a cell; (2) inducing said autophagic/lysosomal system; and (3) increasing production of said lysosomal enzymes.

36. A method of treating a disorder by administering to a subject a therapeutically effective amount of the inhibitor according to any of claims 1 to 26.

37. The method according to claim 36 wherein the disorder is alleviated by the induction of the cell authophagic/lysosomal system.

38. The method according to claim 37 wherein the disorder is selected from the group comprising lysosomal storage disorders, neurodegenerative diseases, hepatic diseases, muscle diseases and metabolic diseases.

39. The method according to claim 38 wherein the disorder is a metabolic disease where the metabolic disease is hypercholesterolemy or fatty liver disease.

40. The method according to claim 38 wherein the disorder is a neurodegenerative disease and the neurodegenerative disease is Alzheimer's disease, Parkinson's disease, Huntington's disease, Creutzfeldt-Jakob disease, or spinocerebellar ataxia.

41. The method according to claim 38 where the disorder is a lysosomal storage disorder and where the lysosomal disorder is: activator deficiency/GM2 gangliosidosis, alpha-mannosidosis, aspartylglucosaminuria, cholesteryl ester storage disease, chronic hexosaminidase A deficiency, cystinosis, Danon disease, Fabry disease, Farber disease, fucosidosis, galactosialidosis, Gaucher disease (including Type I, Type II, and Type III), GM1 gangliosidosis (including infantile, late infantile/juvenile, adult/chronic), I-cell disease/mucolipidosis II, infantile free sialic acid storage disease/ISSD, juvenile hexosaminidase A deficiency, Krabbe disease (including infantile onset, late onset), metachromatic leukodystrophy, pseudo-Hurler polydystrohpy/mucolipidosis IIIA, MPS I Hurler syndrome, MPS I Scheie syndrome, MPS I Hurler-Scheie syndrome, MPS II Hunter syndrome, Sanfilippo syndrome type A/MPS IIIA, Sanfilippo syndrome type B/MPS IIIB, Morquio type A/MPS IVA, Morquio Type B/MPS IVB, MPS IX hyaluronidase deficiency, Niemann-Pick disease (including Type A, Type B, and Type C), neuronal ceroidlipofuscinoses (including CLN6 disease, atypical late infantile, late onset variant, early juvenile Baten-Spielmeyer-Vogt/juvenile NCL/CLN3 disease, Finnish variant late infantile CLN5, Jansky-Bielschowsky disease/late infantile CLN2/TPP1 disease, Kufs/adult-onset NCL/CLN4 disease, northern epilepsy/variant late infantile CLN8, and Santavuori-Haltia/infantile CLN1/PPT disease), beta-mannosidosis, Pompe disease/glycogen storage disease type II, pycnodysostosis, Sandhoff disease/adult onset/GM2 gangliosidosis, Sandhoff disease/GM2 gangliosidosis infantile, Sandhoff disease/GM2 gangliosidosis juvenile, Schindler disease, Salla disease/sialic acid storage disease, Tay-Sachs/GM2 gangliosidosis, Wolman disease, Multiple Sulfatase Deficiency,.

42. The method according to claim 38 wherein the disorder is a hepatic disease and the hepatic disease is Alpha1 antitrypsin deficiency or Fatty liver disease.

43. The method according to claim 38 wherein the disorder is muscle disease and the muscle disease is Autophagic Vacuolar Myopathies or X-linked myopathy with excessive autophagy.

44. A method of treating a disorder comprising the steps of: (1) administering an inhibitor according to any of claims 1 to 26; (2) inducing the autophagic/lysosomal system in a cell; and (3) increasing cellular clearance.

Fig. 1

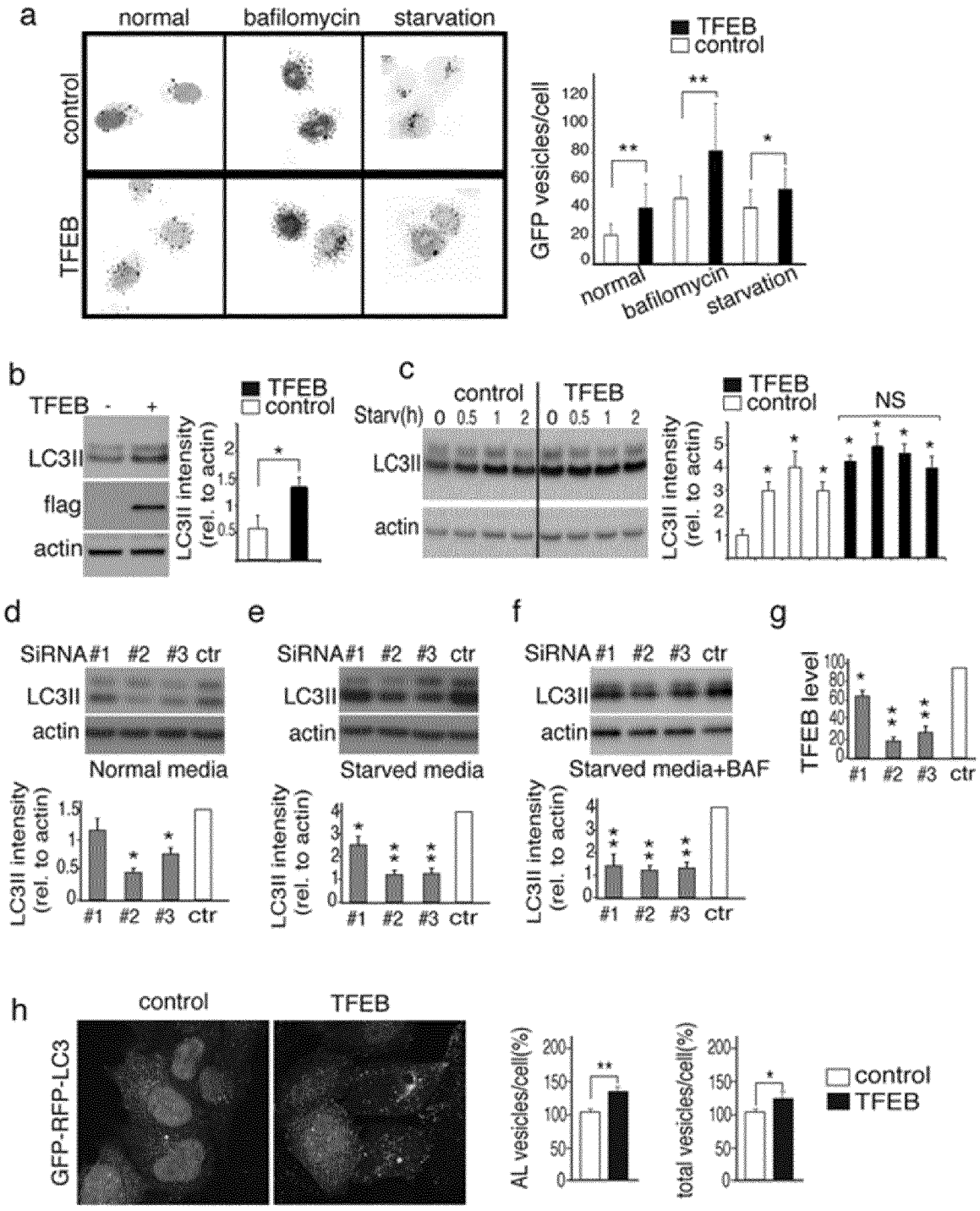
a
normal
bafilomycin
starvation
control
TFEB
TFEB
control
GFP vesicles/cell
normal
bafilomycin
starvation
b
TFEB
LC3II
flag
actin
LC3II intensity (rel. to actin)
c
control
TFEB
Starv(h) 0 0.5 1 2 0 0.5 1 2
LC3II
actin
NS
d
SiRNA #1 #2 #3 ctr
LC3II
actin
Normal media
e
Starved media
f
Starved media+BAF
g
TFEB level
h
control
TFEB
GFP-RFP-LC3
AL vesicles/cell(%)
total vesicles/cell(%)

Fig. 2

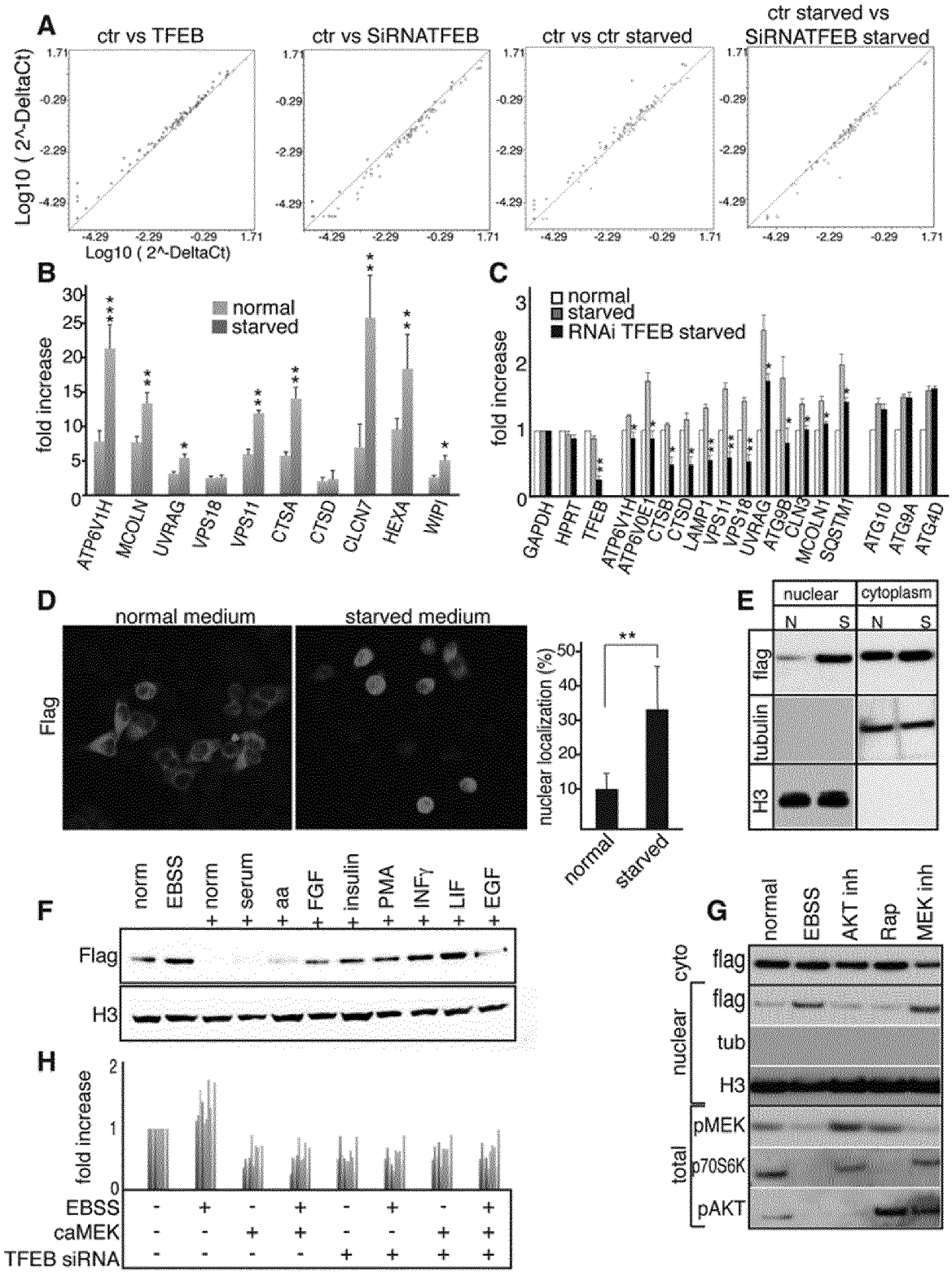
A
ctr vs TFEB
ctr vs SiRNATFEB
ctr vs ctr starved
ctr starved vs SiRNATFEB starved
Log10 (2^-DeltaCt)
B
fold increase
normal
starved
ATP6V1H
MCOLN
UVRAG
VPS18
VPS11
CTSA
CTSD
CLCN7
HEXA
WIPI
C
normal
starved
RNAi TFEB starved
GAPDH
HPRT
TFEB
ATP6V1H
ATP6V0E1
CTSB
CTSD
LAMP1
VPS11
VPS18
UVRAG
ATG9B
CLN3
MCOLN1
SQSTM1
ATG10
ATG9A
ATG4D
D
normal medium
starved medium
Flag
nuclear localization (%)
normal
starved
E
nuclear
cytoplasm
N
S
flag
tubulin
H3
F
norm
EBSS
+ serum
+ aa
+ FGF
+ insulin
+ PMA
+ INFγ
+ LIF
+ EGF
Flag
H3
G
normal
EBSS
AKT inh
Rap
MEK inh
cyto
nuclear
total
flag
tub
H3
pMEK
p70S6K
pAKT
H
fold increase
EBSS
caMEK
TFEB siRNA

Fig. 3

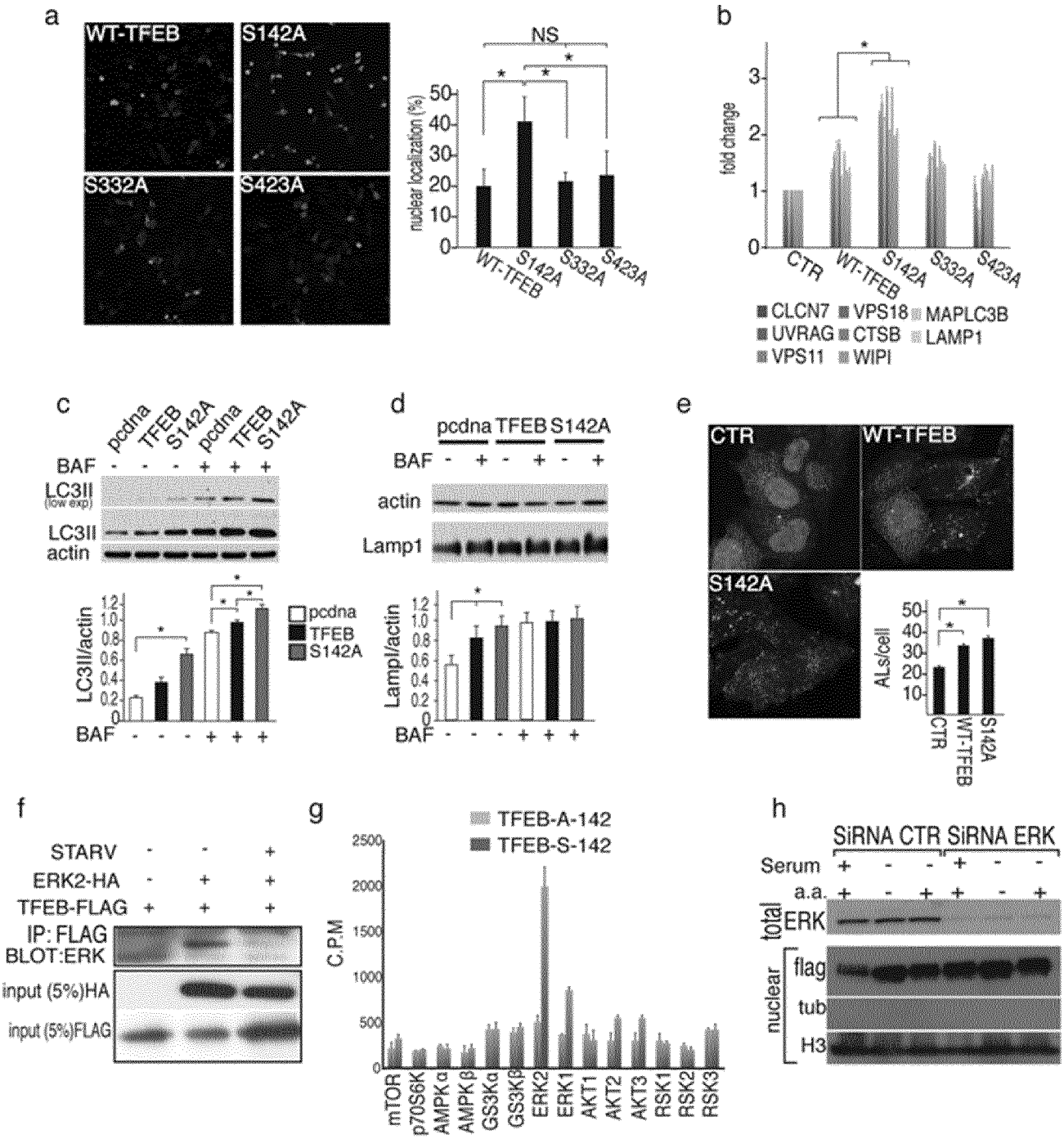
a
WT-TFEB
S142A
S332A
S423A
NS
nuclear localization (%)
WT-TFEB
S142A
S332A
S423A
b
fold change
CTR
WT-TFEB
S142A
S332A
S423A
CLCN7
VPS18
MAPLC3B
UVRAG
CTSB
LAMP1
VPS11
WIPI
c
pcdna
TFEB
S142A
BAF
LC3II (low exp)
LC3II
actin
LC3II/actin
d
pcdna TFEB S142A
BAF
actin
Lamp1
Lamp1/actin
e
CTR
WT-TFEB
S142A
ALs/cell
f
STARV
ERK2-HA
TFEB-FLAG
IP: FLAG
BLOT:ERK
input (5%)HA
input (5%)FLAG
g
TFEB-A-142
TFEB-S-142
C.P.M
mTOR
p70S6K
AMPKα
AMPKβ
GS3Kα
GS3Kβ
ERK2
ERK1
AKT1
AKT2
AKT3
RSK1
RSK2
RSK3
h
SiRNA CTR SiRNA ERK
Serum
a.a.
total
ERK
nuclear
flag
tub
H3

Fig. 4

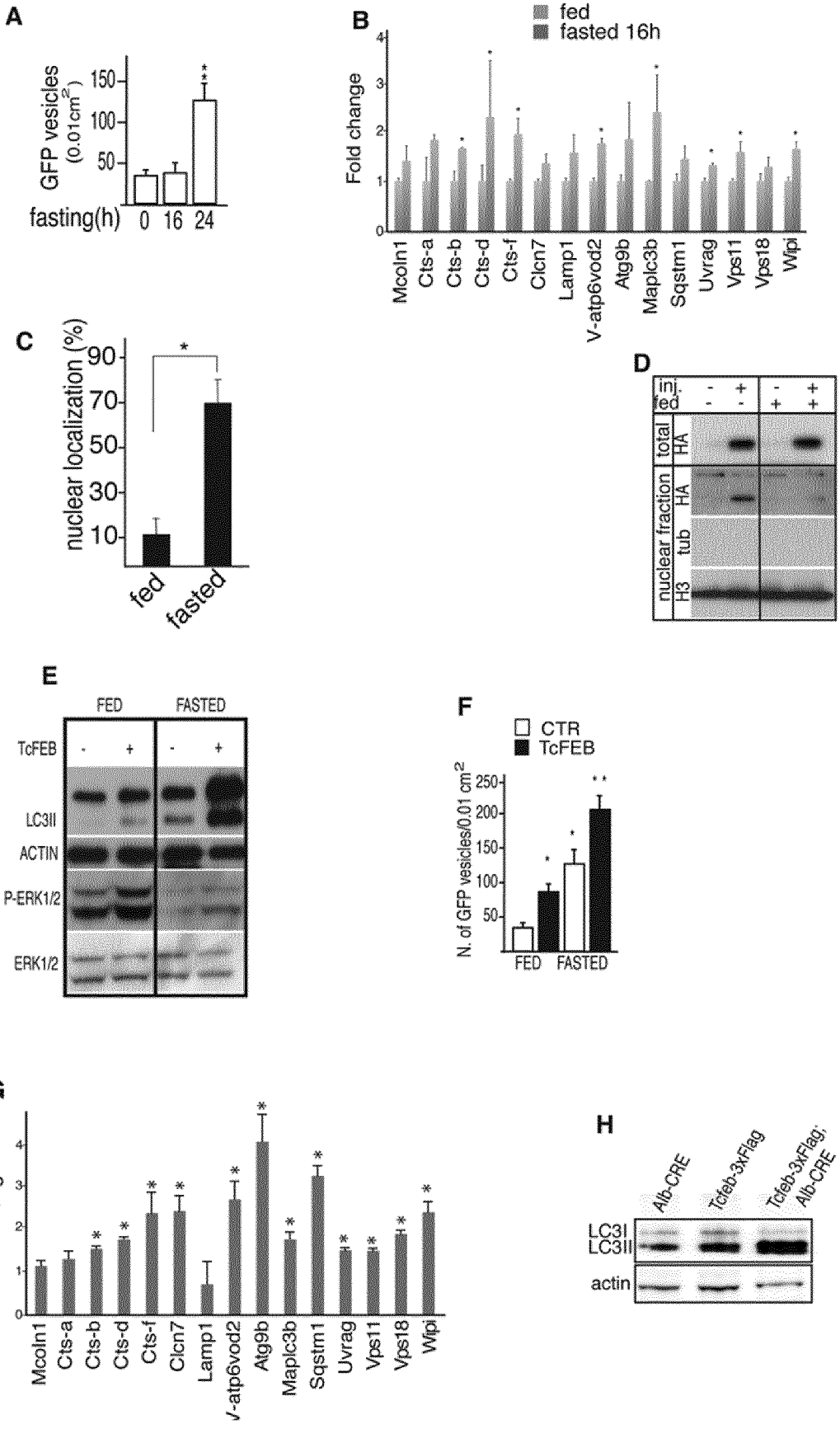
A
GFP vesicles (0.01cm2)
150
100
50
fasting(h) 0 16 24
B
fed
fasted 16h
Fold change
Mcoln1
Cts-a
Cts-b
Cts-d
Cts-f
Clcn7
Lamp1
V-atp6vod2
Atg9b
Maplc3b
Sqstm1
Uvrag
Vps11
Vps18
Wipi
C
nuclear localization (%)
90
70
50
30
10
fed
fasted
D
inj.
fed
total
HA
nuclear fraction
HA
tub
H3
E
FED
FASTED
TcFEB
LC3II
ACTIN
P-ERK1/2
ERK1/2
F
CTR
TcFEB
N. of GFP vesicles/0.01 cm2
250
200
150
100
50
FED
FASTED
G
Fold change
Mcoln1
Cts-a
Cts-b
Cts-d
Cts-f
Clcn7
Lamp1
V-atp6vod2
Atg9b
Maplc3b
Sqstm1
Uvrag
Vps11
Vps18
Wipi
H
Alb-CRE
Tcfeb-3xFlag
Tcfeb-3xFlag; Alb-CRE
LC3I
LC3II
actin

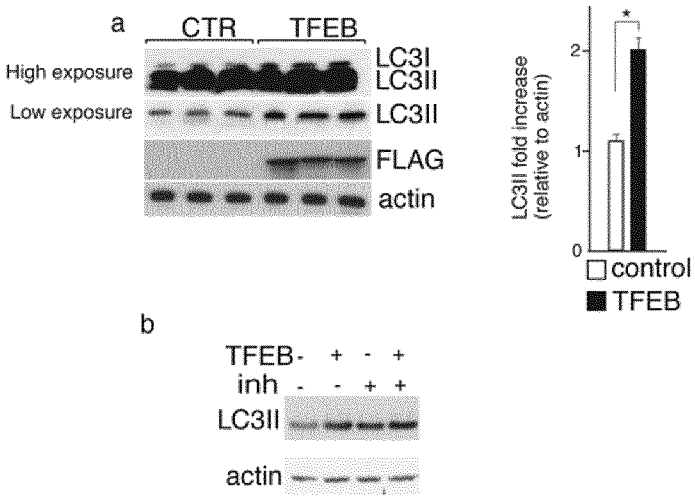
a
CTR
TFEB
High exposure
Low exposure
LC3I
LC3II
LC3II
FLAG
actin
LC3II fold increase (relative to actin)
2
1
0
*
control
TFEB
b
TFEB - + - +
inh - - + +
LC3II
actin

Fig. 5

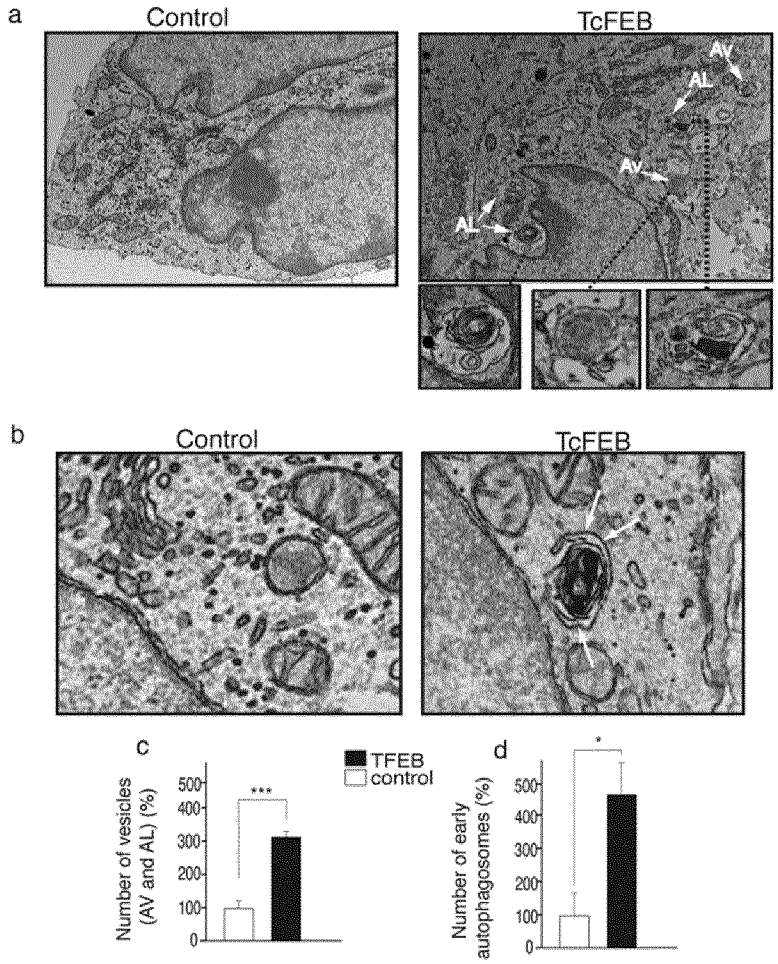
a
Control
TcFEB
AV
AL
Av
AL
b
Control
TcFEB
c
TFEB
control
Number of vesicles (AV and AL) (%)
500
400
300
200
100
0
***
d
Number of early autophagosomes (%)
500
400
300
200
100
0
*

Fig. 6

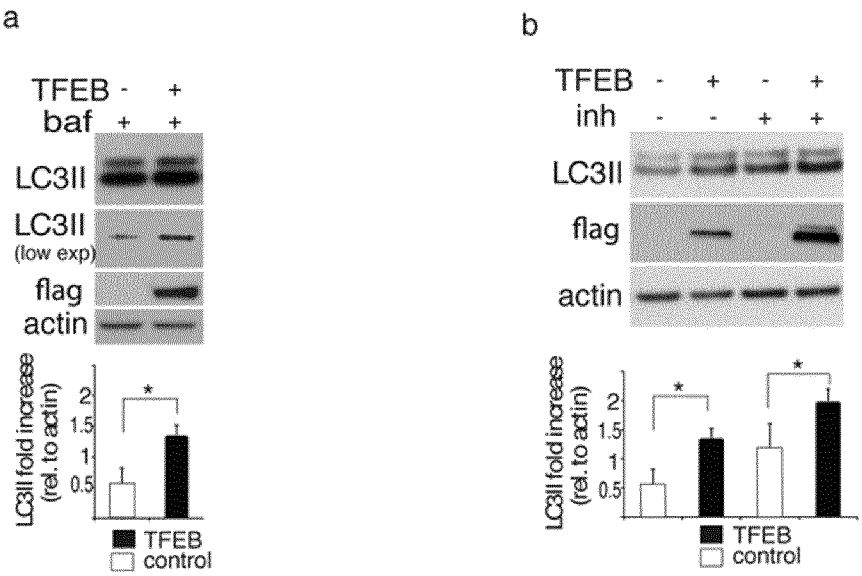
a
TFEB - +
baf + +
LC3II
LC3II
(low exp)
flag
actin
LC3II fold increase
(rel. to actin)
2
1.5
1
0.5
*
TFEB
control
b
TFEB - + - +
inh - - + +
LC3II
flag
actin
LC3II fold increase
(rel. to actin)
2
1.5
1
0.5
*
*
TFEB
control

Fig. 7

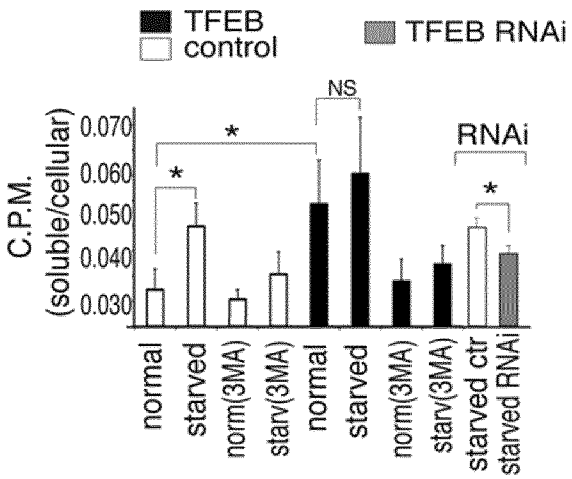
TFEB
control
TFEB RNAi
C.P.M.
(soluble/cellular)
0.070
0.060
0.050
0.040
0.030
*
*
NS
RNAi
*
normal
starved
norm(3MA)
starv(3MA)
normal
starved
norm(3MA)
starv(3MA)
starved ctr
starved RNAi

Fig. 8

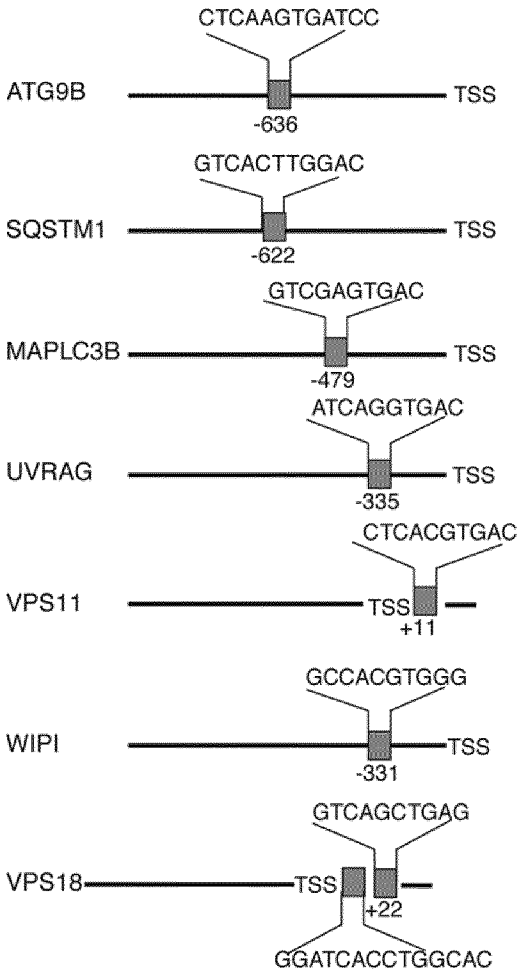
CTCAAGTGATCC
ATG9B
TSS
-636
GTCACTTGGAC
SQSTM1
TSS
-622
GTCGAGTGAC
MAPLC3B
TSS
-479
ATCAGGTGAC
UVRAG
TSS
-335
CTCACGTGAC
VPS11
TSS
+11
GCCACGTGGG
WIPI
TSS
-331
GTCAGCTGAG
VPS18
TSS
+22
GGATCACCTGGCAC

Fig. 9

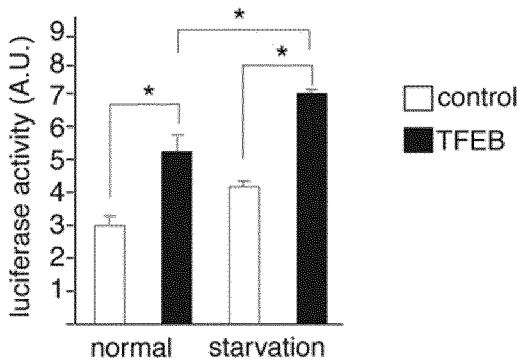
luciferase activity (A.U.)
9
8
7
6
5
4
3
2
1
*
*
*
normal
starvation
control
TFEB

Fig. 10

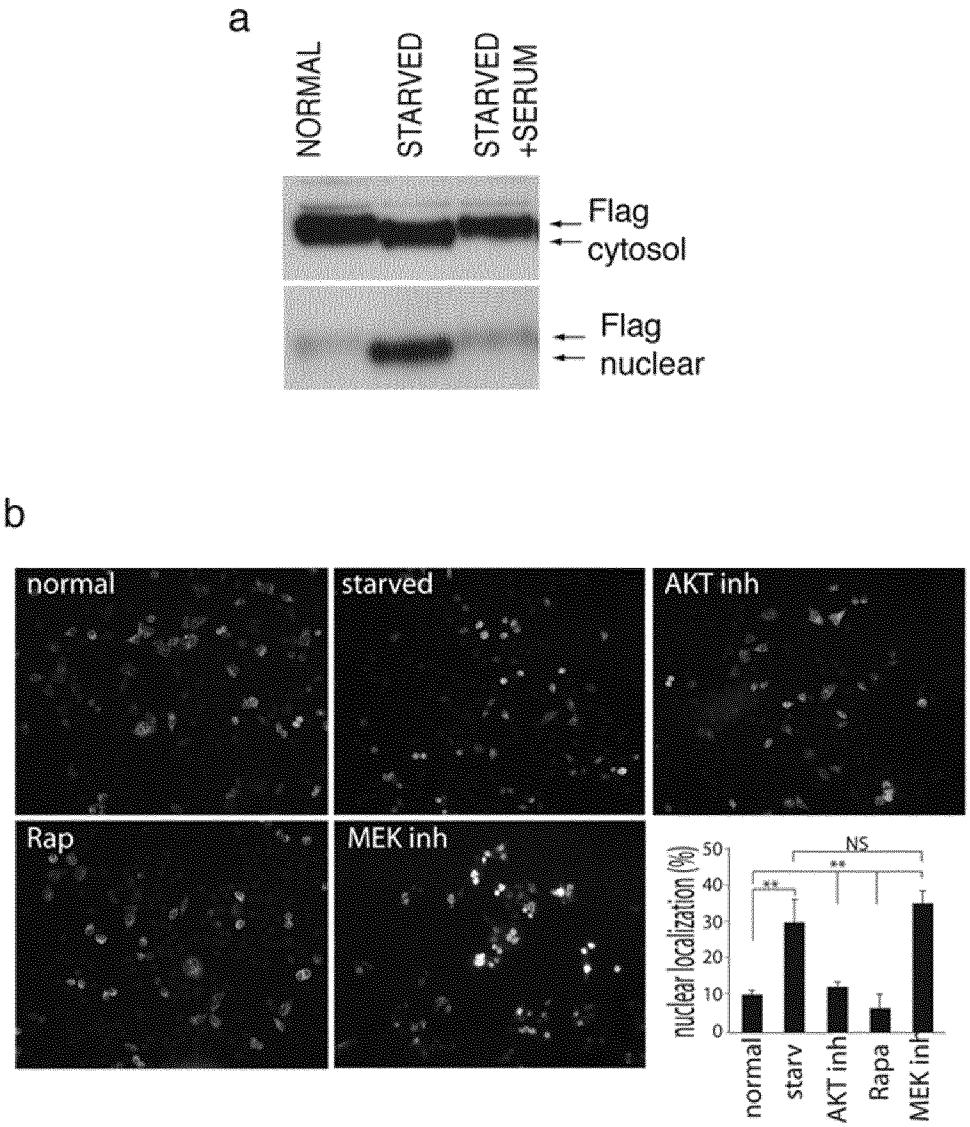
a
NORMAL
STARVED
STARVED +SERUM
Flag cytosol
Flag nuclear
b
normal
starved
AKT inh
Rap
MEK inh
nuclear localization (%)
NS
**
**
normal
starv
AKT inh
Rapa
MEK inh

Fig. 11

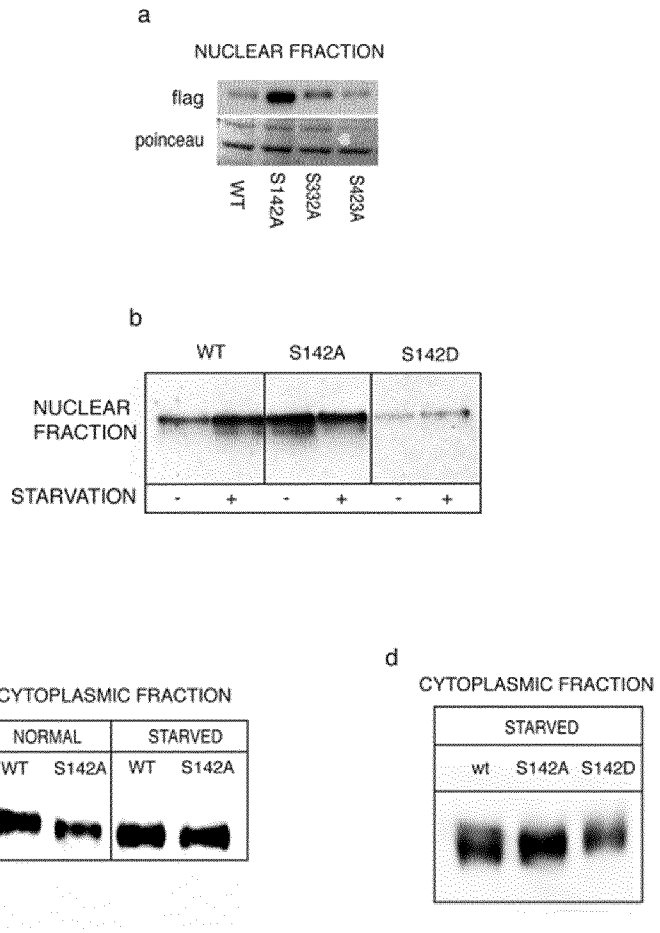
a
NUCLEAR FRACTION
flag
poinceau
WT
S142A
S332A
S423A
b
WT
S142A
S142D
NUCLEAR FRACTION
STARVATION
- + - + - +
c
CYTOPLASMIC FRACTION
NORMAL
STARVED
WT S142A WT S142A
d
CYTOPLASMIC FRACTION
STARVED
wt S142A S142D

Fig. 12

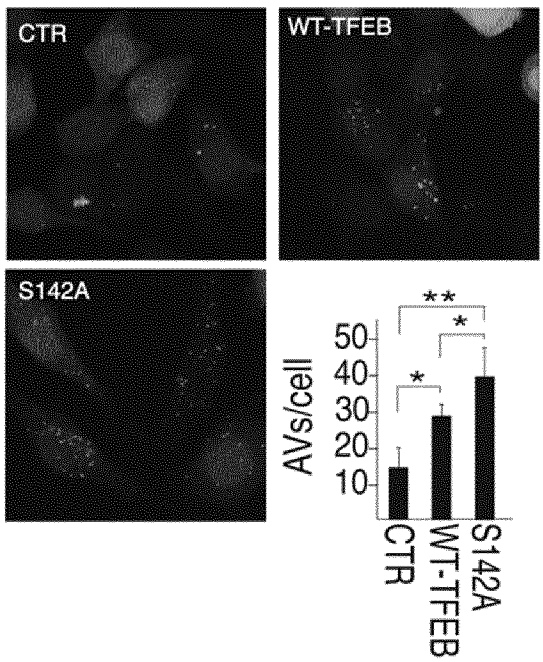

Fig. 13

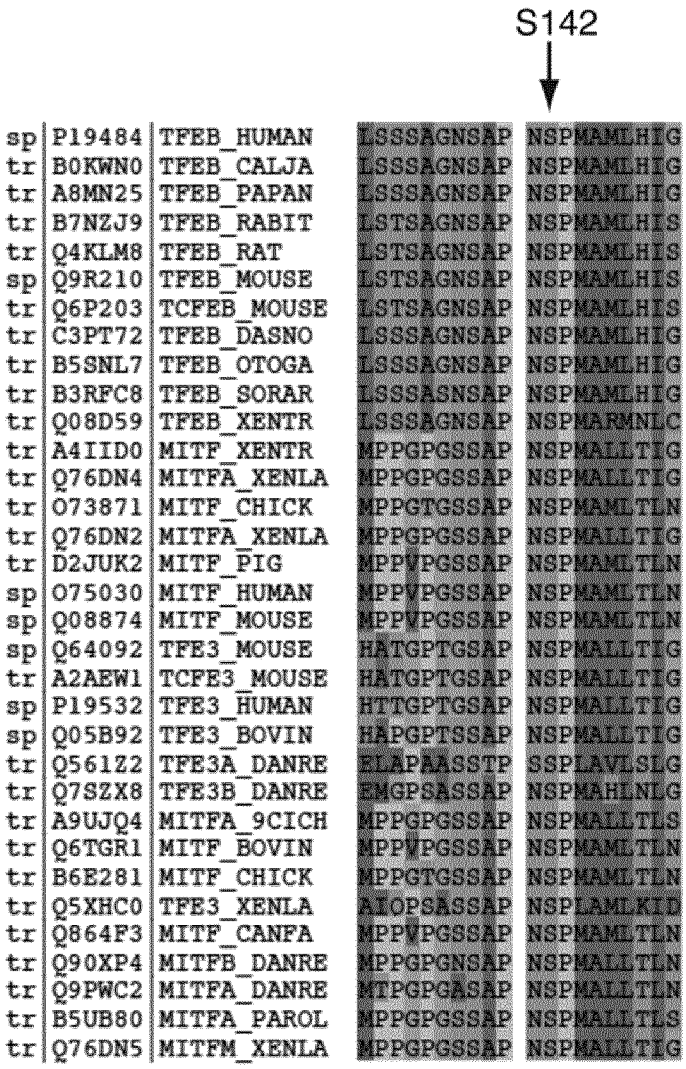
S142
sp P19484 TFEB_HUMAN LSSSAGNSAP NSPMAMLHIG
tr B0KWN0 TFEB_CALJA LSSSAGNSAP NSPMAMLHIG
tr A8MN25 TFEB_PAPAN LSSSAGNSAP NSPMAMLHIG
tr B7NZJ9 TFEB_RABIT LSTSAGNSAP NSPMAMLHIS
tr Q4KLM8 TFEB_RAT LSTSAGNSAP NSPMAMLHIS
sp Q9R210 TFEB_MOUSE LSTSAGNSAP NSPMAMLHIS
tr Q6P203 TCFEB_MOUSE LSTSAGNSAP NSPMAMLHIS
tr C3PT72 TFEB_DASNO LSSSAGNSAP NSPMAMLHIG
tr B5SNL7 TFEB_OTOGA LSSSAGNSAP NSPMAMLHIG
tr B3RFC8 TFEB_SORAR LSSSASNSAP NSPMAMLHIG
tr Q08D59 TFEB_XENTR LSSSAGNSAP NSPMARMNLC
tr A4IID0 MITF_XENTR MPPGPGSSAP NSPMALLTIG
tr Q76DN4 MITFA_XENLA MPPGPGSSAP NSPMALLTIG
tr O73871 MITF_CHICK MPPGTGSSAP NSPMAMLTLN
tr Q76DN2 MITFA_XENLA MPPGPGSSAP NSPMALLTIG
tr D2JUK2 MITF_PIG MPPVPGSSAP NSPMAMLTLN
sp O75030 MITF_HUMAN MPPVPGSSAP NSPMAMLTLN
sp Q08874 MITF_MOUSE MPPVPGSSAP NSPMAMLTLN
sp Q64092 TFE3_MOUSE HATGPTGSAP NSPMALLTIG
tr A2AEW1 TCFE3_MOUSE HATGPTGSAP NSPMALLTIG
sp P19532 TFE3_HUMAN HTTGPTGSAP NSPMALLTIG
sp Q05B92 TFE3_BOVIN HAPGPTSSAP NSPMALLTIG
tr Q561Z2 TFE3A_DANRE ELAPAASSTP SSPLAVLSLG
tr Q7SZX8 TFE3B_DANRE EMGPSASSAP NSPMAHLNLG
tr A9UJQ4 MITFA_9CICH MPPGPGSSAP NSPMALLTLS
tr Q6TGR1 MITF_BOVIN MPPVPGSSAP NSPMAMLTLN
tr B6E281 MITF_CHICK MPPGTGSSAP NSPMAMLTLN
tr Q5XHC0 TFE3_XENLA AIQPSASSAP NSPLAMLKID
tr Q864F3 MITF_CANFA MPPVPGSSAP NSPMAMLTLN
tr Q90XP4 MITFB_DANRE MPPGPGNSAP NSPMALLTLN
tr Q9PWC2 MITFA_DANRE MTPGPGASAP NSPMALLTLN
tr B5UB80 MITFA_PAROL MPPGPGSSAP NSPMALLTLS
tr Q76DN5 MITFM_XENLA MPPGPGSSAP NSPMALLTIG

Fig. 14

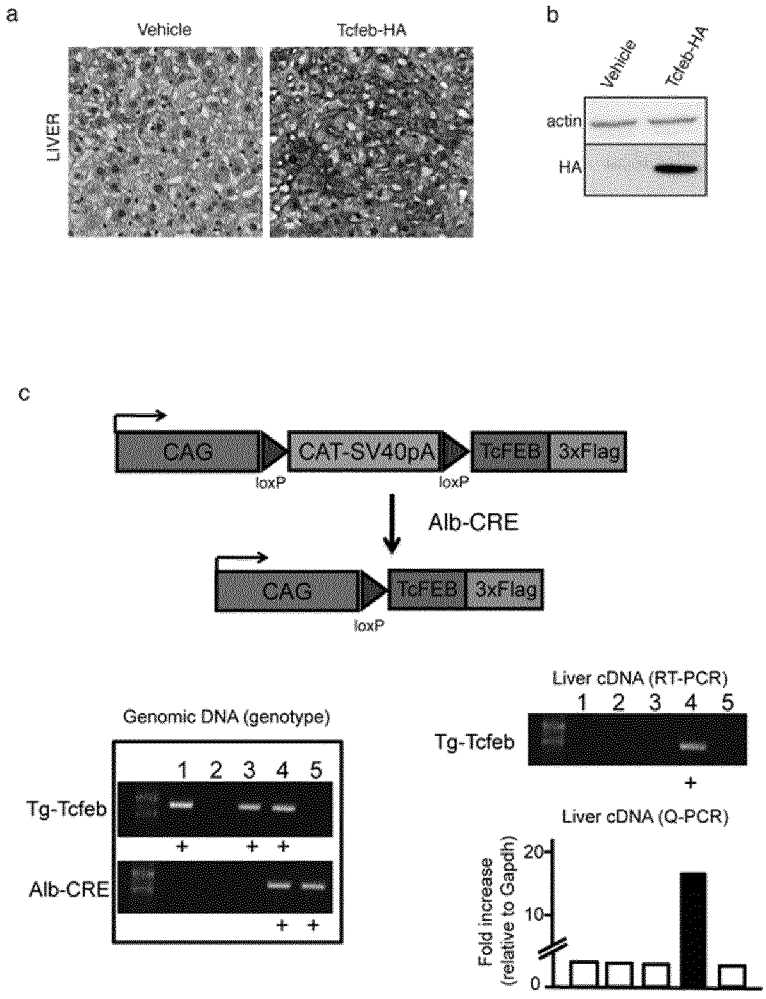
a
Vehicle
Tcfeb-HA
LIVER
b
Vehicle
Tcfeb-HA
actin
HA
c
CAG
CAT-SV40pA
TcFEB
3xFlag
loxP
loxP
Alb-CRE
CAG
TcFEB
3xFlag
loxP
Genomic DNA (genotype)
1 2 3 4 5
Tg-Tcfeb
Alb-CRE
+ + +
+ +
Liver cDNA (RT-PCR)
1 2 3 4 5
Tg-Tcfeb
+
Liver cDNA (Q-PCR)
Fold increase (relative to Gapdh)
20
10
0

Fig. 15

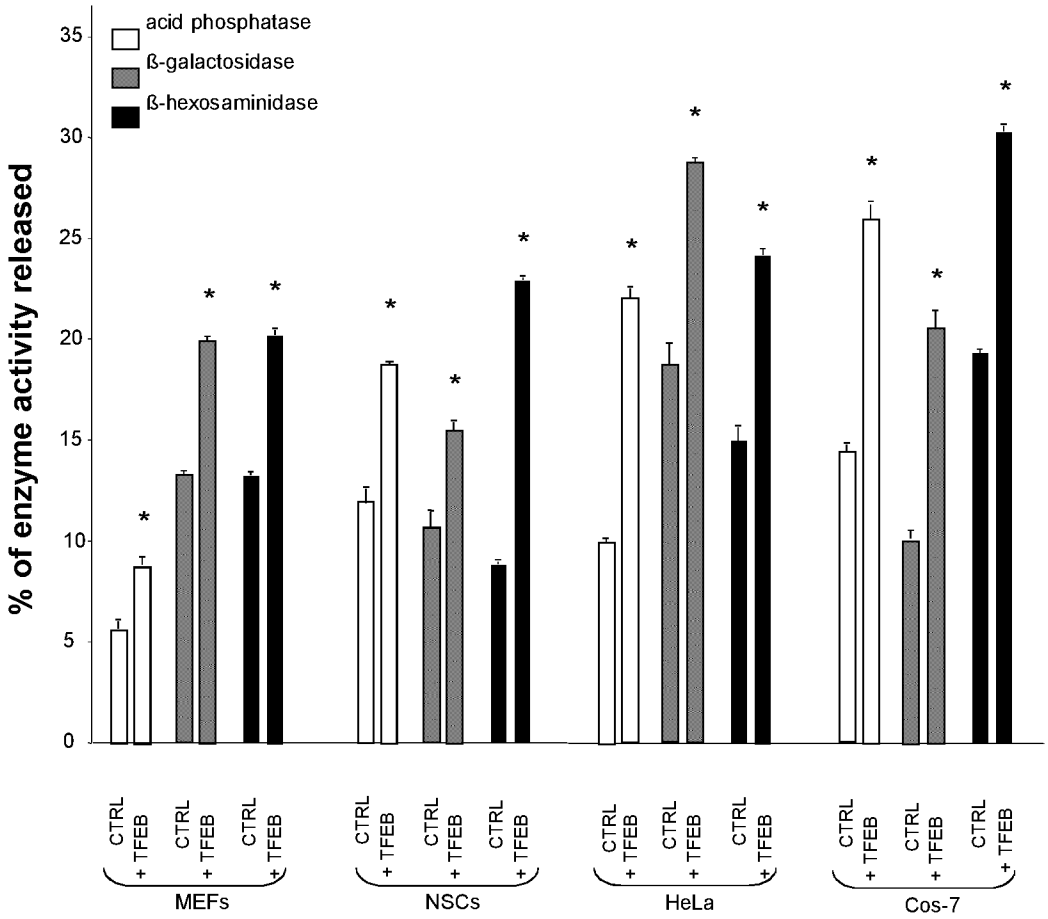
acid phosphatase
ß-galactosidase
ß-hexosaminidase
% of enzyme activity released
35
30
25
20
15
10
5
0
CTRL
+ TFEB
MEFs
NSCs
HeLa
Cos-7

Fig 16

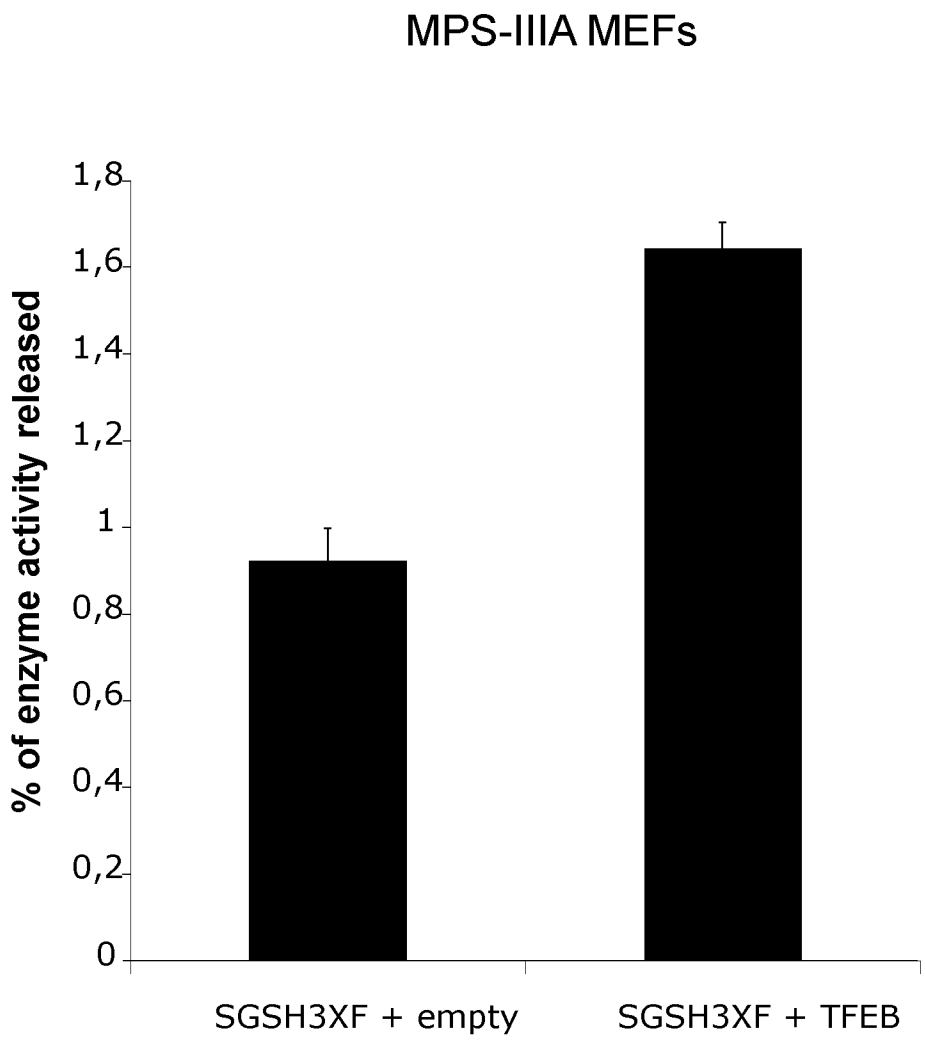
MPS-IIIA MEFs
% of enzyme activity released
1,8
1,6
1,4
1,2
1
0,8
0,6
0,4
0,2
0
SGSH3XF + empty
SGSH3XF + TFEB

Fig. 17

Fig 18

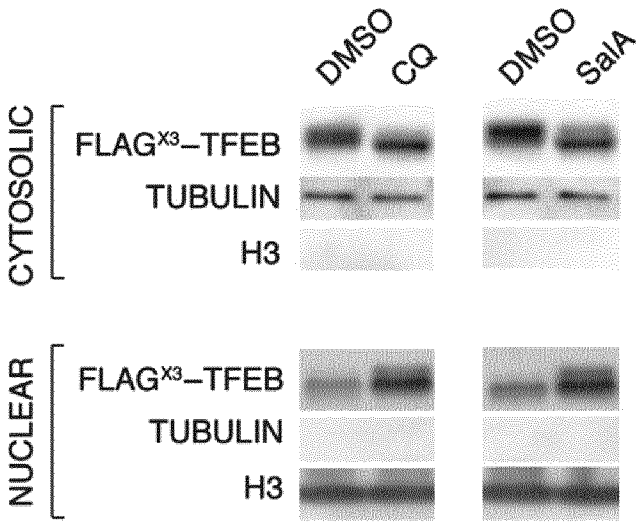
DMSO
CQ
DMSO
SalA
CYTOSOLIC
FLAG^{X3}–TFEB
TUBULIN
H3
NUCLEAR
FLAG^{X3}–TFEB
TUBULIN
H3

Fig 19

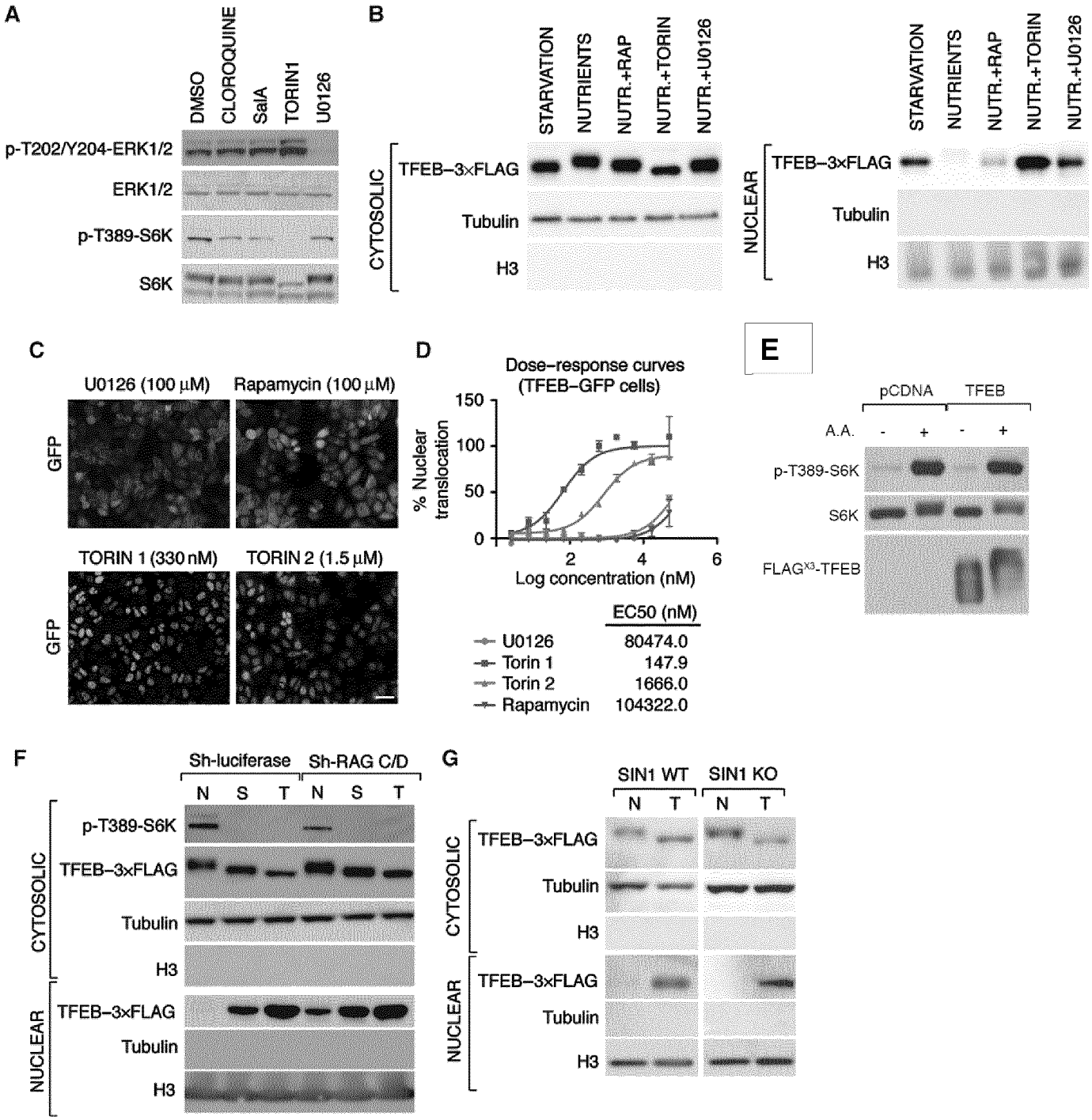
A
DMSO
CLOROQUINE
SalA
TORIN1
U0126
p-T202/Y204-ERK1/2
ERK1/2
p-T389-S6K
S6K
B
STARVATION
NUTRIENTS
NUTR.+RAP
NUTR.+TORIN
NUTR.+U0126
CYTOSOLIC
TFEB–3xFLAG
Tubulin
H3
NUCLEAR
TFEB–3xFLAG
Tubulin
H3
C
U0126 (100 μM)
Rapamycin (100 μM)
GFP
TORIN 1 (330 nM)
TORIN 2 (1.5 μM)
GFP
D
Dose–response curves
(TFEB–GFP cells)
% Nuclear translocation
150
100
50
0
2
4
6
Log concentration (nM)
EC50 (nM)
U0126 80474.0
Torin 1 147.9
Torin 2 1666.0
Rapamycin 104322.0
E
pCDNA
TFEB
A.A. - + - +
p-T389-S6K
S6K
FLAG^X3-TFEB
F
Sh-luciferase
Sh-RAG C/D
N S T N S T
CYTOSOLIC
p-T389-S6K
TFEB–3xFLAG
Tubulin
H3
NUCLEAR
TFEB–3xFLAG
Tubulin
H3
G
SIN1 WT
SIN1 KO
N T N T
CYTOSOLIC
TFEB–3xFLAG
Tubulin
H3
NUCLEAR
TFEB–3xFLAG
Tubulin
H3

Fig 20

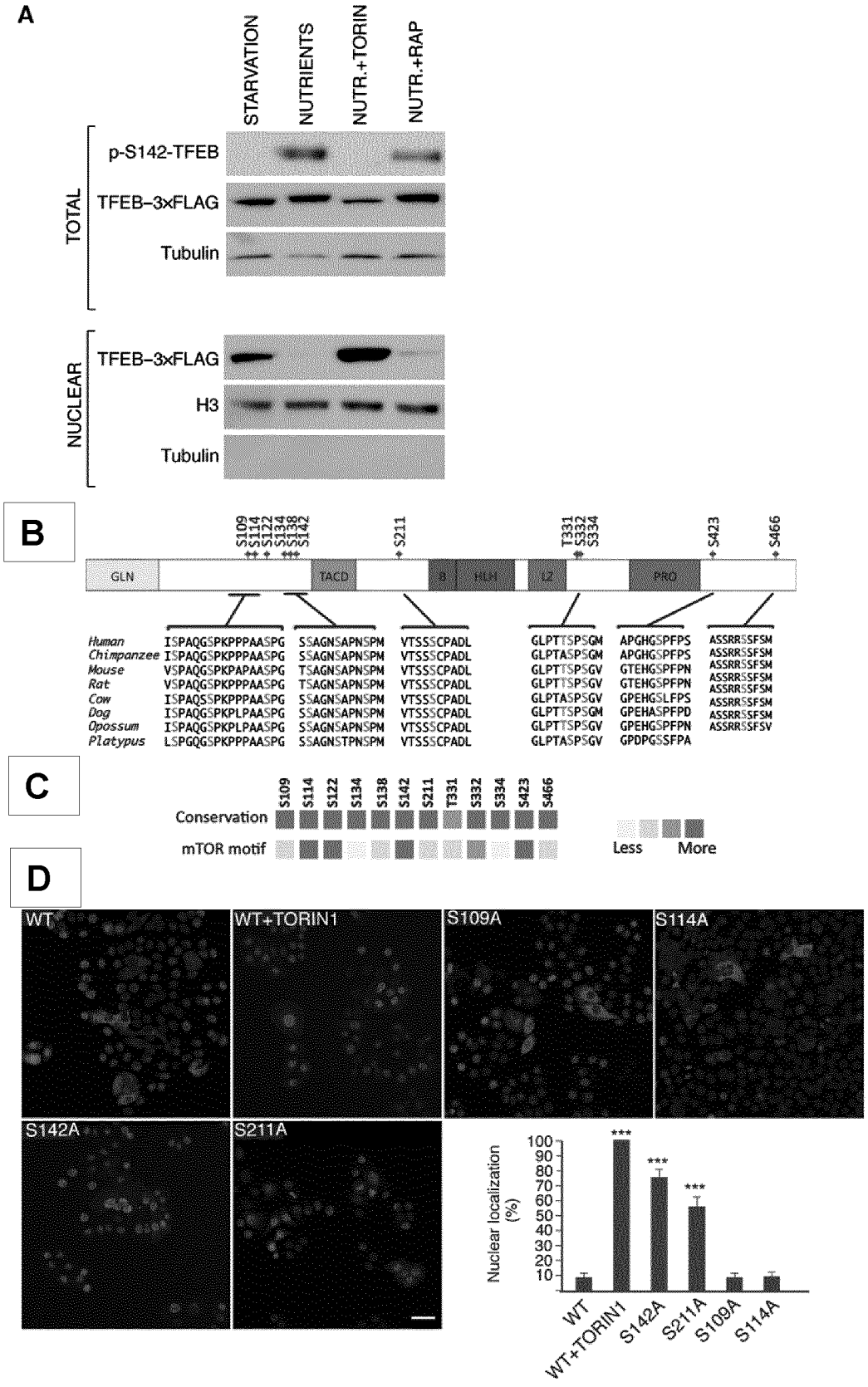
A
STARVATION
NUTRIENTS
NUTR.+TORIN
NUTR.+RAP
TOTAL
p-S142-TFEB
TFEB-3xFLAG
Tubulin
NUCLEAR
TFEB-3xFLAG
H3
Tubulin
B
S109 S114 S122 S134 S138 S142 S211 T331 S332 S334 S423 S466
GLN
TACD
B
HLH
LZ
PRO
Human ISPAQGSPKPPPAASPG SSAGNSAPNSPM VTSSSCPADL GLPTTSPSGM APGHGSPFPS ASSRRSSFSM
Chimpanzee ISPAQGSPKPPPAASPG SSAGNSAPNSPM VTSSSCPADL GLPTASPSGM APGHGSPFPS ASSRRSSFSM
Mouse VSPAQGSPKPAPAASPG TSAGNSAPNSPM VTSSSCPADL GLPTTSPSGV GTEHGSPFPN ASSRRSSFSM
Rat VSPAQGSPKPPPAASPG TSAGNSAPNSPM VTSSSCPADL GLPTTSPSGV GTEHGSPFPN ASSRRSSFSM
Cow ISPAQSSPKPPPAASPG SSAGNSAPNSPM VTSSSCPADL GLPTASPSGV GPEHGSLFPS ASSRRSSFSM
Dog ISPAQGSPKPLPAASPG SSAGNSAPNSPM VTSSSCPADL GLPTTSPSGM GPEHASPFPD ASSRRSSFSM
Opossum ISPAQGSPKPLPAASPG SSAGNSAPNSPM VTSSSCPADL GLPTTSPSGV GPEHGSPFPN ASSRRSSFSM
Platypus LSPGQGSPKPPPAASPG SSAGNSTPNSPM VTSSSCPADL GLPTASPSGV GPDPGSSFPA ASSRRSSFSV
C
S109 S114 S122 S134 S138 S142 S211 T331 S332 S334 S423 S466
Conservation
mTOR motif
Less More
D
WT
WT+TORIN1
S109A
S114A
S142A
S211A
Nuclear localization (%)
100 90 80 70 60 50 40 30 20 10
***
***
***
WT
WT+TORIN1
S142A
S211A
S109A
S114A

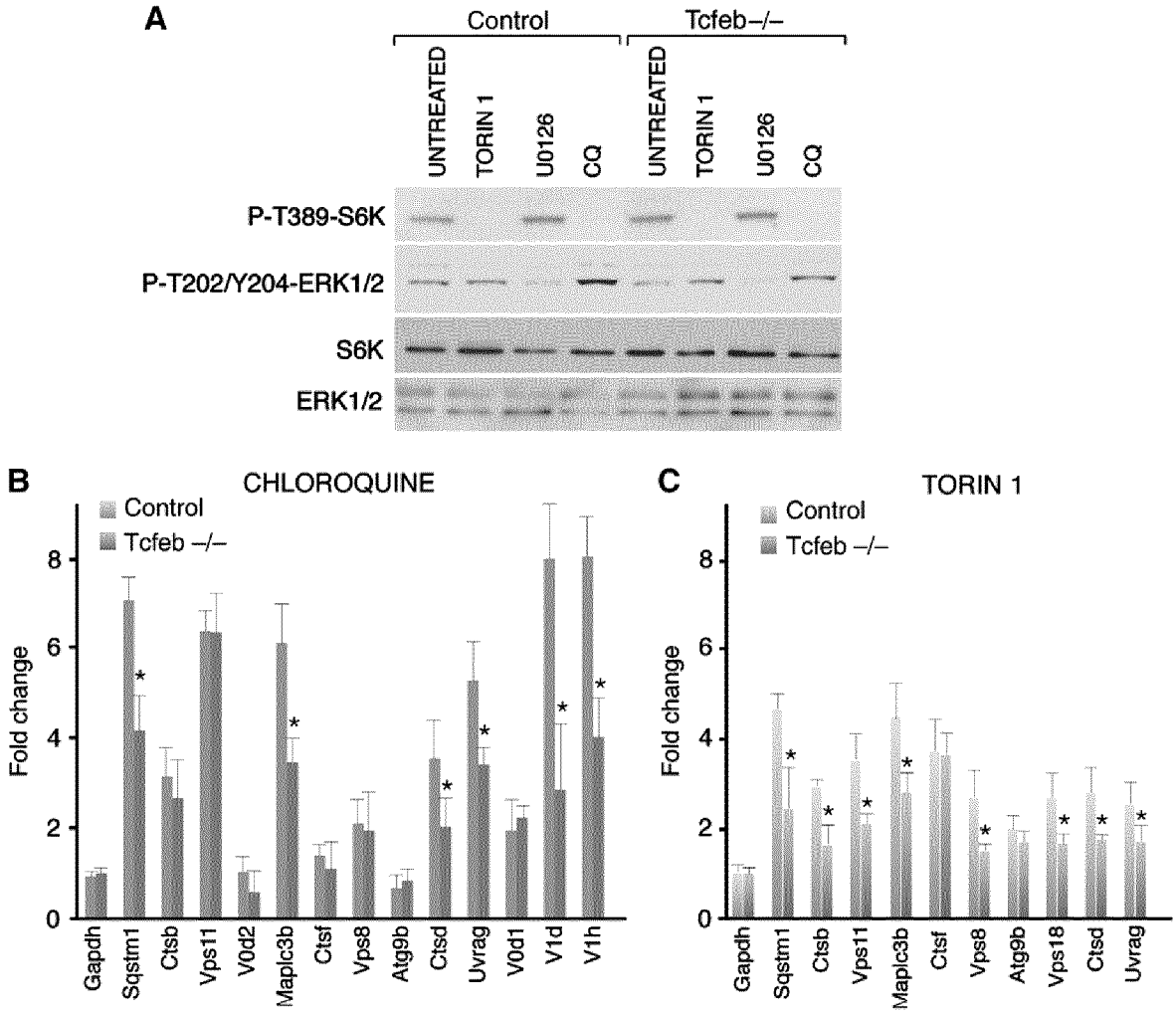
A
Control
Tcfeb–/–
UNTREATED
TORIN 1
U0126
CQ
UNTREATED
TORIN 1
U0126
CQ
P-T389-S6K
P-T202/Y204-ERK1/2
S6K
ERK1/2
B
CHLOROQUINE
Control
Tcfeb –/–
Fold change
0
2
4
6
8
Gapdh
Sqstm1
Ctsb
Vps11
V0d2
Maplc3b
Ctsf
Vps8
Atg9b
Ctsd
Uvrag
V0d1
V1d
V1h
C
TORIN 1
Control
Tcfeb –/–
Fold change
0
2
4
6
8
Gapdh
Sqstm1
Ctsb
Vps11
Maplc3b
Ctsf
Vps8
Atg9b
Vps18
Ctsd
Uvrag

Fig 21

Fig. 22

MSD+DMSO MSD+Torin1 MSD+Torin2

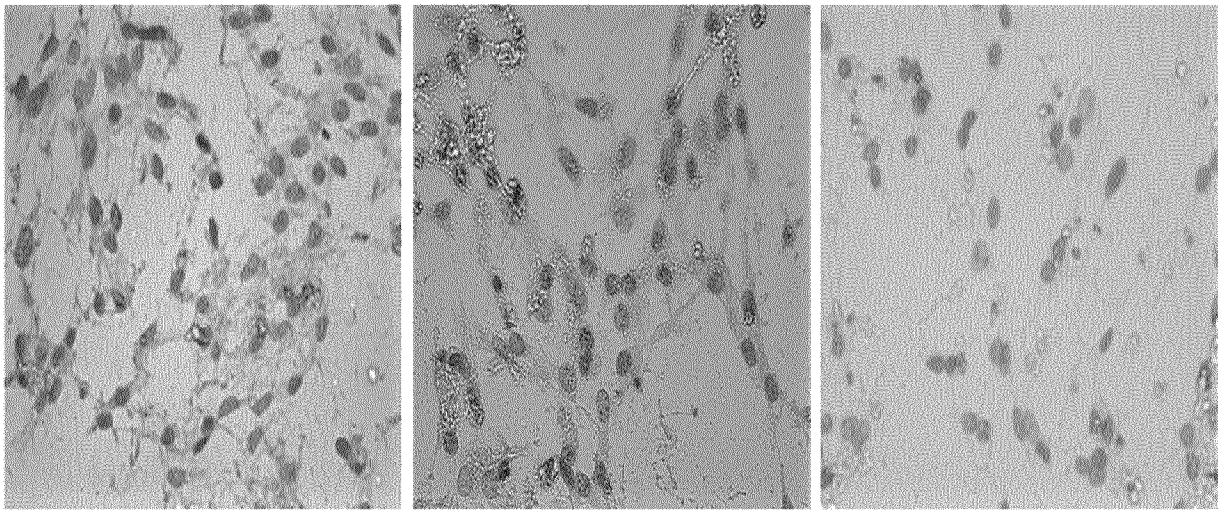

WT NSCs

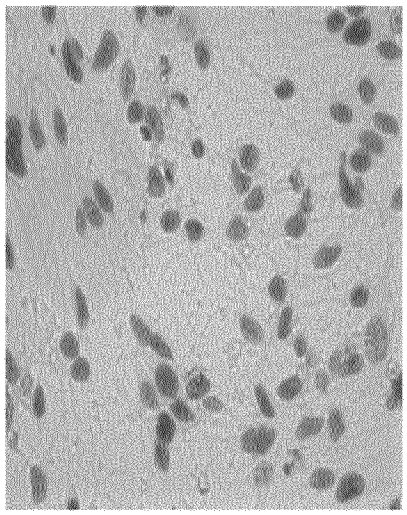

Fig. 23

MSD+DMSO

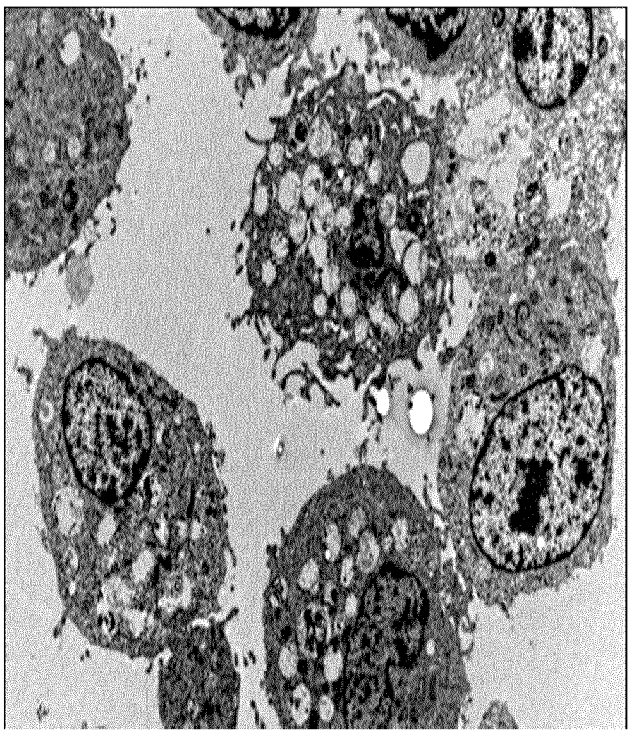

MSD+Torin2

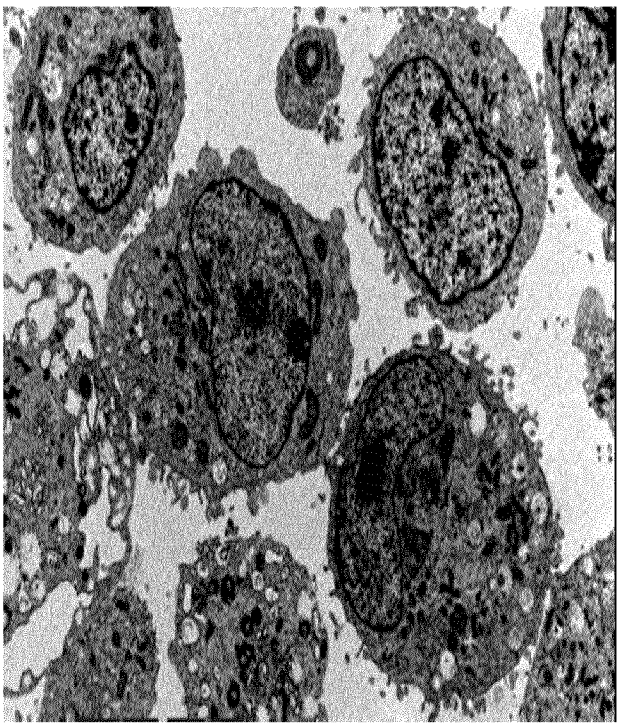

Fig. 24

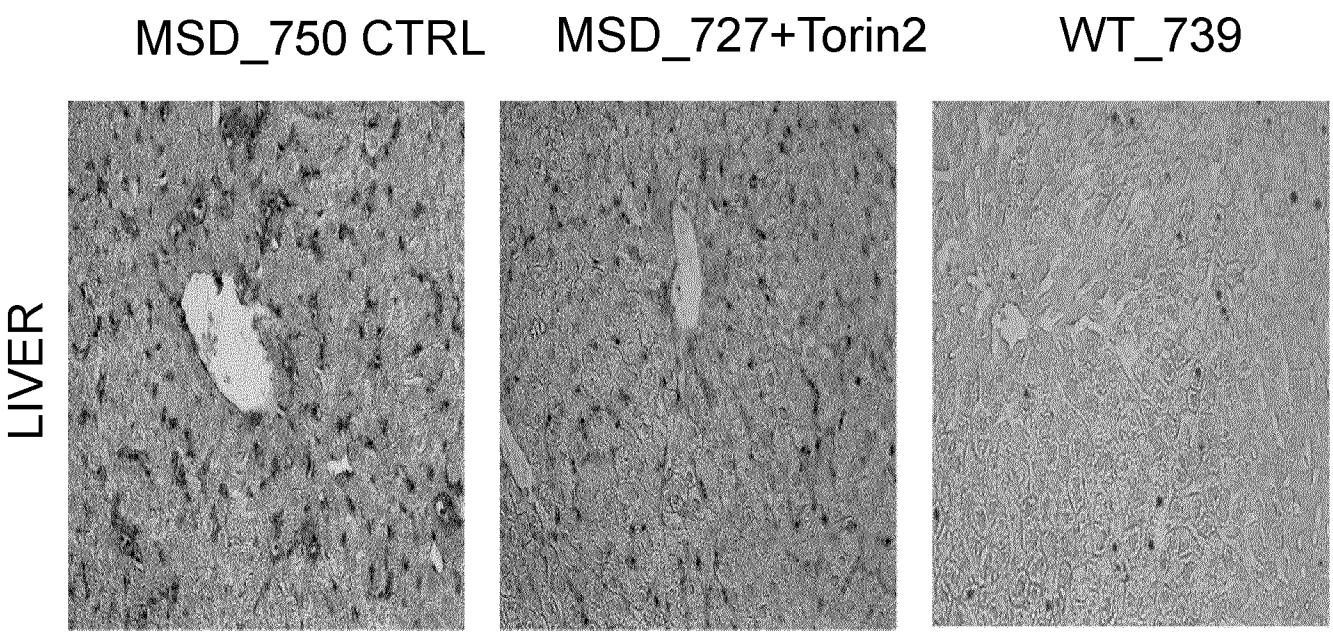

INTERNATIONAL SEARCH REPORT

International application No
PCT/EP2012/053928

A. CLASSIFICATION OF SUBJECT MATTER
INV. A61P1/00 A61P3/00 A61P21/00 A61P25/00 A61K31/00
ADD.

According to International Patent Classification (IPC) or to both national classification and IPC

B. FIELDS SEARCHED

Minimum documentation searched (classification system followed by classification symbols)
A61K A61P C12N

Documentation searched other than minimum documentation to the extent that such documents are included in the fields searched

Electronic data base consulted during the international search (name of data base and, where practicable, search terms used)
EPO-Internal, WPI Data, BIOSIS, EMBASE, CHEM ABS Data

C. DOCUMENTS CONSIDERED TO BE RELEVANT

Category*	Citation of document, with indication, where appropriate, of the relevant passages	Relevant to claim No.
X	WO 2010/044885 A2 (WHITEHEAD BIOMEDICAL INST [US]; DANA FARBER CANCER INST INC [US]; GRAY) 22 April 2010 (2010-04-22)	1-4,27, 28,34-38
A	paragraph [0003] Summary paragraph [0027] - paragraph [0072] paragraph [0079] Examples claims 75-79, 83-87	5-26, 29-33, 39-44

-/--

[X] Further documents are listed in the continuation of Box C.

[X] See patent family annex.

* Special categories of cited documents :

"A" document defining the general state of the art which is not considered to be of particular relevance

"E" earlier application or patent but published on or after the international filing date

"L" document which may throw doubts on priority claim(s) or which is cited to establish the publication date of another citation or other special reason (as specified)

"O" document referring to an oral disclosure, use, exhibition or other means

"P" document published prior to the international filing date but later than the priority date claimed

"T" later document published after the international filing date or priority date and not in conflict with the application but cited to understand the principle or theory underlying the invention

"X" document of particular relevance; the claimed invention cannot be considered novel or cannot be considered to involve an inventive step when the document is taken alone

"Y" document of particular relevance; the claimed invention cannot be considered to involve an inventive step when the document is combined with one or more other such documents, such combination being obvious to a person skilled in the art

"&" document member of the same patent family

Date of the actual completion of the international search	Date of mailing of the international search report
29 May 2012	14/08/2012

Name and mailing address of the ISA/	Authorized officer
European Patent Office, P.B. 5818 Patentlaan 2 NL - 2280 HV Rijswijk Tel. (+31-70) 340-2040, Fax: (+31-70) 340-3016	Hornich-Paraf, E

1

Form PCT/ISA/210 (second sheet) (April 2005)

INTERNATIONAL SEARCH REPORT

International application No.
PCT/EP2012/053928

Box No. II Observations where certain claims were found unsearchable (Continuation of item 2 of first sheet)

This international search report has not been established in respect of certain claims under Article 17(2)(a) for the following reasons:

1. ☐ Claims Nos.:
because they relate to subject matter not required to be searched by this Authority, namely:

2. ☐ Claims Nos.:
because they relate to parts of the international application that do not comply with the prescribed requirements to such an extent that no meaningful international search can be carried out, specifically:

3. ☐ Claims Nos.:
because they are dependent claims and are not drafted in accordance with the second and third sentences of Rule 6.4(a).

Box No. III Observations where unity of invention is lacking (Continuation of item 3 of first sheet)

This International Searching Authority found multiple inventions in this international application, as follows:

see additional sheet

1. ☐ As all required additional search fees were timely paid by the applicant, this international search report covers all searchable claims.

2. ☐ As all searchable claims could be searched without effort justifying an additional fees, this Authority did not invite payment of additional fees.

3. ☐ As only some of the required additional search fees were timely paid by the applicant, this international search report covers only those claims for which fees were paid, specifically claims Nos.:

4. ☒ No required additional search fees were timely paid by the applicant. Consequently, this international search report is restricted to the invention first mentioned in the claims; it is covered by claims Nos.:

3, 4(completely); 1, 2, 27-33, 36-44(partially)

Remark on Protest

☐ The additional search fees were accompanied by the applicant's protest and, where applicable, the payment of a protest fee.

☐ The additional search fees were accompanied by the applicant's protest but the applicable protest fee was not paid within the time limit specified in the invitation.

☐ No protest accompanied the payment of additional search fees.

C(Continuation). DOCUMENTS CONSIDERED TO BE RELEVANT

Category*	Citation of document, with indication, where appropriate, of the relevant passages	Relevant to claim No.
X	WO 2010/056754 A2 (OF THE UNIVERSITY OF TEXAS SYS [US]; SHARP ZELTON DAVE [US]; STRONG JO) 20 May 2010 (2010-05-20) 'Summary of the invention' in particular page 4, paragraph 5 page 6, line 12 page 6, paragraph 4 page 7, paragraph 1 'mTOR Inhibitors and Rapamycin' on p. 14, last paragraph to p. 16 '2. Age-Related Diseases Associated with the TOR Pathway' on p. 21, in particular 2 and 3 page 22, line 4 - line 8 Claims, in particular claims 1-4, 9, 14, 15, 19-24, 27-29	1-4,27, 28,33, 36-38, 40,44
X	WO 2010/049481 A1 (NOVARTIS AG [CH]; GARCIA-ECHEVERRIA CARLOS [CH]; MAIRA SAUVEUR-MICHEL) 6 May 2010 (2010-05-06)	1-4,27, 28,33, 36-38, 40,44
A	the whole document in particular 'Summary of the invention' page 2, paragraph 7 page 6, paragraph 3 page 10, paragraph 2 last paragraph; page 10 page 11, paragraph 1 Claims, in particular claims 9, 10, 13	5-26, 29-32, 39,41-43
X	SETTEMBRE C ET AL: "Lysosomal storage diseases as disorders of autophagy", AUTOPHAGY, LANDES BIOSCIENCE, US, vol. 4, no. 1, 1 January 2008 (2008-01-01) , pages 113-114, XP009159089, ISSN: 1554-8627 the whole document	1-4,27, 28,33, 36-38, 40,44
X	DEHAY BENJAMIN ET AL: "Pathogenic Lysosomal Depletion in Parkinson's Disease", JOURNAL OF NEUROSCIENCE, NEW YORK, NY, US, vol. 30, no. 37, 15 September 2010 (2010-09-15), pages 12535-12544, XP002674196, ISSN: 0270-6474 abstract 'Discussion'	1-4,27, 28,33, 36-38, 40,44

-/--

C(Continuation). DOCUMENTS CONSIDERED TO BE RELEVANT

Category*	Citation of document, with indication, where appropriate, of the relevant passages	Relevant to claim No.
A	Carmine Settembre: "A block of autophagy in lysosomal storage disorders", , 1 September 2008 (2008-09-01), XP055026273, Retrieved from the Internet: URL:http://hmg.oxfordjournals.org/content/17/1/119.full.pdf#page=1&view=FitH [retrieved on 2012-05-07] abstract 'Discussion'	1-4, 27-33, 36-44
A	SARDIELLO MARCO ET AL: "A gene network regulating lysosomal biogenesis and function", SCIENCE, AMERICAN ASSOCIATION FOR THE ADVANCEMENT OF SCIENCE, WASHINGTON, DC; US, vol. 325, no. 5939, 24 July 2009 (2009-07-24), pages 473-477, XP002588778, ISSN: 0036-8075, DOI: 10.1126/SCIENCE.1174447 [retrieved on 2009-06-25] abstract the whole document	1-4, 27-33, 36-44
A,P	A. M. CUERVO: "Autophagy's Top Chef", SCIENCE, vol. 332, no. 6036, 16 June 2011 (2011-06-16), pages 1392-1393, XP055026308, ISSN: 0036-8075, DOI: 10.1126/science.1208607 the whole document	1-4, 27-33, 36-44
A	WO 2010/092112 A1 (FOND TELETHON [IT]; BALLABIO ANDREA [IT]; SARDIELLO MARCO [IT]) 19 August 2010 (2010-08-19) 'Description ot the invention' page 3 - page 6 Claims, in particular claims 1, 9-13	1-4, 27-33, 36-44

1

FURTHER INFORMATION CONTINUED FROM PCT/ISA/ 210

This International Searching Authority found multiple (groups of) inventions in this international application, as follows:

1. claims: 3, 4(completely); 1, 2, 27-33, 36-44(partially)

   An inhibitor of TFEB phosphorylation for medical use / for use in the treatment of a disorder that needs the induction of the cell autophagic / lysosomal system, wherein the inhibitor is an inhibitor of TFEB phosphorylation acting on a kinase of the pathway of the TFEB phosphorylation, wherein the kinase is mTOR and/or PI3K; the inhibitor belonging to the group of compounds listed in table 4 par. 1 PI3I-mTOR pathway

   ---

2. claims: 5-8(completely); 1, 2, 27-33, 36-44(partially)

   An inhibitor of TFEB phosphorylation for medical use / for use in the treatment of a disorder that needs the induction of the cell autophagic / lysosomal system, wherein the inhibitor is an inhibitor of TFEB phosphorylation acting on a kinase that directly phosphorylates TFEB molecule; inhibiting a serine specific Extracellular Regulated Kinase (ERK); wherein the ERK kinase is the ERK2 kinase; the inhibitor belonging to the group of compounds listed in table 4 par. 2 Ras-ERK pathway

   ---

3. claims: 9, 10(completely); 1, 2, 27-33, 36-44(partially)

   An inhibitor of TFEB phosphorylation for medical use / for use in the treatment of a disorder that needs the induction of the cell autophagic / lysosomal system, wherein the inhibitor is an inhibitor of TFEB phosphorylation acting on a kinase wherein the kinase is a Mitogen activated protein kinase; the inhibitor belonging to the group of compounds listed in Table 4 par. 3 of Mitogen activated protein kinases

   ---

4. claims: 11, 12(completely); 1, 2, 27-33, 36-44(partially)

   An inhibitor of TFEB phosphorylation for medical use / for use in the treatment of a disorder that needs the induction of the cell autophagic / lysosomal system, wherein the inhibitor is an inhibitor of TFEB phosphorylation acting on a kinase wherein the kinase is Aurora kinase; the inhibitor belonging to the group of compounds listed in Table 4 par. 4 Aurora kinases

   ---

5. claims: 13, 14(completely); 1, 2, 27-33, 36-44(partially)

   An inhibitor of TFEB phosphorylation for medical use / for use in the treatment of a disorder that needs the induction

of the cell autophagic / lysosomal system, wherein the inhibitor is an inhibitor of TFEB phosphorylation acting on a kinase wherein the kinase is a Receptor Tyrosine kinase; the inhibitor belonging to the group of compounds listed in Table 4 par. 5 Receptor Tyrosine kinases

---

6. claims: 15, 16(completely); 1, 2, 27-33, 36-44(partially)

An inhibitor of TFEB phosphorylation for medical use / for use in the treatment of a disorder that needs the induction of the cell autophagic / lysosomal system, wherein the inhibitor is an inhibitor of TFEB phosphorylation acting on a kinase wherein the kinase is a Polo-like kinase; the inhibitor belonging to the group of compounds listed in Table 4 par. 6 Polo-like kinases

---

7. claims: 17, 18(completely); 1, 2, 27-33, 36-44(partially)

An inhibitor of TFEB phosphorylation for medical use / for use in the treatment of a disorder that needs the induction of the cell autophagic / lysosomal system, wherein the inhibitor is an inhibitor of TFEB phosphorylation acting on a kinase wherein the kinase belongs to the JAK-STAT pathway; the inhibitor belonging to the group of compounds listed in Table 4 par. 7 JAK-STAT pathway

---

8. claims: 19, 20(completely); 1, 2, 27-33, 36-44(partially)

An inhibitor of TFEB phosphorylation for medical use / for use in the treatment of a disorder that needs the induction of the cell autophagic / lysosomal system, wherein the inhibitor is an inhibitor of TFEB phosphorylation acting on a kinase wherein the kinase is a cyclin dependent kinase; the inhibitor belonging to the group of compounds listed in Table 4 par. 8 cyclin dependent kinases

---

9. claims: 21, 22(completely); 1, 2, 27-33, 36-44(partially)

An inhibitor of TFEB phosphorylation for medical use / for use in the treatment of a disorder that needs the induction of the cell autophagic / lysosomal system, wherein the inhibitor is an inhibitor of TFEB phosphorylation acting on a kinase wherein the kinase belongs to the Wnt signaling pathway; the inhibitor belonging to the group of compounds listed in Table 4 par. 9 Wnt signaling pathway

---

10. claims: 23, 24(completely); 1, 2, 27-33, 36-44(partially)

An inhibitor of TFEB phosphorylation for medical use / for use in the treatment of a disorder that needs the induction

of the cell autophagic / lysosomal system, wherein the inhibitor is an inhibitor of TFEB phosphorylation acting on a kinase wherein the kinase is a Src family kinase; the inhibitor belonging to the group of compounds listed in Table 4 par. 10 Src family kinases

---

11. claims: 25, 26(completely); 1, 2, 27-33, 36-44(partially)

An inhibitor of TFEB phosphorylation for medical use / for use in the treatment of a disorder that needs the induction of the cell autophagic / lysosomal system, wherein the inhibitor is an inhibitor of TFEB phosphorylation acting on a kinase wherein the kinase belongs to the family of Protein kinases C; the inhibitor belonging to the group of compounds listed in Table 4 par. 11 Protein kinases C family

---

12. claims: 34, 35

Use of the inhibitor according to any of claims 1 to 26 for increasing the productivity of cells producing endogeneous or recombinant lysosomal enzymes (claim 34);
A method of producing lysosomal endogeneous or recombinant enzymes comprising: contacting the inhibitor according to any of claims 1 to 26 with the autophagic/lysosomal system in a cell; inducing said autophagic/lysosomal system; and increasing production of said lysosomal enzymes (claim 35).

INTERNATIONAL SEARCH REPORT

Information on patent family members

International application No
PCT/EP2012/053928

Patent document cited in search report	Publication date	Patent family member(s)	Publication date
WO 2010044885 A2	22-04-2010	CN 102256966 A	23-11-2011
		EP 2350053 A2	03-08-2011
		US 2011288091 A1	24-11-2011
		WO 2010044885 A2	22-04-2010
WO 2010056754 A2	20-05-2010	CA 2743491 A1	20-05-2010
		CN 102292078 A	21-12-2011
		EP 2365802 A2	21-09-2011
		US 2012064143 A1	15-03-2012
		WO 2010056754 A2	20-05-2010
WO 2010049481 A1	06-05-2010	AU 2009309616 A1	06-05-2010
		CA 2736361 A1	06-05-2010
		CN 102202668 A	28-09-2011
		EP 2349275 A1	03-08-2011
		JP 2012506898 A	22-03-2012
		KR 20110090911 A	10-08-2011
		US 2011195966 A1	11-08-2011
		WO 2010049481 A1	06-05-2010
WO 2010092112 A1	19-08-2010	AU 2010212854 A1	08-09-2011
		CA 2752433 A1	19-08-2010
		EP 2218458 A1	18-08-2010
		EP 2396022 A1	21-12-2011
		US 2012040451 A1	16-02-2012
		WO 2010092112 A1	19-08-2010